NUMERICAL STUDIES OF REACTION-DIFFUSION IN PHYSIOLOGICAL PROCESSES

by

ANNA FRANCINA MEIRING

A thesis submitted in partial fulfilment of the requirements for the degree of

DOCTOR OF SCIENCE

in the

Faculty of Mathematics and Natural Science,

University of Pretoria,

Pretoria.

November, 1980.

ACKNOWLEDGEMENTS

Sincere thanks to the following persons:

Prof A R Mitchell of the Mathematics Department, University of Dundee, Scotland, under whose guidance this study was commenced. His encouragement and enthusiasm was a constant source of inspiration. It was a priviledge to study with such an able person;

Prof J A Snyman of the Department of Applied Mathematics, University of Pretoria and promotor of this thesis. His invaluable assistance and enthusiasm and the many hours he spent reading this manuscript are much appreciated;

Prof B D Sleeman of the Mathematics Department, University of Dundee, Scotland, for his interest and useful discussions;

Prof P J Zietsman and other colleagues and friends in the Mathematics Department, University of Pretoria, for their compliance in many aspects and for helping with the painstaking task of proofreading;

Mrs Schickerling for the excellent typing of this manuscript;

My parents for their constant encouragement and care throughout my years of study.

Thanks be to God, creater of all things.

The Author.

SUMMARY

The aim of this study is to conduct a numerical investigation into mathematical models representing two physiological processes, both being examples of reaction-diffusion processes. The first of these processes comes from the field of population genetics when two types of individuals are allowed to mate at random. The governing equation of the relevant model is Fisher's equation [1]

$$\frac{\partial u}{\partial t} = \frac{\partial^2 u}{\partial x^2} + f(u) .$$

The second process comes from the field of neurobiology and concerns the conduction of an impulse in the nervous system, the principal model being the Hodgkin-Huxley system of differential equations [45] with simplifications due to FitzHugh [28] and Nagumo, Arimoto and Yoshizawa [64].

Chapter 1 is an introductory chapter, introducing the reader to reaction-diffusion equations, mathematical modelling in general and giving an exposition as to the purpose of the present study.

In Chapter 2 the relevant two physiological processes are discussed and a description is given of the construction of the mathematical models which represent these processes respectively. Assumptions are motivated and refinements to the original models are discussed.

In Chapter 3 a general system of reaction-diffusion equations is given, of which the governing equations of the various models are particular examples. A literature survey is then presented which covers both the pure analytical results and numerical results available on the various models.

In Chapter 4 a numerical study is conducted on Fisher's equation, using the Finite Element method. The numerical results are assessed with reference to the available analytical results quoted in the preceding chapter. The study concentrates on three aspects, namely the stability of solutions, the asymptotic speed of propagation and the convergence to wave fronts.

In Chapter 5 a numerical study is conducted on the Hodgkin-Huxley model and it's simplifications, namely Nagumo's model, the Fitz-Hugh-Nagumo model and the BVP model. The initiation of travelling wave solutions and the effect of initial and boundary data is investigated. Speed diagrams are constructed for both Nagumo's model and the Hodgkin-Huxley model. Aspects such as the relationship between stimulus strength and pulse speed and the one-to-one correspondence between stimuli and impulses initiated are investigated.

We conclude the study in Chapter 6 with an overview of the present investigation.

OPSOMMING

Die doel van hierdie studie is om 'n numeriese ondersoek te doen na wiskundige modelle wat twee fisiologiese prosesse verteenwoordig, albei voorbeelde van reaksie-diffusieprosesse. Die eerste proses kom uit die gebied van bevolkingsgenetika wanneer twee tipes individue gelaat word om lukraak te paar. Die beheervergelyking van dié betrokke model is Fisher se vergelyking [1]

$$\frac{\partial u}{\partial t} = \frac{\partial^2 u}{\partial x^2} + f(u).$$

Die tweede proses kom uit die gebied van neurobiologie en het betrekking op die geleiding van 'n impuls in die senuweestelsel. Hier is die belangrikste model die Hodgkin-Huxley-stelsel van differensiaalvergelykings [45], met vereenvoudigings deur FitzHugh [28] en Nagumo, Arimoto en Yoshizawa [64].

Hoofstuk 1 is 'n inleidende hoofstuk en stel die leser bekend aan reaksie-diffusievergelykings en wiskundige modellering in die algemeen en gee 'n uiteensetting van die doel van hierdie studie.

In Hoofstuk 2 word die betrokke twee fisiologiese prosesse bespreek en 'n beskrywing word gegee van die konstruksie van die wiskundige modelle wat die twee prosesse verteenwoordig. Aannames word gemotiveer en verfynings van die oorspronklike modelle word bespreek.

In Hoofstuk 3 word 'n algemene stelsel van reaksie-diffusievergelykings beskou, waarvan die beheervergelykings van die verskillende modelle spesifieke voorbeelde is. 'n Literatuuroorsig word dan aangebied wat beide die beskikbare suiwer analitiese sowel as numeriese resultate dek.

In Hoofstuk 4 word 'n numeriese studie op Fisher se vergelyking gedoen deur die Eindigelementmetode te gebruik. Die numeriese oplossings word benader met verwysing na die beskikbare analitiese resultate wat aangehaal is in die voorafgaande hoofstuk. Die studie lê klem op veral drie aspekte, naamlik die stabiliteit van oplossings, die asimptotiese voortplantingsspoed en die konvergensie na golffronte.

In Hoofstuk 5 word 'n numeriese studie gedoen op die Hodgkin-Huxley-model en sy vereenvoudigings, naamlik Nagumo se model, die FitzHugh-Nagumo-model en die BVP-model. Die inisiëring van bewegende golfoplossings en die effek van begin- en randgegewens hierop word ondersoek. Spoed-diagramme word opgestel vir beide Nagumo se model en die Hodgkin-Huxley-model. Aspekte soos die verband tussen stimulussterkte en pulsspoed en die een-een-duidige verband tussen stimuli en impulse wat geïnisieer word, word ondersoek.

Die werk word afgesluit in Hoofstuk 6 met 'n oorsig van hierdie studie.

I N D E X

CHAPTER 1

INTRODUCTION

CHAPTER 2

MATHEMATICAL MODELS OF REACTION-DIFFUSION

CHAPTER 3

ANALYSIS OF GOVERNING EQUATIONS — A SURVEY OF EXISTING LITERATURE

CHAPTER 4

A FINITE ELEMENT STUDY OF FISHER'S EQUATION

CHAPTER 5

A FINITE ELEMENT STUDY OF THE HODGKIN-HUXLEY EQUATIONS

"A mathematical model is something simple made by a scientist to help him understand something complicated".

R FitzHugh

CHAPTER 1

INTRODUCTION

1.1. Reaction-Diffusion problems in physiology

In fields such as physiology, biology or chemistry the concepts of interaction (reaction) between species and diffusion in a process are common phenomena.

The term species describes in general the individuals active during the process - genotypes in models from population genetics, chemical substances in reaction kinetics or taxonomic species in ecological problems. Diffusion is the term describing the movement of particles - random flow of genes in population genetics or active migration of individuals or flow of charge in nerve conduction models. Reaction in the medium refers to processes such as chemical reactions, reproduction processes or deaths in biological population or ion transfer across the membrane of the nerve.

Reaction and diffusion in a process lead, in many cases, to a mathematical description by a system of non-linear second order partial differential equations of the form

$$\frac{\partial \underline{u}}{\partial t} = F(\underline{u}) + D \nabla^2 \underline{u}$$

where $\underline{u}(\underline{x},t)$ is a vector which defines the state of the system at a given point $\underline{x}$ and time t. The non-linear function F describes the reaction of the system while the diffusion enters via the term $D \nabla^2 \underline{u}$ where D is a matrix with non-negative entries and ∇^2 the Laplacian.

An indication of the importance of equations of this type is the

wide range of excitable media which can be modelled by a system of reaction-diffusion equations. A few examples are; models for the cardiac muscle, spread of epidemics, travelling bands of bacteria, concentration fronts in chemical reactor theory and quench front problems in water-cooled reactors [14, 32, 34, 62, 63, 87].

The first of two examples of reaction-diffusion processes which will be investigated in the present study comes from the field of population genetics when two types of individuals are allowed to mate at random [1, 26, 27]. The other example comes from the field of neurobiology and concerns the process of conduction of a nerve impulse along a nerve fibre [44, 45].

1.2. Progress in mathematical modelling

The concept of a mathematical model for a physical process is a very old one, mathematicians have been busy constructing mathematical models for various processes for the past few centuries.

A mathematical model in physiology is a translation of classical physiological concepts in a more definite and logical language than one composed of words alone [29]. In doing so one hopes that the mathematical formulation will give a clearer indication of the degree of dependence of the process on the various parameters included in the model. The basic dynamic relationships between the variables of state, exhibited by the model, should explain the working of the process as clearly as possible. Results obtained from a model should quantitatively, as well as qualitatively, agree with experimental evidence. In this way, conclusions of greater generality may be made with greater confidence.

Some authors have indicated [41] that mathematical models of physiological processes are not usually received with enthusiasm by the general physiologists. This attitude on the part of the physiologists can be explained by the fact that construction of an adequate model for an intricate physiological process is never easy and difficulties such as incomplete biological theory and lack of sufficient experimental data from which to determine all of the parameters in the model may lead to an inaccurate mathematical formulation. The aim of the scientist constructing the model is to do so in the simplest possible way while still retaining the most important features of the process. Once this aim has been reached, refinements may follow.

A particular model in physiology which has a long and interesting history and which is partly the subject of this study is that of the conduction of an impulse along the nervous system.

Attempts to construct models of nerve cells date back more than 150 years [44] but it is only since 1930 that serious attempts have been made to develop models of the mechanism which enables nerve fibres to carry messages about the bodies of men and animals.

Two important facts had firmly been established by the end of the eighteenth century, namely, that nerves or muscles could be stimulated by electrical shocks and that some animals produce electricity. Hodgkin [44] in a book on impulse conduction mentions these and other interesting facts known for many centuries before our time. For example a fifth-dynasty Egiptian mural in a tomb at Sakkara (2600 B.C.) contains a clear representation

of Malapterurus, the electrical catfish. An amusing anecdote is that Scribonius, a Roman physician in the first century A.D., should have recommended the discharge of the Torpedo as a cure for gout, headaches and epilepsy.

The study of electric fish showed that animals produce electricity, but the discovery of action currents of nerve and muscle had to wait for the development of suitable recording instruments. These experiments got underway during the 1930 s and reached a climax with the work of Hodgkin and Huxley [45] in 1952.

In 1952 A.L. Hodgkin and A.F. Huxley concluded a series of papers concerning the flow of electrical current through the surface of the giant axon of the squid Loligo. They constructed the first relatively complete model of impulse transmission along the nerve membrane.

Hodgkin and Huxley were awarded the Nobel Prize in 1963 for this remarkable achievement. Their work was highly acclaimed the world over as the brilliant combination of difficult experimental work and mathematical ingenuity. The construction of Hodgkin and Huxley's model was the climax of a long and interesting accumulation of knowledge of the nervous system throughout history.

Simplifications of the Hodgkin-Huxley model followed subsequently. The first of these appeared in 1961, called the BVP model and was due to R. FitzHugh [28]. Although this model does not match the voltage changes in the nerve quantitatively, as does the Hodgkin-Huxley model, it does give a qualitative description.

Two further simplifications followed, namely the FitzHugh-

Nagumo model and the Nagumo model [64]. Although simpler in form, these models have no other advantage over the original model and certainly cannot be seen as a substitute for the original model.

The history surrounding the construction of the other example of a physiological model which will be studied here, comes from the field of population genetics and does not date back as far as that of the study of the nervous system. We pick up the history in 1937 when R.A. Fisher [27] published a paper concerned with the construction of a model of the genetics of a population consisting of two types of individuals, allowed to mate at random. Under assumptions on fertilities and mortalities a partial differential equation is constructed to describe temporal and spatial changes of the gene frequencies.

The model describes the form of a steadily progressing wave of gene increase due to the local establishment of a favourable mutation. The resulting equation formulated in this historical paper is known today as Fisher's equation. It has been suggested by Cohen in [1] that Fisher's equation is a model for a nerve axon which has been treated with certain toxins, so that there may indeed be a connection between the two different models, although as considered here they originate from completely different fields. Subsequent refinements and extensions to the Fisher model are due to Aronson and Weinberger [1]. Their work is not experimental but mathematical and more specifically concerned with an assessment of the assumptions contained in the model, followed by results on existence and stability of solutions to the model.

1.3. Purpose of the present study

The purpose of the present study is to conduct a numerical investigation into the governing equations of the models of the two physiological processes introduced in the previous paragraph.

Although these models have been the subject of various papers up to the present moment, they have not yet been fully investigated. In particular, very little work seems to have been done in applying numerical techniques to the analysis of these models.

In this study the intention is to bring together, in one work, the rationale underlying the construction of the models themselves, a review of the most significant analytical and numerical results available in the literature to date, and to combine this with a systematic numerical study of features of the models which, as yet, have not been carried out. In doing the latter, extensive use of the Finite Element method is made.

The task of a numerical study, such as presented here, is complementary to that of the pure analyst. Where analytical solutions to the models do exist, it is both interesting and useful to verify these numerically and where analytical results do not exist, solutions should be determined numerically and the qualitative behaviour of these solutions should be investigated which, in turn then, can be verified analytically. Furthermore, a comparison between different numerical methods should be useful.

To carry out the above in a meaningful manner it is therefore necessary to include in this study a description of the models, as well as a review of the most important available analytical and numerical results.

We start our study in Chapter 2 with a description of the two processes which are represented by the two models respectively. We discuss certain features of the processes; in the case of the model of population genetics the reader is introduced to the genetical background and in the case of the model of the nervous system the nature of the nerve along which conduction takes place and the changes in permeability of the nerve membrane during an action potential are described. For both models the construction is discussed explicitly, pointing to assumptions made, the role of experimental data and the principles which lead to the governing partial differential equations.

In Chapter 3 a general classification of the governing equations of the models is presented followed by a literature survey. This survey can be divided into two sections - firstly concerning pure analytical results such as existence, uniqueness and stability of certain types of solutions and secondly concerning numerical results obtained from digital computer solutions. Deficiencies in our existing knowledge of the analysis of these models will be pointed out.

In Chapter 4 a Finite Element scheme is constructed to solve Fisher's equation. Fisher's equation is studied numerically with the purpose of verifying and clarifying existing analytical results and possibly obtaining new information. Certain features of the model will be explained numerically to give more insight into the process.

In Chapter 5 the Hodgkin-Huxley system is studied numerically. A Finite Element scheme is constructed for each of the simplified models and also for the full Hodgkin-Huxley system.

Numerical solutions obtained for the models are then compared to existing results. Special attention is given to the boundary and initial conditions required to initiate non-zero solutions.

In Chapter 6 conclusions will be drawn from an overview of the present study.

CHAPTER 2

MATHEMATICAL MODELS OF REACTION-DIFFUSION

2.1. Introduction

This chapter consists of a description of two physiological processes, each followed by an explanation of the construction of the models which represent these processes respectively. The first of these concerns itself with population genetics and the second with impulse transmission in the nervous system.

2.2. Fisher's model

2.2.1. Introduction

In this section we study the construction of Fisher's model of population genetics. A brief outline of the most important features of Fisher's classical paper of 1937 [27] is presented in § 2.2.2. The genetical background is given, the assumptions for the model are motivated and the construction of the model is explained. We then discuss a refinement of the model due to Aronson and Weinberger [1] and conclude the paragraph with a physical interpretation of certain features of the model.

2.2.2. The original model

Consider a population of allelomorphs distributed in a linear habitat such as a shoreline which it occupies with uniform density. If at any point of the habitat a mutation occurs and the circumstances are favourable we may expect the mutant gene to increase at the expense of the allelomorphs previously occupying the same position and there will be, advancing from the origin, a wave of increase in the intensity of the mutant gene.

The mathematical model is then constructed as follows:

1. Let x be the co-ordinate measuring position in the linear habitat and let t stand for time, measured in generations.

2. If $p(x,t)$ is the relative density of the mutant gene and $q(x,t)$ the relative density of it's parent allelomorph, it follows that

$$p(x,t) + q(x,t) = 1$$

3. Suppose that the rate of increase of the density of the mutant gene is the sum of a source term and a diffusion term, the former due to the birth of mutant gene and the latter due to diffusion of population density.

4. Restricting the argument, first of all, to the increase due to diffusion we consider an element, δx, of the shoreline and determine the net influx into the element per unit time.

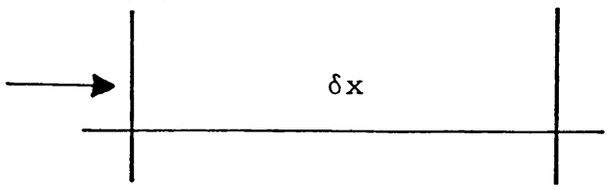

We assume the magnitude of the flux (mutants/time unit) across the boundary at any point x to be proportional to the concentration gradient. The exact relationship being

$$\phi(x) = - k \left.\frac{\partial p}{\partial x}\right|_x$$

where k is the so-called diffusion coefficient and is assumed to be constant for the particular species. Considering the flux at x and $x + \delta x$ gives the net rate of increase in the element due to diffusion as

$$\frac{\partial}{\partial t}(p\delta x) = -k\frac{\partial p}{\partial x}\Big|_x - \left(-k\frac{\partial p}{\partial x}\Big|_{x+\delta x}\right)$$

$$= -k\frac{\partial p}{\partial x}\Big|_x + k\frac{\partial p}{\partial x}\Big|_x + k\frac{\partial^2 p}{\partial x^2}\Big|_x \delta x + 0(\delta x^2)$$

Therefore in the limit as $\delta x \to 0$ we have

$$\frac{\partial p}{\partial t}\ (\text{due to diffusion}) = k\frac{\partial^2 p}{\partial x^2} \qquad \ldots\ldots \quad (D)$$

5. Suppose now that the source term is a quantity proportional to the densities p and q. This term is then given by the product rpq where r is the intensity of selection in favour of the mutant gene, supposed independent of p, i.e.

$$\frac{\partial p}{\partial t}\ (\text{due to source}) = rpq = rp(1-p) \qquad \ldots\ldots \quad (S)$$

6. The sum of the diffusion term (D) and the source term (S) yields the governing equation of the system

$$\frac{\partial p}{\partial t} = k\frac{\partial^2 p}{\partial x^2} + rp(1-p) \qquad \ldots\ldots \quad (2.1$$

7. Possible complications such as unequal increase in population in opposite directions, position dependence of the diffusion-coefficient k, variations in the density of the population and changes in the ability of the mutant gene to survive at a given place were ignored in the construction of equation (2.1) which therefore represents one of the simplest possible models

8. As an example of how to treat such complications, consider unequal increase in population in opposite directions. Suppose that for a population distributed along the shoreline at time t, in addition to the normal changes due to the diffusion and reaction, the distribution is moving to the right with constant velocity m due to some external force.

The implication is that for an x-co-ordinate moving to the right with velocity m the changes in the distribution would occur as without the drift to the right.

Let $X = x - mt$

$T = t$

then $\frac{\partial p}{\partial t} = \frac{\partial p}{\partial X} \cdot \frac{\partial X}{\partial t} + \frac{\partial p}{\partial T} \cdot \frac{\partial T}{\partial t}$

$= - m \frac{\partial p}{\partial X} + \frac{\partial p}{\partial T}$

and $\frac{\partial^2 p}{\partial x^2} = \frac{\partial^2 p}{\partial X^2}$

Therefore $\frac{\partial p}{\partial T} = \frac{\partial^2 p}{\partial X^2} - m \frac{\partial p}{\partial X} + p(1-p)$

The unequal drift therefore involves a first space derivative, which we call the drift term.

2.2.3. Refinements to the model

A more recent discussion of the same problem and a classification of the various forms in which Fisher's equation may occur are given by Aronson and Weinberger [1]. They reformulate Fisher's problem as follows: Consider a population of deploid (two kinds of) individuals. Suppose that the gene at a specific locus in a particular chromosome pair occurs in two forms, called alleles, which we denote by a and A. The population is then divided into three classes or genotypes. Two of these consist of individuals called homozygotes which carry only one kind of allele. The members of these classes are denoted by aa or AA, depending on the alleles they carry. The third class consists of individuals, called heterozygotes, which carry only one of each allele. These individuals are denoted by aA.

The following assumptions are made:

1. Let the population be distributed in a one-dimensional habitat. (For a treatment of the population genetics in a multi-dimensional environment the reader is referred to [2]). The linear densities of the genotypes aa, aA and AA at the point x of the habitat at time t are denoted by $\rho_1(x,t)$, $\rho_2(x,t)$ and $\rho_3(x,t)$, respectively. Let

$$\rho(x,t) = \rho_1(x,t) + \rho_2(x,t) + \rho_3(x,t).$$

The situation is presented schematically as follows:

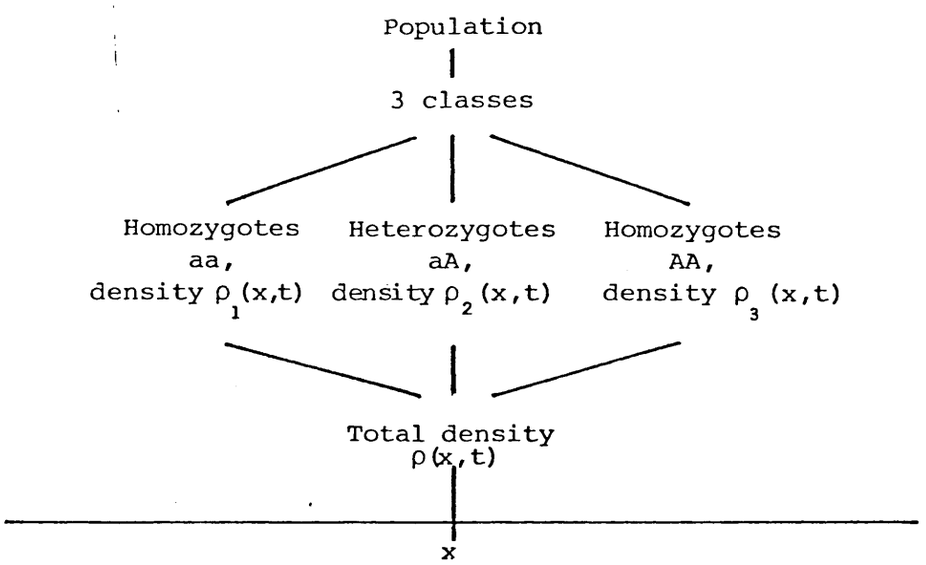

2. Assume now that the population mates at random, thereby producing offspring with an overall birth-rate (births per unit density per unit time) denoted by r, and that the population diffuses through the habitat with diffusion constant 1.

3. A further assumption is that the death-rates depend only on the genotype with respect to the alleles a and A. Denote the death-rates of genotypes aa, aA and AA by τ_1, τ_2 and τ_3 (deaths per unit density per unit time), respectively.

In general, these death-rates differ slightly, so that some genotypes are more viable than others. Reproduction by cell division can be incorporated into this model by adding negative quantities to the death-rates. Therefore no assumption about the sign of τ_i is made.

4. At a given point x and time t:

Rate of increase of ρ_i = entry rate + birth-rate - death-rate

(due to diffusion)

Entry rate of ρ_i: $\frac{\partial^2 \rho_i}{\partial x^2}$ (as before in (D) of §2.2.2; here $k = 1$).

Death rate of ρ_i: $\tau_i \rho_i$.

Total rate of births:

$$r\rho = \frac{r}{\rho}[\rho^2]$$

$$= \frac{r}{\rho}\left[\rho_1 + \frac{\rho_2}{2} + \frac{\rho_2}{2} + \rho_3\right]^2$$

$$= \underbrace{\frac{r}{\rho}\left[\rho_1 + \frac{\rho_2}{2}\right]^2}_{\text{rate of aa births}} + \underbrace{\frac{2r}{\rho}\left[\rho_1 + \frac{\rho_2}{2}\right]\left[\rho_3 + \frac{\rho_2}{2}\right]}_{\text{rate of aA births}} + \underbrace{\frac{r}{\rho}\left[\rho_1 + \frac{\rho_2}{2}\right]^2}_{\text{rate of AA births}}$$

(See Appendix A for an explanation of the genetics involved).

Under the assumptions stated above the population densities satisfy the system of partial differential equations:

$$\begin{aligned}
\frac{\partial \rho_1}{\partial t} &= \frac{\partial^2 \rho_1}{\partial x^2} - \tau_1 \rho_1 + \frac{r}{\rho}\left(\rho_1 + \tfrac{1}{2}\rho_2\right)^2 \\
\frac{\partial \rho_2}{\partial t} &= \frac{\partial^2 \rho_2}{\partial x^2} - \tau_2 \rho_2 + \frac{2r}{\rho}\left(\rho_1 + \tfrac{1}{2}\rho_2\right)\left(\rho_3 + \tfrac{1}{2}\rho_2\right) \qquad \ldots\ldots (2.2) \\
\frac{\partial \rho_3}{\partial t} &= \frac{\partial^2 \rho_3}{\partial x^2} - \tau_3 \rho_3 + \frac{r}{\rho}\left(\rho_3 + \tfrac{1}{2}\rho_2\right)^2
\end{aligned}$$

Aronson and Weinberger [1] consider the case where the derivatives of the initial data are small, r very large and the quantity

$$\varepsilon = |\tau_1 - \tau_2| + |\tau_3 - \tau_2| \quad \text{very small.}$$

They show that under these conditions and for times which are small relative to ε^{-1} equations (2.2) may be approximated by the single equation

$$\frac{\partial u}{\partial t} = \frac{\partial^2 u}{\partial x^2} + f(u) \qquad \ldots\ldots \quad (2.3)$$

with

$$f(u) = u(1-u)\{(\tau_1 - \tau_2)(1-u) - (\tau_3 - \tau_2)u\} \qquad \ldots\ldots \quad (2.4)$$

and where u is the so-called relative density defined by

$$u(x,t) = \frac{\rho_3 + \frac{1}{2}\rho_2}{\rho_1 + \rho_2 + \rho_3} \qquad \ldots\ldots \quad (2.5)$$

Equation (2.3) is generally referred to as Fisher's equation.

It is clear that the genetic composition of an isolated population will not change with time if the population consists entirely of individuals of either genotype AA or genotype aa: The first case implies that $\rho_1 \equiv \rho_2 \equiv 0$ which in turn implies that $u \equiv 1$. It follows that $f(u) = 0$. In the second case $\rho_2 \equiv \rho_3 \equiv 0$ which implies that $u \equiv 0$. It follows again that $f(u) = 0$. In both cases $\frac{\partial^2 u}{\partial x^2} = 0$ and therefore $\frac{\partial u}{\partial t} = 0$ from which it follows that the composition does not change.

Regardless of the values of τ_i the function f(u) has the properties:

$$f \in C^1[0,1], \quad f(0) = f(1) = 0.$$

Without loss of generality we can assume that $\tau_1 \geqslant \tau_3$ since we

can always interchange the labels a and A and hence the values of τ_1 and τ_3.

There are then three cases:

Case 1 $(\tau_3 \leq \tau_2 \leq \tau_1)$.

This is called the heterozygote intermediate case. The relevant properties of the function f in (2.3) are

$$f'(0) > 0, \quad f(u) > 0 \text{ in } (0,1) \qquad \ldots\ldots \quad (2.6)$$

[See figure 2.1(i)]

This is the case which had been considered by Fisher [27] and Kolmogoroff et al [50].

Case 2 $(\tau_2 < \tau_3 \leq \tau_1)$.

This is called the heterozygote superior case. The relevant properties of the function f in (2.3) are

$$f'(0) > 0, \quad f'(1) > 0, \quad f(u) > 0 \text{ in } (0,\alpha), \quad f(u) < 0 \text{ in } (\alpha,1) \text{ for some } \alpha \in (0,1) \qquad \ldots\ldots \quad (2.7)$$

[See figure 2.1(ii)].

Case 3 $(\tau_3 \leq \tau_1 < \tau_2)$.

This is called the heterozygote inferior case. The relevant properties of the function f in (2.3) are

$$f'(0) < 0, \quad f'(1) < 0, \quad f(u) < 0 \text{ in } (0,\alpha), \quad f(u) > 0 \text{ in } (\alpha,1) \text{ for some } \alpha \in (0,1) \qquad \ldots\ldots \quad (2.8)$$

and $\int_0^1 f(u)du > 0$.

[See figure 2.1(iii)].

Typical example functions to represent cases 1,2 and 3 are shown in Figure 2.1 below.

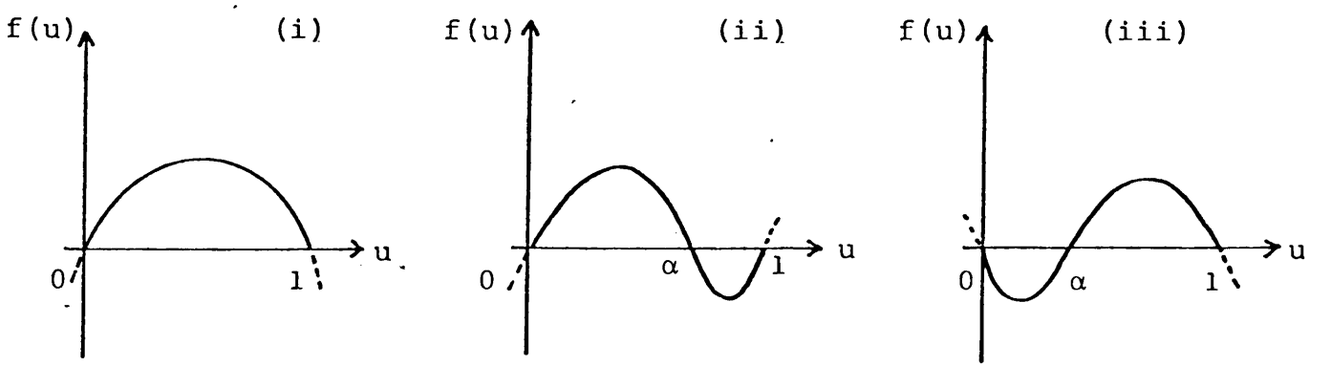

$f(u) = u(1-u)$ $\quad (\tau_2 = \frac{\tau_1 + \tau_3}{2})$

$f(u) = u(1-u)(a-u), a \in (0,1)$ $\quad (\tau_2 = \frac{-1 + \tau_1 + \tau_3}{2})$

$f(u) = u(1-u)(u-a), a \in (0, \frac{1}{2})$ $\quad (\tau_2 = \frac{1 + \tau_1 + \tau_3}{2})$

Figure 2.1

Questions immediately arising are: How does a given initial distribution of the allele AA evolve in time? Is the allele AA ultimately wiped out or does it persist and if so do both alleles coexist in an equilibrium distribution?
In mathematical terms the problem is to determine the nature of the stability of the equilibrium states $u \equiv 0$, $u \equiv 1$ and any others which may occur. This will be discussed in Chapter 3.

2.3.4. Interpretation of features of the model.

In this paragraph we give a brief explanation of some of the features of the model and try to give preliminary answers to some of the questions in the preceding paragraph.

The relative density was defined by Aronson and Weinberger [1] in equation (2.5):

$$u(x,t) = \frac{\rho_3 + \frac{1}{2}\rho_2}{\rho_1 + \rho_2 + \rho_3}$$

where $\rho_1(x,t)$, $\rho_2(x,t)$ and $\rho_3(x,t)$ are the linear densities of the genotypes aa, aA and AA, respectively. From equation (2.4) and the facts that

$\rho_1(x,t) + \rho_2(x,t) + \rho_3(x,t) = \rho(x,t)$,

$\rho_1(x,t) > 0$, $\rho_2(x,t) > 0$ and $\rho_3(x,t) > 0$ we observe that

$u(x,t) = 0 \Rightarrow \rho_2 = \rho_3 = 0$ and so the population consists only of the first genotype (aa).

$u(x,t) = 1 \Rightarrow \rho_1 = \rho_2 = 0$ and so the population consists only of the third genotype (AA).

$u(x,t) = \frac{1}{2} \Rightarrow$ The density of the second genotype (aA) attains a maximum and $\rho_1 = \rho_3$.

Graphically we represent this as follows:

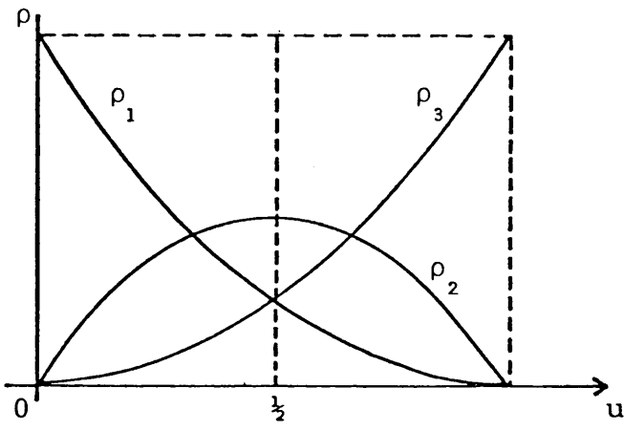

Figure 2.2.
Graphical representation of the relation between the densities ρ_1, ρ_2 and ρ_3.

The maximum height of ρ_2 can vary between 0 and ρ.

We next look at the function f defined in (2.4) as

$$f(u) = u(1-u)\{(\tau_1 - \tau_2)(1-u) - (\tau_3 - \tau_2)u\}$$

where τ_1, τ_2 and τ_3 represent the death-rates of aa, aA and AA respectively.

For the particular examples of f pictured in Figure 2.1:

(i) $f(u) = u(1-u)$:

It follows that $\tau_1 = \tau_2 + 1$

$\tau_3 = \tau_2 - 1$

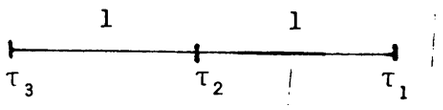

(ii) $f(u) = u(1-u)(a-u)$:

It follows that $\tau_2 = \tau_3 - 1 + a$

$\tau_1 = \tau_3 + 2a - 1$

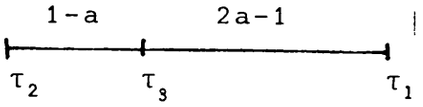

This satisfies $\tau_2 < \tau_3 \leqslant \tau_1$ <u>only</u> if $a \geqslant \frac{1}{2}$

which implies $\int_0^1 f(u)du > 0$.

(iii) $f(u) = u(1-u)(u-a)$:

It follows that $\tau_3 = \tau_1 + 2a - 1$

$\tau_2 = \tau_1 + a$

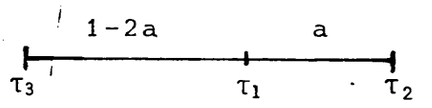

This satisfies $\tau_3 \leqslant \tau_1 < \tau_2$ <u>only</u> if $a \leqslant \frac{1}{2}$

which implies $\int_0^1 f(u)du > 0$.

The death-rates denote deaths/(unit density * unit time) and therefore vary between -1 and 1. The following can then be noted:

<u>Case 1</u>. In this case $\tau_3 \leqslant \tau_2 \leqslant \tau_1 \leqslant 1$. The situation $\tau_3 = \tau_2 - 1$ and $\tau_1 = \tau_2 + 1$ has only one possible interpretation, namely that

$$\tau_1 = 1, \quad \tau_2 = 0, \quad \tau_3 = -1$$

which implies that the death-rate τ_3 is actually a 100% birth-rate, whereas τ_1 represents a 100% death-rate. This would mean that any initial non-zero distribution of population, no matter how small, will grow to $u \equiv 1$. This implies that the whole of the population will eventually consist of AA individuals.

Case 3. First of all we note the dependence of the death-rates on the parameter a. A small value of a will mean that the death-rate τ_3 is significantly smaller than the death-rates τ_1 and τ_2, causing the rate at which the homozygotes AA increases to be high. This will probably imply that the speed at which the increase is propagated will be higher when a is small. The death-rates are dependent on a so that the speed at which the increase is propagated is actually dependent on a.

Consider an initial distribution of a population:

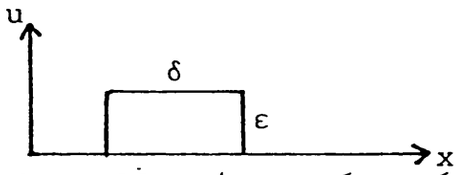

If ε and δ are both small and $\tau_3 \leqslant \tau_1 < \tau_2$ this may be interpreted as:

A small number of AA are present but few of them die per unit time whereas a larger number of aa are present although more die per unit time. This causes a situation in which the outcome cannot easily be predicted. If ε and δ are both small enough the homozygotes aa would probably take over and the AA would be wiped out. Larger values of ε and δ can be interpreted as follows: A larger number of AA are present and the death-rate is low, whereas few aa are present and their death-rate is high. It stands to reason that the AA wil increase at the expense of the aa.

An interesting case arises when $a = \frac{1}{2}$. This implies that $\tau_1 = \tau_3$. The death-rates are equal, so that neither the aa nor the AA has any advantage concerning rate of increase. Furthermore $\int_0^1 f(u)\,du = 0$ so that the source term provides no scope either for increase or decrease. The initial distribution is expected to remain stationary.

Case 2. The death-rate of aA is lower than that of AA or aa. The death-rate of the aa is the highest and that of AA is in between. As soon as the aa decreases because of the high death-rate it is compensated by the low death-rate of aA and subsequent increases of aa, aA and AA. It follows that neither the aa, nor AA will be wiped out for any non-zero initial distribution. It is likely that an equilibrium state will be reached eventually, with the value of u depending on a.

2.3. The Hodgkin-Huxley model

2.3.1. Introduction

When constructing a mathematical model of a physiological process such as impulse transmission in the nervous system the physiological nature of the nerve axon, as well as the physical aspects (such as electrical changes), are of prime importance. Both these aspects are discussed in the next paragraph. We then explain the construction of the Hodgkin-Huxley model, pointing to the required assumptions.

2.3.2. The nerve axon

2.3.2.1. Physical nature of the nerve axon ([44, 45, 85])

All nervous messages have certain features in common and results obtained from animals can be applied in a fairly general manner because of the universality of the physical nature of the nervous system.

A nerve fibre (axon)(See Figures 2.3a, 2.3b) is regarded as a long cylinder with a conducting core and a surface membrane of relatively high resistance. The core consists of semifluid

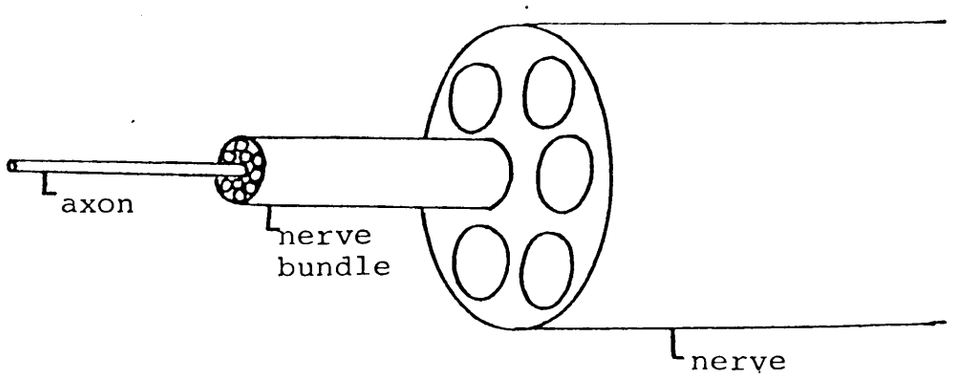

Figure 2.3a: Representation of a nerve in the human being.

conducting axoplasm and the nerve axon is surrounded by salt solution. The diameter of an axon is usually between 0,1 μ and 20 μ (one fiftieth of a millimeter), the length varies between a fraction of a millimeter to several meters in a large mammal. At the surface of the axon the membrane acts as a barrier and prevents ions in the external solution from mixing rapidly with the internal solution.

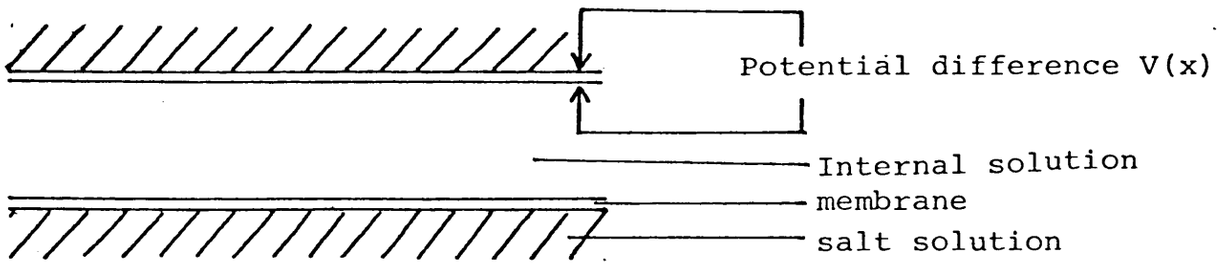

Figure 2.3b: Representation of a nerve axon.

In the resting state potassium ions are more concentrated inside the membrane and sodium ions are more concentrated outside the membrane. The membrane is assumed to be more permeable to potassium than to sodium in the resting state so that a potential difference is set up with the inside of the membrane negative and the outside positive. The constant potential difference, maintained in the absence of stimulation, is called the resting

potential.

2.3.2.2. Impulse propagation ([44, 85])

When the membrane of an axon in the resting state is stimulated electrically, chemically, thermically or mechanically the sodium permeability increases and subsequent changes in the membrane potential are brought about. Sodium ions flow to the inside of the membrane and the potential difference is changed to being positive inside and negative outside. These changes are called depolarization.

The rise in sodium permeability is short-lived, however, and the potassium permeability soon increases. Potassium ions flow to the outside of the membrane and the original potential difference across the membrane is restored. This process is called repolarization. The process of depolarization and the subsequent repolarization are together referred to as an action potential.

By a "membrane" action potential is meant one in which the membrane potential is uniform, at each one instant, over the whole length of the fibre. This is also referred to as the space-clamped case.

When a stimulus is given at a certain point on the membrane, an action potential can originate at the point of stimulation. This local action potential activates adjacent parts of the membrane, so that the depolarization (and subsequent repolarization) spreads along the whole of the fibre. This is called the conduction of an impulse (or a propagated action potential)

and can be explained as follows:

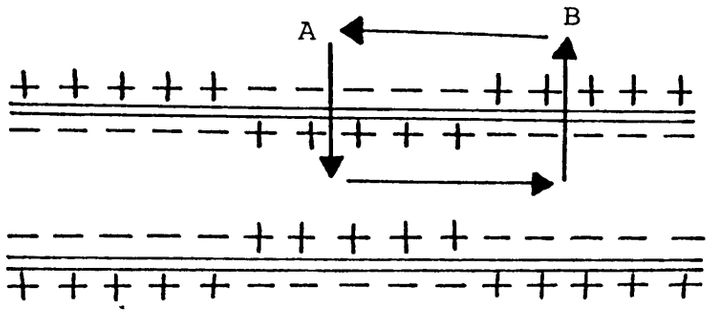

Figure 2.4: Propagation of an impulse (Redrawn after [44])

Suppose point A is "active" and point B is "resting". At A the membrane is depolarized. The change in potential difference acts as stimulus for the adjacent part and the sodium permeability increases just ahead of the active region. In this way a wave of internal positivity and of increased sodium permeability spreads along the nerve. Electrical current flows in a local circuit between the resting region and the active region of the nerve.

One notices that after an action potential the sodium concentration inside the membrane is higher than before and the potassium concentration is higher outside than before. In the minutes or hours following the action potential the sodium and potassium interchange slowly to restore the original potential difference. A large number of impulses conducted in a short period of time would bring about fatigue.

2.3.3. Experimental evidence ([29, 44, 45, 85])

Some of the experimental facts concerning the transmission of impulses along the nerve axon is now described:

The experimental work of A.L. Hodgkin and A.F. Huxley is de-

scribed by Hodgkin [44]. The experiments were conducted on a nerve fibre using the microelectrode technique which means that the electrical potential across the surface of the fibre is measured directly by means of an internal electrode. The internal electrode is pushed into one end of the fibre for a distance of 10 - 30 mm. (The presence of an internal electrode does not have any obvious effect on the activity of the nerve).

These experiments were conducted on an isolated axon in which the action potential differs slightly from that in the intact animal, the essential features of the conduction mechanism are, however, the same in both cases.

If the stimulus is applied in the form of a brief current pulse at the one end of the axon through a stimulating electrode touching the membrane, the potential changes according to the amplitude of the stimulus.

A weak and short stimulus will cause a slight deviation in the axon potential which will die away in time and distance.

If the stimulus is increased in both strength and duration a critical level called the threshold is reached eventually. Such a threshold causes the potential to increase abruptly in amplitude to reach a maximum after which it decreases slowly to a minimum and increases even slower again to the resting state (See figure 2.5).

An impulse is formed which is propagated at a constant velocity and amplitude along the axon. The potential can be recorded at any point along the fibre as the impulse passes but there is no way to deduce from the recording alone where it originated or what the strength of the stimulus was that produced it.

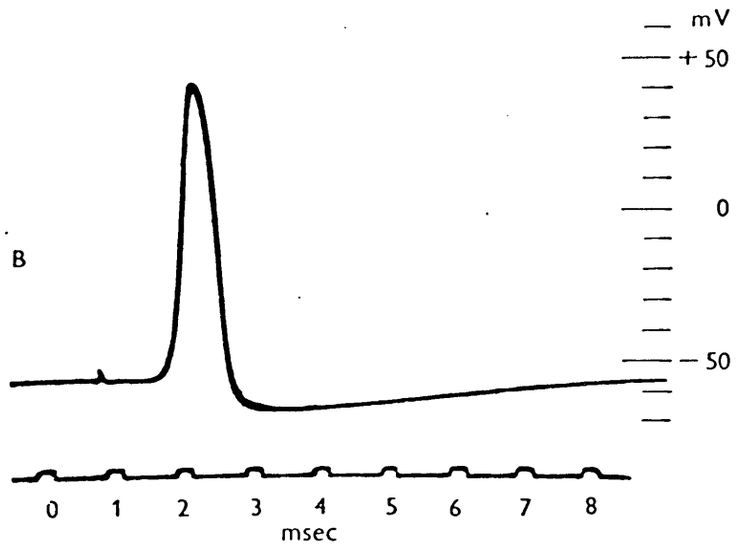

Figure 2.5: Form of an action potential at a stimulated point x (Reprinted from [44])

The characteristics of an impulse can therefore not be altered by changing the strength or quality of the stimulus (provided it is above threshold). A second stimulus can be applied at the same end after the first one with the hope that a second impulse will appear, giving rise to a train of impulses if the process is repeated continuously. It has been determined experimentally that this will only happen provided that a certain time-interval, called the absolute refractory period has elapsed after the application of the first stimulus. If a second stimulus, no matter how strong, is applied during this interval no second impulse will be produced. This initial period is followed by a period called the relative refractory period during which a second impulse can be produced requiring, however, a much higher threshold than the first impulse. This new threshold decreases gradually with time until it reaches it's original value.

The application of a very long stimulus may produce more than one impulse, therefore giving rise to a train of impulses.

The threshold to stimulation observed in experiments is embodied in the so-called all-or-none-law of physiology [85] which states that an impulse occurs either full size or not at all with no intermediate response possible.

If a nerve has not been excited by a comparitively long application of a constant current a yet longer application will not produce an impulse. This implies that a minimum current strength is needed to fire an impulse. The so-called rheobase is a value such that a current of which the strength exceeds it, will fire an impulse. Furthermore, a current exceeding the rheobase need only be applied for a finite duration of time to fire an impulse. This phenomenon gives rise to the so-called threshold strength and duration relation.

Although nerves normally conduct impulses in one direction, all nerves can conduct impulses in both directions and the velocity at which the impulse propagates is independent of the direction in which it is travelling.

2.3.4. The Mathematical Model

A. L. Hodgkin and A. F. Huxley [45] attempted to simulate the physical behaviour of the giant axon of a squid (Loligo) by means of an appropriate mathematical model. Their first attempt was to consider only the space-clamped axon for which the potential difference is constant all along it's length.

In the construction of the model the following assumptions, partly based on their own experimental results, were made:

1. The electrical behaviour of the nerve axon may be represented by the network in Figure 2.6.

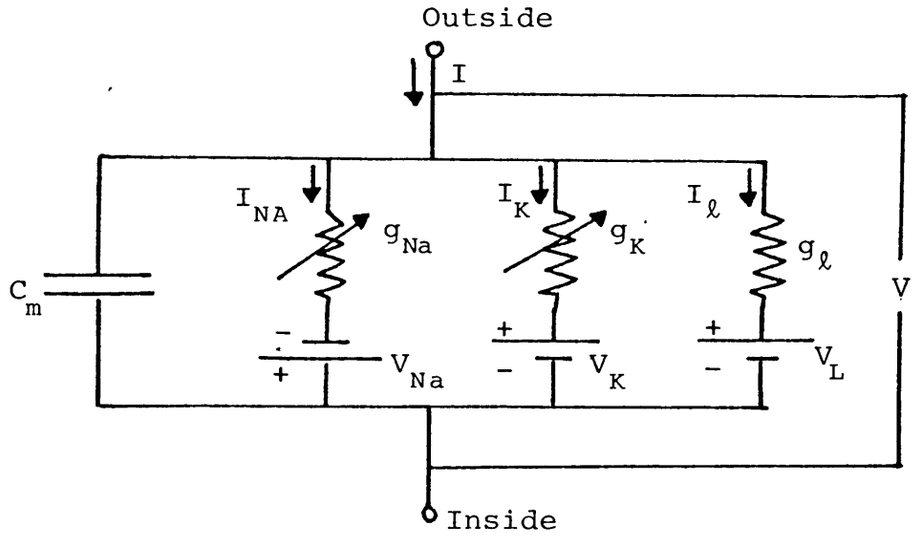

Figure 2.6: Electrical circuit representing the membrane showing the three ionic pathways for sodium, potassium and leakage ions. After Hodgkin and Huxley [45].

2. Current can be carried through the membrane either by charging the membrane capacitor or by movement of ions through the resistances in parallel with the capacitor.

3. The total membrane current is divided into the capacity current and an ionic current. Thus the simplest equation which can be used is

$$I = C_m \frac{\partial V}{\partial t} + I_i \qquad \ldots\ldots (2.9)$$

where

I is the total membrane current density;

I_i is the ionic current density;

V is the displacement of the membrane potential from it's resting value;

C_m is the membrane capacity per unit area (assumed constant $1\ \mu F/cm^2$);

t is time.

4. The ionic current I_i in (2.9) is divided into three independent components carried by sodium and potassium ions (I_{Na} and I_K) and a small "leakage" current I_ℓ made up by chloride and other ions.

Thus $I_i = I_{Na} + I_K + I_\ell$ ..... (2.10)

Each component of the ionic current is determined by a driving force which may be measured as the product of a permeability coefficient (which has the dimensions of a conductance) and an electrical potential difference:

$$I_{Na} = g_{Na} (E - E_{Na})$$
$$I_K = g_K (E - E_K)$$
$$I_\ell = \bar{g}_\ell (E - E_\ell)$$

where E_{Na} and E_K are the equilibrium potentials for the sodium and potassium ions and E_ℓ is the potential at which the "leakage current" due to chloride and other ions is zero. (Equilibrium potential can be defined as the membrane potential at which there will be no netto flow of the involved ions across the membrane). E is the true potential difference.

For practical purposes it is convenient to write these equations in the form:

$$I_{Na} = g_{Na} (V - V_{Na})$$
$$I_K = g_K (V - V_K) \quad ..... \quad (2.11)$$
$$I_\ell = \bar{g}_\ell (V - V_\ell)$$

where

$$V = E - E_r$$

$$V_{Na} = E_{Na} - E_r$$

$$V_K = E_K - E_r$$

$$V_\ell = E_\ell - E_r$$

and E_r is the absolute value of the resting potential. V, V_{Na}, V_K and V_ℓ can then be measured directly as displacements from the resting potential.

5. An important assumption based on experimental observation is that the changes in permeability depend on membrane potential rather than on membrane current. One of the most striking properties of the membrane is the extreme steepness of the relation between ionic conductances and membrane potential.

Hodgkin and Huxley [45] pursued two main lines of thought on the changes of sodium and potassium permeability of the membrane. The hypothesis they finally decided upon was acceptable both from the point of the simplicity of application as well as experimental justification. This hypothesis is based on the assumption that sodium movement depends on the distribution of charged particles which do not act as carriers but which allow sodium to pass through the membrane when they occupy particular sites in the membrane. The rate of movement of the activating particles therefore determines the rate at which the sodium conductance approaches it's maximum but has little effect on the magnitude of the conductance. The decline of sodium conductance is attributed to the relatively slow movement of another kind of particle

(inactivating) which blocks the flow of sodium ions when it reaches a certain position in the membrane. An alternative here is to assume that the decline in sodium conductance is due to a change in the same particles which cause the rise in sodium conductance. The choice here is actually between two variables each of which satisfies a first order differential equation or one variable satisfying a second-order differential equation. The former was decided upon.

To model the changes in potassium permeability the assumption is that a completely separate system determines the potassium permeability and it differs from the sodium system in the following aspects: The activating molecules have an affinity for potassium but not for sodium, they move slower and they are not blocked or inactivated.

6. (i) In the case of <u>potassium conductance</u> the simplified assumption that g_K is proportional to the fourth power of a variable which obeys a certain prescribed first-order equation is justifiable both from the point of accuracy and of calculation ease. The potassium conductance is then described by

$$g_K = \bar{g}_K \, n^4 \qquad \ldots\ldots \quad (2.12)$$

with $n(V,t)$ satisfying

$$\frac{dn}{dt} = \alpha_n(1-n) - \beta_n n \qquad \ldots\ldots \quad (2.13)$$

where

$\bar{g}_K$ is a constant, α_n and β_n are rate constants varying with voltage but not with time and have dimensions of $[\text{time}]^{-1}$, n is a dimensionless variable which may vary

between zero and one.

The physical interpretation of (2.12) and (2.13) would be to assume that potassium can only cross the membrane when four similar particles occupy a certain region of the membrane. The proportion of the particles in a certain position (for example inside the membrane) is represented by n. The proportion that are somewhere else are represented by $1 - n$. α_n determines the rate of transfer from outside to inside, while β_n determines the rate of transfer in opposite direction. If the particle has a negative charge, α_n should increase and β_n should decrease when the membrane is depolarized.

The continuous curves α_n and β_n which fit experimental data best are given in Appendix B.

(ii) In the case of the sodium conductance the assumption is that g_{Na} is determined by two variables. The two variables m and h are referred to as sodium activation and sodium inactivation respectively.

The equations are

$$g_{Na} = m^3 h \bar{g}_{Na} \qquad \ldots\ldots \quad (2.14)$$

$$\frac{dm}{dt} = \alpha_m(1-m) - \beta_m m \qquad \ldots\ldots \quad (2.15)$$

$$\frac{dh}{dt} = \alpha_h(1-h) - \beta_h h \qquad \ldots\ldots \quad (2.16)$$

where $\bar{g}_{Na}$ is a constant and α_m, β_m, α_h and β_h are functions of V but not of t, variables m, n and h are functions of both V and t.

These equations are given physical interpretation if sodium

conductance is assumed to be proportional to the number of sites on the inside of the membrane which are occupied simultaneously by three activating molecules but are not blocked by an inactivating molecule. m then represents the proportion of activating molecules on the inside and 1 - m the proportion on the outside of the membrane; similarly h represents the proportion of inactivating molecules on the outside and 1 - h the proportion on the inside of the membrane. α_m and β_h, β_m and α_h represent the transfer rate functions in two directions, respectively.

The expressions for the rate functions obtained from experimental data are given in Appendix B.

(iii) In the case of <u>leakage conductance</u> the change of $\bar{g}_\ell$ is negligible small so that $\bar{g}_\ell$ is assumed to be constant.

Substituting equations (2.12) and (2.14) in (2.11) and using the latter in (2.10) yields the total ionic current. It follows from (2.9) and (2.10) that the total current I is given by

$$I = C_m \frac{dV}{dt} + \bar{g}_K n^4(V - V_K) + \bar{g}_{Na} m^3 h(V - V_{Na}) + \bar{g}_\ell(V - V_\ell) \quad \ldots\ldots \quad (2.17)$$

Equation (2.17) is known as the '<u>space-clamped</u>' <u>Hodgkin-Huxley equation</u>.

The respective constants are given in Appendix B, n,m and h satisfying the differential equations (2.13, 2.15, 2.16).

7. If in the space-clamped case the stimulus is a short shock at $t = 0$, the form of the action potential should be obtained from solving (2.17) with $I = 0$ and the initial conditions $V = V_o \neq V_R$ and m, n and h taken at their resting state values

when $t = 0$.

In the case of the propagated action potential the situation is far more complicated:

Consider a cylindrical element of the axon of radius a and length δx as shown in Figure 2.7.

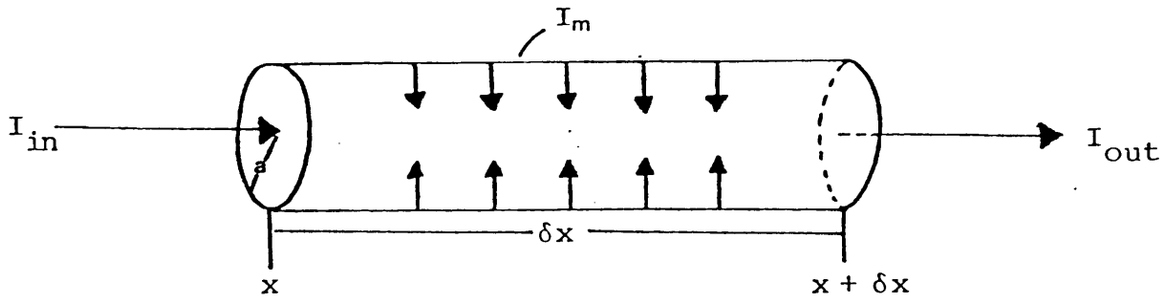

Figure 2.7.

We require that the net inflow of charge/sec be equal to the net outflow, i.e.

$I_m \times$ membrane surface area + $I_{in} \times$ cross-sectional area of axon = $I_{out} \times$ cross-sectional area of axon

where I_m is the membrane current

$$\Rightarrow I_m 2\pi a\delta x = \frac{1}{R}\frac{\partial V}{\partial x}(x+\delta x)\pi a^2 - \frac{1}{R}\frac{\partial V}{\partial x}(x)\pi a^2$$

$$= \{\frac{1}{R}\frac{\partial V}{\partial x} + \frac{1}{R}\frac{\partial^2 V}{\partial x^2}\cdot\delta x + 0(\delta x^2)\}\pi a^2 - \frac{1}{R}\frac{\partial V}{\partial x}(x)\pi a^2$$

Thus in the limit as $\delta x \to 0$ we have

$$I_m = \frac{a}{2R}\frac{\partial^2 V}{\partial x^2} \qquad \ldots\ldots (2.18)$$

where R is the internal resistance per unit length (the external resistance being negligible when the axon is surrounded by a large volume of conducting fluid).

Inserting equation (2.18) into (2.17) we have

$$\frac{a}{2R}\frac{\partial^2 V}{\partial x^2} = C_m \frac{\partial V}{\partial t} + \bar{g}_K n^4 (V - V_K) + \bar{g}_{Na} m^3 h (V - V_{Na}) + \bar{g}_\ell (V - V_\ell) \quad \ldots\ldots (2.19)$$

In the case of a propagated action potential the variables V, m, n and h are functions of time as well as of distance x along the axon (and of the potential V in the case of m, n and h).

8. Temperature: All constants are independent of temperature. The only effect of temperature is to change the rates of m, h and n. This has the effect that the right-hand sides of equations (2.13, 2.15, 2.16) are multiplied by the factor $\phi = 3^{(T-6.3)/10}$ which is strictly positive for any temperature other than $T = 6{,}3\ ^\circ C$.

9. Sign convention:
Hodgkin and Huxley measured depolarization of the membrane from the resting value as negative. Recent physiological practice is to change the sign of V and I by taking a depolarization of the membrane to be positive. In this new convention a cathodal current stimulating pulse I is positive and an anodal one negative. We follow the original formulation but will depict the potential difference on a -V-axis.

10. We mention a few of the subsequent developments concerning the Hodgkin-Huxley model. Refinements to the original model have been investigated in [48,46], and extensions of the nerve membrane modelling, such as for coupled nerve fibres is treated in [15]. A comparison of Hodgkin and Huxley's model to other models of the electrical behaviour of the nerve membrane is presented in [7, 12]. Applications of the Hodgkin-Huxley equations to excitable tissues including the cardiac muscle is presented in [66]. The reader is referred to these very interesting papers.

2.3.5. The BVP simplification

The BVP model was constructed in 1961 by R. FitzHugh [28] as an over-simplification of the Hodgkin-Huxley model of an excitable membrane.

The motivation behind this model lies in the fact that it could be useful to have a model which is mathematically simpler to handle than the Hodgkin-Huxley model (from the theoretical point of view) while still retaining the more important and characteristic features of the electrical behaviour of the membrane.

FitzHugh considers such a "pilot model" as being useful in explaining general properties and for preliminary analysis.

We now present the arguments carried through in the construction of FitzHugh's model:

In 1926 B van der Pol [86] proposed a differential equation to describe non-linear "relaxation oscillators". He made use of the linear differential equation describing an oscillating quantity with damping constant k:

$$\ddot{x} + k\dot{x} + x = 0, \qquad \dot{} = \frac{d}{dt} \qquad \ldots\ldots (2.20)$$

The construction of equation (2.20) is illustrated by the following example:

Consider a steel spring attached to a support and hanging downward with a mass, m, suspended from it as seen in Figure 2.8. By x we denote the displacement of the mass from it's equilibrium position.

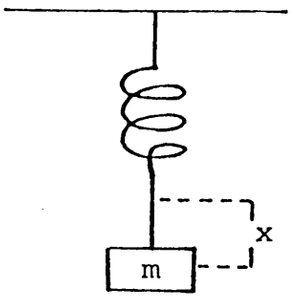

FIGURE 2.8: Mass m suspended downward.

According to Newton's law

$$m\ddot{x} = F \qquad \ldots\ldots \quad (2.21)$$

where F is the sum of the forces acting on the mass.

Now let $F = F_1 + F_2 + F_3$

where F_1 = restoring force of the spring which by Hooke's law is assumed to be directly proportional to the magnitude of the displacement x but in the opposite direction, i.e., $F_1 = -cx$, $(c > 0)$;

F_2 = damping force, assumed to be directly proportional to the magnitude of the velocity x but in the opposite direction, i.e., $F_2 = -k\dot{x}$, $(k > 0)$;

F_3 = external forces, assumed to be zero during free oscillations.

If we choose $m = 1$ and $c = 1$ equation (2.21) reduces to

$$\ddot{x} = -x - k\dot{x}$$

or $$\ddot{x} + x + k\dot{x} = 0 \qquad \ldots\ldots \quad (2.22)$$

For the actual case of a spring-mass system moving through a fluid, the damping constant k is, of course, positive and the mass will oscillate with decreasing amplitude. If, however, we allow for a damping constant k which is negative, the amplitude of the oscillations will increase to infinity which implies

that for actual physical systems for which a negative k is possible, the linear differential equation (2.22) will only be valid for values of x within a certain finite range. To express the limitation of the amplitude we must assume that the damping coefficient is a function of the amplitude itself, becoming positive at higher values.

Van der Pol [86] replaced the damping constant k by a damping coefficient which depend quadratically on x, i.e.,

$$k = k(x^2) = c(x^2 - 1),\ c > 0 \text{ constant.} \qquad \ldots\ldots (2.23)$$

This varying damping coefficient provides for negative damping (increasing amplitude) for small oscillations and positive damping (decreasing amplitude) for larger ones. The amplitude of the oscillations therefore tends towards a fixed intermediate value. Substituting (2.23) into equation (2.22) yields the so-called relaxation oscillator model:

$$\ddot{x} + c(x^2 - 1)\dot{x} + x = 0 \qquad \ldots\ldots (2.24)$$

Although the solutions of the simple equation (2.24) do not accurately correspond to the actual behaviour of physical oscillators, they nevertheless successfully model the qualitative properties of a wide class of such oscillators.

One particular example of a relaxation oscillator model of a physiological process is that of the heartbeat [87]. This particular model may have sparked off the idea of using relaxation oscillators as models of similar physiological processes.

On a suggestion of Dr. K.S. Cole, FitzHugh [28] tried to generalize equation (2.24) with the purpose of constructing a model which could serve as a simple representative of a class of

excitable-oscillatory systems including the Hodgkin-Huxley model of the excitable membrane of the squid giant axon. This is a reasonable conjecture, since a train of pulses is basically an oscillation relative to the constant amplitude of the potential difference across the membrane.

Integrating equation (2.24) with respect to time and introducing a new variable y yields two equations

$$\dot{x} + c(\frac{x^3}{3} - x) - y = 0$$

and $$\dot{y} = -x$$

or $$\dot{x} = c(y - \frac{x^3}{3} + x) \qquad \ldots\ldots \quad (2.25)$$

$$\dot{y} = -\frac{x}{c} \qquad \ldots\ldots \quad (2.26)$$

To complete the construction of his model FitzHugh adds various new terms to equations (2.25) and (2.26) on which subsequent restrictions are placed to obtain:

$$\dot{x} = c(y + x - \frac{x^3}{3} + z) \qquad \ldots\ldots \quad (2.27)$$

$$\dot{y} = -(x - a + by)/c \qquad \ldots\ldots \quad (2.28)$$

where $1 - \frac{2b}{3} < a < 1$, $0 < b < 1$, $b < c^2$. The physical role of parameter z will be discussed later.

The reason for the addition of these terms and the restrictions on the constants can only be motivated satisfactorily from a detailed phase plane analysis. It is a lengthy study and the interested reader is referred to the original text [28]. Summarizing one can say that the addition of the new terms produce a pair of non-linear differential equations with either a stable singular point or a limit cycle.

The model of FitzHugh is named the BVP model due to the facts

that van der Pol's equation was primarily used in it's construction and that the phase plane analysis show a qualitative resemblance to a theoretical iron wire (non-mathematical) model of the nerve which had previously been constructed by Bonhoeffer [3].

By renaming the variables in equations (2.27) and (2.28) the BVP model becomes

$$J = \frac{1}{c}\frac{du}{dt} - w - (u - \frac{u^3}{3}) \qquad \ldots\ldots (2.29)$$

$$c\frac{dw}{dt} + bw = a - u \qquad \ldots\ldots (2.30)$$

where $1 - \frac{2b}{3} < a < 1, \qquad 0 < b < 1, \qquad b < c^2$

In the phase plane analysis of FitzHugh the plane is divided into regions corresponding to the physiological states of the nerve fibre to form a "physiological state diagram" with the help of which many physiological phenomena concerning the nerve can be explained, such as the threshold phenomenon, stimulation by a constant current to produce a single pulse or infinite train of pulses, stimulation by rectangular positive current pulses of different durations and a number of other properties.

Without elaborating further on the phase plane analysis of FitzHugh we now point out the similarities between the BVP model and the original Hodgkin-Huxley model:

1. Equations (2.29) and (2.30) which describe the BVP model correspond to the space-clamped Hodgkin-Huxley model.

2. The variable J in equation (2.29) represents the stimulus intensity corresponding to the membrane current I in the

Hodgkin-Huxley model. J is specified as an arbitrary function of t.

3. The variable u in the BVP model corresponds to the pair of variables (V,m) in the Hodgkin-Huxley model. It represents excitability and is a rapidly changing function.

4. The variable w in the BVP model corresponds to the pair of variables (h,n) in the Hodgkin-Huxley model. It represents refractoriness and is a relatively slow-changing function.

5. The fact that the BVP model has only two variables of state (u,w) instead of the four of the Hodgkin-Huxley model (V, m, n, h) simplifies the analysis considerably.

FitzHugh did not generalize his model to cover the case of a propagated action potential. This was done later by Nagumo et al [64] whose work is discussed in the following paragraph.

2.3.6. The FitzHugh-Nagumo model

In 1962 J. Nagumo, S. Arimoto and S. Yoshizawa [64] constructed an active transmission line using tunnel diodes to electronically simulate the electrical behaviour of an animal nerve axon. The model they tried to simulate was that of FitzHugh, namely the BVP model. The transmission line is diagrammatically represented in Figure 2.9.

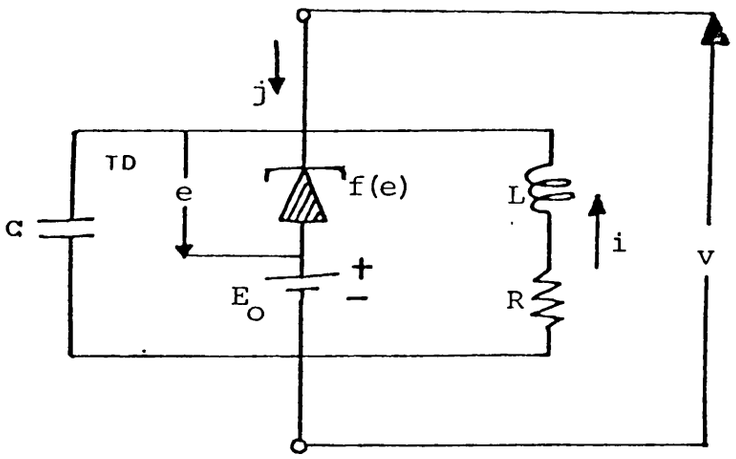

Figure 2.9: An electrical simulator of the BVP model as constructed by Nagumo et al (Redrawn after [64])

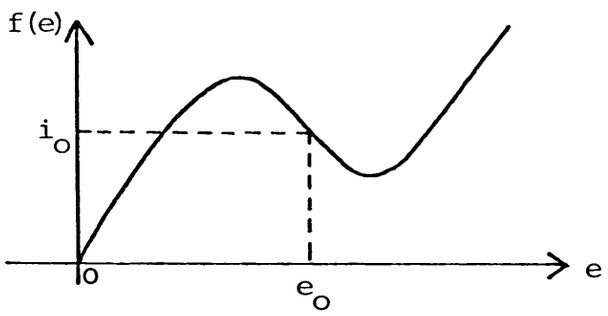

Figure 2.10: The voltage-current characteristic of the tunnel diode (Redrawn after [64])

The circuit equations are

$$j = C \frac{\partial v}{\partial \tau} - i - f(e) \qquad \ldots\ldots \quad (2.31)$$

$$L + \frac{di}{d\tau} + Ri = - v = e - E_o \qquad \ldots\ldots \quad (2.32)$$

where f(e) is given by

$$f(e) = i_o - \frac{1}{\rho} \{(e - e_o) - \frac{(e-e_o)^3}{3K^2}\} \quad (\rho > 0,\ K > 0,\ f(e_o) = i_o)$$

as shown in Figure 2.10.

By introducing the variables

$$t = \frac{\tau}{\sqrt{LC}}, \quad u = \frac{v + (e_o - E_o)}{K}, \quad w = \frac{\rho}{K} (i + i_o)$$

$$J = \frac{\rho}{K} j, \quad a = \frac{Ri_o + (e_o - E_o)}{K}, \quad b = \frac{R}{\rho}$$

and $$c = \frac{1}{\rho}\sqrt{\frac{L}{C}} \qquad \ldots\ldots \quad (2.33)$$

the system (2.31, 2.32) reduces to the BVP system (2.29, 2.30). An examination of the restrictions on the constants in the BVP model leads to the following conclusions:

The condition $0 < b < 1$ in the BVP model is equivalent to $\rho > R$,

$c^2 > b$ is equivalent to $\frac{L}{R} > \rho C$ and

$1 - \frac{2}{3}b < a < 1$ is equivalent to

$$Ri_o + e_o - K < E_o < R\,(i_o + \frac{3K}{2\rho}) + e_o - K$$

or $e_3 < E_o < e_1$ as shown in Figure 2.11.

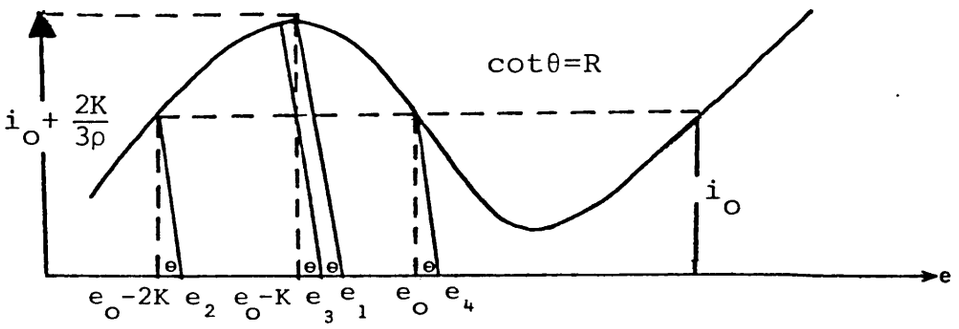

Figure 2.11: When the bias voltage is set between e_1 and e_2 the circuit in Figure 2.9 is monostable. If $E_o = e_4$ the circuit oscillates spontaneously. (Redrawn after [64])

Nagumo et al state that the restriction on E_o is too severe and can be weakened to $e_2 < E_o < e_1$. This would still ensure that the circuit in Figure 2.9 is monostable. Therefore

$$1 - \frac{2}{3}b < a < 2 \qquad \text{instead of}$$

$$1 - \frac{2}{3}b < a < 1.$$

To obtain the equations which describe the propagation of excitation along the nerve axon Nagumo et al [64] consider the circuit shown in Figure 2.12 which is constructed by cascading the many two-terminal circuits in Figure 2.9 through interstage coupling resistance.

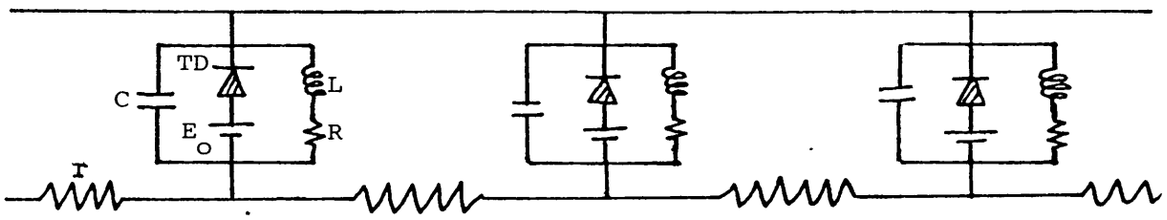

Figure 2.12: Electrical model to simulate propagation along the nerve axon (Redrawn after Nagumo et al [64])

Regarding the circuit above as a distributed line it follows that

$$j = \frac{1}{r} \frac{\partial^2 V}{\partial s^2} \qquad \ldots\ldots (2.34)$$

where s is distance along the line. This corresponds to (2.18) in the Hodgkin-Huxley model, provided the interstage coupling resistance per unit length of the line is r. By using the transformations of (2.33) equation (2.34) reduces to

$$J = \frac{\rho}{r} \frac{\partial^2 u}{\partial s^2} \qquad \ldots\ldots (2.35)$$

The BVP model of a propagated action potential then becomes

$$h \frac{\partial^2 u}{\partial s^2} = \frac{1}{c} \frac{\partial u}{\partial t} - w - (u - \frac{u^3}{3}), \quad h = \frac{\rho}{r} \qquad \ldots\ldots (2.36)$$

$$c \frac{\partial w}{\partial t} + bw = a - u, \quad 1 - \frac{2b}{3} < a < 2, \quad 0 < b < 1, \quad b < c^2 \qquad \ldots (2.37)$$

The system (2.36, 2.37) can be written as a single equation

$$ch\frac{\partial^3 u}{\partial t \partial s^2} + bh\frac{\partial^2 u}{\partial s^2} = \frac{\partial^2 u}{\partial t^2} - c\{(1 - \frac{b}{c^2}) - u^2\}\frac{\partial u}{\partial t}$$

$$+ \{(1-b)u + \frac{b}{3}u^3\} - a \qquad \ldots\ldots \quad (2.38)$$

Nagumo et al simplify equation (2.38) even further by setting $R = 0$ $(b = 0)$ and state that even in this oversimplified form the equation may still be considered as a model of the nerve axon in the sense that it contains certain characteristics thereof.

In this case (2.38) reduces to

$$ch\frac{\partial^3 u}{\partial t \partial s^2} = \frac{\partial^2 u}{\partial t^2} - c(1 - u^2)\frac{\partial u}{\partial t} + u - a$$

$$\text{where } c > 0, \quad 2 > a > 1, \quad h > 0 \qquad \ldots\ldots \quad (2.39)$$

By setting $x = \frac{s}{\sqrt{ch}}$, $\quad z = \frac{2a}{a^2-1}(a - u)$

$$\mu = c(a^2 - 1), \quad \varepsilon = \frac{a^2 - 1}{4a^2}$$

equation (2.39) is transformed to

$$\frac{\partial^3 z}{\partial t \partial x^2} = \frac{\partial^2 z}{\partial t^2} + \mu(1 - z + \varepsilon z^2)\frac{\partial z}{\partial t} + z \qquad \ldots\ldots \quad (2.40)$$

$$\text{where } \mu > 0, \quad \frac{3}{16} > \varepsilon > 0$$

Nagumo et al [64] state that the partial differential equation (2.40) probably represents the simplest realistic mathematical model of the nerve axon.

2.3.7. Further simplification of the BVP and FitzHugh-Nagumo models.

One disadvantage of the BVP model, as represented by equations (2.31, 2.32) or (2.36, 2.37) and the simplification of Nagumo (2.40) is the large number of constants present, many of which could have been eliminated through appropriate transformations. Furthermore, the rest states of the variables u and w in these models are not uniformly zero which might prove to be another disadvantage. Reformulated versions may be obtained by changing both the dependent and independent variables as is described in Appendix C to obtain the FitzHugh-Nagumo system:

$$\frac{\partial u}{\partial t} = \frac{\partial^2 u}{\partial x^2} + u(1-u)(u-a) - w \qquad \ldots\ldots (2.41)$$

$$\frac{\partial w}{\partial t} = b(u - dw), \qquad b > 0,\ d \geqslant 0 \qquad \ldots\ldots (2.42)$$

$$a \in (0,1)$$

When $d = 0$ the system (2.41, 2.42) is simply referred to as Nagumo's equation.

Sleeman [79] notes that the transformations to obtain (2.41, 2.42) breaks down when $d = 0$ so that one should rather consider $d > 0$ and not $d \geqslant 0$. When $d = 0$ the model is simply referred to as Nagumo's model which can be obtained from (2.40) through appropriate transformations. Nagumo's model is given by:

$$\frac{\partial u}{\partial t} = \frac{\partial^2 u}{\partial x^2} + u(1-u)(u-a) - w \qquad \ldots\ldots (2.43)$$

$$\frac{\partial w}{\partial t} = b\,u \qquad b > 0,\ a \in (0,1) \qquad \ldots\ldots (2.44)$$

Returning to the BVP model, as represented by equations (2.36, 2.37) we apply the transformations

$$x = \frac{s}{\sqrt{h}}, \quad t = ct,$$

rename the constants and let $u = -u$ to obtain

$$\frac{\partial u}{\partial t} = \frac{\partial^2 u}{\partial x^2} + u - \frac{1}{3}u^3 - w \qquad \ldots\ldots (2.45)$$

$$\frac{\partial w}{\partial t} = \phi(u + a - bw) \qquad \ldots\ldots (2.46)$$

$$1 - \frac{2b}{3} < a < 2, \quad 0 < b < 1, \quad b < \frac{1}{\phi^2}$$

Popular values for ϕ, a and b are 0,08, 0,7 and 0,8 respectively.

CHAPTER 3

ANALYSIS OF GOVERNING EQUATIONS — A SURVEY OF EXISTING LITERATURE

3.1. Introduction

In this chapter a general mathematical classification of the various models introduced and discussed in the previous chapter is presented by considering the relationship of the governing equations to a general system of reaction-diffusion equations. Theoretical as well as computational results existing in the literature on the various governing equations are then discussed.

3.2. General classification of governing equations

3.2.1. Reaction-Diffusion systems [56, 59]

Let $\Omega \subseteq \mathbb{R}^m$, $m \geq 1$ be a bounded or unbounded domain. If Ω is bounded we suppose it has a smooth boundary.
For $(\underline{x},t) \in \Omega \times [t \geq 0]$ consider the system of reaction-diffusion equations

$$\frac{\partial \underline{u}}{\partial t} = D \nabla^2 \underline{u} + \sum_{j=1}^{m} M_j(\underline{x},\underline{u}) \frac{\partial \underline{u}}{\partial x_j} + \underline{f}(\underline{u}) \qquad \ldots\ldots (3.1)$$

where $\underline{u} = (u_1, \ldots, u_n)^T$, $m \geq 1$, D is a "diffusion matrix" with non-negative constant entries and is usually diagonal. The coefficients $M_j (j=1, \ldots, m)$ are continuous matrix-valued functions. The terms on the right-hand side of (3.1) describe diffusion, convection and non-linear reaction respectively.

Along with (3.1) we have the initial condition

$$\underline{u}(\underline{x},0) = \underline{u}_o(\underline{x}), \quad \underline{x} \in \Omega \qquad \ldots\ldots (3.2)$$

and for initial boundary value problems we have in addition to (3.2) the boundary condition

$$P \frac{\partial \underline{u}}{\partial n} + Q \underline{u} = \underline{a}, \quad (\underline{x},t) \in \partial\Omega \times [t \geqslant 0] \qquad \ldots\ldots \quad (3.3)$$

where P,Q are matrix - valued functions of $\underline{x}$ and t, $\underline{a}$ depends on $\underline{x}$ and t and $\frac{\partial}{\partial n}$ denotes the normal derivative. We mainly consider the case m = 1, so that Ω is one-dimensional.

3.2.2. Fisher's equation

Fisher's equation as given by (2.3):

$$\frac{\partial u}{\partial t} = \frac{\partial^2 u}{\partial x^2} + f(u)$$

represents the simplest case of (3.1), namely that with n = m = 1. The diffusion matrix D becomes a diffusion constant of unity and the convection coefficient M_j is identically zero. In the case of a drift term added to (2.3) (see § 2.2.2), the convection coefficient is non-zero. The associated initial and boundary conditions will be discussed in § 3.3.2.

3.2.3. Nerve axon equations

3.2.3.1. The general class of models

The general class of models for impulse propagation in the nerve axon, based on an equivalent circuit consisting of a capacitor in parallel with a conductor (as discussed in § 2.3.4) can be described by the system:

$$\frac{\partial^2 u}{\partial x^2} = \frac{\partial u}{\partial t} + I(u,\underline{w}) \qquad \ldots\ldots \quad (3.4)$$

$$\frac{\partial \underline{w}}{\partial t} = P(u)\underline{w} + \underline{q}(u) \qquad \ldots\ldots \quad (3.5)$$

where u(x,t) is the electrical potential across the membrane as a function of time t and distance x along the axon. The

current density I is a function of the potential u and one or more state variables $w_1, \ldots, w_n$.

Equations (3.4, 3.5) correspond to the general equations (3.1) by setting $m = 1$, $n \geqslant 2$ and splitting the vector $\underline{u} = (u_1, \ldots, u_n)^T$ into a single function u and a vector $\underline{w} = (w_1, \ldots, w_{n-1})^T$. The diffusion matrix D has only one non-zero entry, namely the first, which is one. In the space-clamped case the matrix D is identically zero. The convection coefficients are set to zero once again. The functions $I(u,\underline{w})$, $P(u)\,\underline{w}$ and $\underline{q}(u)$ are all incorporated by the term $f(\underline{u})$ in (3.1).

3.2.3.2. The Hodgkin-Huxley model

In the case of the Hodgkin-Huxley system as given in Appendix B, $\underline{w}(x,t)$ is a three-dimensional vector function, P is a 3×3 matrix function and q is a vector function, both depending non-linearly on u. The function $I(u,\underline{w})$ is linear in u but non-linear in w. Assuming the axon to be of infinite length we study the system on the quarter plane $x \geqslant 0$, $t \geqslant 0$ with appropriate initial and boundary conditions.

3.2.3.3. Simplifications of the Hodgkin-Huxley model

The BVP model as given by (2.45, 2.46) and the FitzHugh-Nagumo model as given by (2.41, 2.42) are two-variable simplifications of the Hodgkin-Huxley system. Both these models are examples of the general model (3.4, 3.5) where the functions I, P and q are different for the two models but similar in form; both u(x,t) and w(x,t) are one-dimensional vectors.

Here the function I(u,w) is non-linear in u but linear in w. This is in contrast to the Hodgkin-Huxley system. P is a con-

stant scalar and the function q(u) is linear in u. The severe non-linearities in the Hodgkin-Huxley system have been reduced to a single non-linear term in these two models. Nagumo's equation (2.43, 2.44) is the simplified version of the FitzHugh-Nagumo model where the constant P is zero.

3.3. Theoretical treatment

3.3.1. Introduction

We consider the system of reaction-diffusion equations (3.1). One of the basic problems associated with systems of the form (3.1, 3.2, 3.3) is that of establishing existence and uniqueness of solutions. A comprehensive survey of known results concerning these matters are contained in the work of Rauch and Smoller [69] and Schonbek [77, 78].

Another important question, both from the mathematical point of view and that of biology is how the solutions of (3.1, 3.2, 3.3) evolve in time and space and in particular how they are affected by initial and boundary data. These problems have been studied in the literature although results are far from complete.

However, it is known that a large class of systems of the form (3.1, 3.2, 3.3) exhibit "travelling wave" type of solutions.

These are defined as follows ([18]):

- Travelling waves: These are solutions $u(\underline{x},t)$ of the form $u(\underline{x},t) = U(\underline{x} - \underline{c}t)$ for some velocity vector $\underline{c}$.

Two special types of travelling waves are:

- Wave fronts: These are travelling wave solutions U which satisfy the conditions: $U(-\infty)$, $U(\infty)$ exist but are unequal.

- Pulses: These are travelling wave solutions U which satisfy the conditions: $U(-\infty)$, $U(\infty)$ exist and are equal but U is not constant.

We will also need the following definitions:

- A steady state (or equilibrium state) is a solution to (3.1) which is time-independent, i.e. for which $\frac{\partial u}{\partial t} = 0$.

- When referring to a stable state, C^0-stability is implied. This is defined as follows: A steady state solution $\psi(x)$ of (3.1) is C^0-stable if, given any $\varepsilon > 0$, there is a $\delta > 0$ such that every solution $u(x,t)$ of (3.1) defined for $x \in \mathbb{R}$, $t \geq 0$, satisfying $|u(\cdot,0) - \psi|_0 \equiv \sup_{x \in \mathbb{R}} |u(x,0) - \psi(x)| < \delta$ also satisfies $|u(\cdot,t) - \psi|_0 < \varepsilon$ for all $t > 0$.

In practice this would mean that a stable steady state is one for which a slight disturbance from this state will cause a return to the state as time progresses, whereas an unstable state is one for which a slight disturbance will cause the solution to develop into another, stable, equilibrium state as time progresses.

3.3.2. Fisher's equation

3.3.2.1. Analysis of Fisher's equation

In this section we review the known results concerning the pure initial value problem and the initial boundary value problem for various forms of Fisher's equation (2.3).

The pure initial value problem is represented by

$$\frac{\partial u}{\partial t} = \frac{\partial^2 u}{\partial x^2} + f(u) \qquad (-\infty < x < \infty,\ t > 0)$$

$$u(x,o) = \phi(x) \qquad (-\infty < x < \infty) \qquad \ldots\ldots (3.6)$$

and the initial boundary value problem by

$$\frac{\partial u}{\partial t} = \frac{\partial^2 u}{\partial x^2} + f(u) \qquad (0 \leqslant x < \infty,\ t > 0)$$

$$u(x,o) = 0 \qquad , x > 0$$

$$u(o,t) = \psi(t) \qquad , t \geqslant 0 \qquad \ldots\ldots (3.7)$$

To begin with it is a standard result [24] to prove that if $f \in C^1$, $f(o) = f(1) = 0$ and ψ is piece-wise continuous with $0 \leqslant \phi(x) \leqslant 1$ then there exists one and only one bounded solution $u(x,t)$ of the problems (3.6, 3.7). Furthermore, it can be shown that $0 \leqslant u(x,t) \leqslant 1$.

Before proceeding with results on stability we state again the three types of conditions which may apply to the function $f(u)$ associated with Fisher's equation (2.3). Henceforth they will be referred to as Case 1, 2 or 3, respectively, of Fisher's equation (§ 2.2.3).

Case 1 (The heterozygote intermediate case)

$f'(u) > 0$, $f(u) > 0$ in $(0,1)$

e.g. 

Case 2 (The heterozygote superior case)

$f'(0) > 0$, $f'(1) > 0$, $f(u) > 0$ in $(0,\alpha)$,

$f(u) < 0$ in $(\alpha,1)$ for some $\alpha \in (0,1)$

e.g. 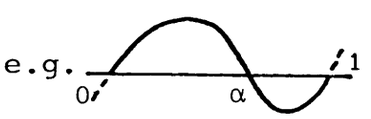

Case 3 (The heterozygote inferior case)

$f'(0) < 0$, $f'(1) < 0$, $f(u) < 0$ in $(0,\alpha)$,
$f(u) > 0$ in $(\alpha,1)$ for some $\alpha \in (0,1)$
and $\int_0^1 f(u)\,du > 0$.

e.g. 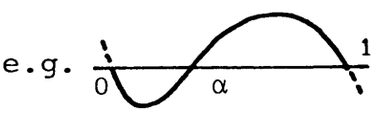

The following theorems provide important information regarding the stability of solutions to Fisher's equation (2.3). These theorems have been proved by Aronson and Weinberger [1] using a comparison type of argument.

We first consider results on the pure initial value problem (3.6):

Theorem 3.1

Let $u(x,t) \in [0,1]$ be a solution of (3.6).

1. If $f(u)$ satisfies the conditions of case 1
   then either $u(x,t) \equiv 0$ or $\lim_{t\to\infty} u(x,t) = 1$.

2. If $f(u)$ satisfies the conditions of case 2
   then either $u(x,t) \equiv 0$ or $\lim_{t\to\infty} u(x,t) = \alpha$.

In other words $u \equiv 1$ is the only stable equilibrium state in case 1, whereas $u = \alpha$ is the only stable equilibrium state in case 2.

In case 3 the situation is not as simple as in the previous two cases. Aronson and Weinberger prove the instability of the state $u \equiv \alpha$ and the conditional stability of the states $u \equiv 0$ and $u \equiv 1$. More explicitly, this means that a disturbance of bounded support of the state $u \equiv 0$ which is sufficiently large on a sufficiently large interval grows to one while a disturbance which is not sufficiently large on a sufficiently large interval dies away (to reach the steady state $u \equiv 0$ eventually). A threshold phenomenon is exhibited, therefore. The analytical theorems concerning this matter are rather complicated and lengthy to state here, we refer the reader to the original text [1].

Let us now consider a few asymptotic results particularly relevant to the initial-boundary value problem (3.7).

Here Aronson and Weinberger [1] prove for case 1:

Theorem 3.2

Let $u(x,t) \in [0,1]$ be the solution of (3.7) where $f(u)$ satisfies the conditions of case 1. If $u(x,t) \not\equiv 0$ then

$$\lim_{t\to\infty} \inf\, u(x,t) \geqslant \tau(x)$$

where $\tau(x)$ is the unique positive solution of the problem

$$q'' + f(q) = 0 \quad \text{in} \quad 0 < x < \infty$$

$$q(0) = \beta$$

where $$\beta = \lim_{t\to\infty} \inf\, \psi(t)$$

In particular $$\lim_{x\to\infty} \lim_{t\to\infty} \inf\, u(x,t) = 1$$

Thus if $\psi(t) \not\equiv 0$, $u(x,t)$ approaches values near one far from the boundary regardless of the behaviour of $\psi(t)$.

In the same way it can be proved that if $f(u)$ satisfies the conditions of case 2 then

$$\lim_{x\to\infty} \lim_{t\to\infty} \inf\, u(x,t) = \lim_{x\to\infty} \lim_{t\to\infty} \sup\, u(x,t) = \alpha$$

unless $\psi(t) \equiv 0$.

Finally, in case 3 the threshold property is exhibited again. In general

$$\lim_{x\to\infty} \lim_{t\to\infty} \sup u(x,t) = 0 \quad \text{if} \quad \sup \psi(t) \quad \text{is suitably}$$

bounded, while

$$\lim_{x\to\infty} \lim_{t\to\infty} \inf u(x,t) = 1 \quad \text{if} \quad \psi(t) \quad \text{is large enough}$$

on a suitably large time interval.

We quote the following result from Aronson and Weinberger [1] on this matter

Theorem 3.3.

Let $u(x,t) \in [0,1]$ be the solution of (3.7) and let $f(u)$ satisfy the conditions of case 3. Let $K \in [\alpha,1)$ be defined as the unique number for which $\int_0^K f(u)du = 0$

For any $\beta \in (K,1)$ there is a positive time T_β with the property that the condition

$$\psi(t) \geqslant \beta \quad \text{on} \quad (t_o,\ t_o + T_\beta)$$

for some non-negative t_o, implies

$$\lim_{x\to\infty} \lim_{t\to\infty} \inf u(x,t) = 1$$

With this we conclude the results on stability and investigate the existence of travelling wave solutions in the next paragraph.

3.3.2.2. Travelling wave solutions

We introduce the travelling wave coordinate $\xi = x - ct$, $c > 0$. A travelling wave solution to Fisher's equation is a function $U(\xi)$ satisfying the ordinary differential equation

$$U'' + cU' + f(U) = 0 \qquad \text{where } ' = \frac{d}{d\xi} \qquad \ldots\ldots \quad (3.8)$$

Here c denotes the speed of the front and it can be shown in some cases to be unique while in others wave fronts are known to exist for a half line of speeds c greater than some minimal critical speed c^* [1].

The existence of travelling wave solutions is established in the following theorem due to Aronson and Weinberger [1].

THEOREM 3.4

If $f(u)$ satisfy the conditions of either cases 1, 2 or 3 there exists a travelling wave solution

$$U = q^*(x - c^*t)$$

of Fisher's equation. Moreover $q^{*\prime}(\xi) < 0$

$\lim_{\xi\to\infty} q^*(\xi) = 0$ and

$\lim_{\xi\to-\infty} q^*(\xi) = \begin{cases} 1 & \text{in cases 1 and 3} \\ \alpha & \text{in case 2.} \end{cases}$

Theorem 3.4 establishes the existence of a particular type of travelling wave solution, namely a wave front type of solution.

Throughout our discussion of solutions to Fisher's equation we define such fronts as solutions of the form $u(x,t) = U(x - ct)$ where $U(-\infty) = 1$, $U(\infty) = 0$. For the conditions $U(-\infty) = 0$, $U(\infty) = 1$ these solutions need to be replaced by $U(-x + ct) = U(-\xi)$.

We now give two results concerning the asymptotic speed of propagation, due to Rothe [75]:

THEOREM 3.5

For Fisher's equation satisfying the conditions of case 1 there exists a positive minimal speed $c^*(f)$. For every velocity $c \geqslant c^*(f)$ there exists a travelling wave solution (satisfying $\lim_{\xi \to -\infty} U(\xi) = 1$ and $\lim_{\xi \to \infty} U(\xi) = 0$)

whereas there are no travelling wave solutions for velocities less than $c^*(f)$. Aronson and Weinberger [1] gives the value $\sqrt{4f'(0)}$ as a lower bound for the minimal speed $c^*(f)$

THEOREM 3.6

For Fisher's equation satisfying the conditions of case 3 and for a particular function f there exists exactly one velocity c^* admitting wave front solutions.

3.3.2.3. Convergence to wave fronts

We now investigate the convergence of solutions of the various forms of Fisher's equation to wave fronts, for various types of initial or boundary data.

Suppose, as in Case 1, that $f(u) > 0$ for $u \in (0,1)$, $f'(0) > 0$ and in addition $f'(1) < 0$, $f'(u) \leqslant f'(0)$ then Kolmogorov,

Petrovskii and Piskounov [50] have shown that if the initial function $\phi(x)$ is chosen so that $\phi(x) \equiv 0$ for $x < 0$ and $\phi(x) \equiv 1$ for $x > 0$, then in a certain sense there exists a travelling front $U(x - ct)$ and a function $\psi(t)$ such that as $t \to \infty$

$$|u(x,t) - U(x - ct - \psi(t))| \to 0$$

uniformly in x and $\psi'(t) \to 0$. [simplified proof in [54]]. More recently Stokes [82] has improved on the result of [50] in that if ϕ is taken to be a step function or a sufficiently steep monotone function and $c^2 > 4f'(0)$ then ψ is constant. Further improvements and extensions of these results are due to Rothe [75]. He investigates the asymptotic behaviour for a large class of monotone initial data and proves that all solutions with initial data in this class evolve to wave-type solutions. These results are too complicated to state in full and we refer the reader to the original text [75].

The interesting case is, as before, Case 3 where a threshold property exists. The convergence to a wave front type of solution from arbitrary initial or boundary data has been investigated in various papers [19, 20, 21, 25, 35, 36, 75] but perhaps the most complete results to date are due to Fife and McLeod [23, 24]. These results are of such generality and importance as to be worth stating in full.

Theorem 3.7 establishes the convergence to a travelling wave front from montonone initial data whereas Theorem 3.8 is a result concerning the threshold property and the convergence to two wave fronts travelling in opposite directions.

THEOREM 3.7

Let $f \in C^1[0,1]$ satisfy, for some $\alpha \in (0,1)$, $f(0) = f(1) = 0$, $f(u) \leq 0$ for $u \in (0,\alpha)$, $f(u) > 0$ for $u \in (\alpha,1)$, $\int_0^1 f(u)du > 0$. Then there exists a travelling front $U(x - ct)$, unique modulo translation and necessarily monotonic, and if $\phi \in C^1(-\infty,\infty)$ with $\phi(-\infty) = 0$, $\phi(\infty) = 1$, $\phi'(x) > 0$ for all x, then there exists a function $\gamma \in C^1(0,\infty)$ with $\gamma'(t) \to 0$ as $t \to \infty$ such that uniformly in x

$$|u(x,t) - U(x - ct - \gamma(t))| = o(1)$$

where u is the solution to the initial value problem (3.6) with $u(x,0) = \phi(x)$.

THEOREM 3.8

Let f satisfy the hypotheses of Theorem 3.7. Let ϕ satisfy $0 \leq \phi \leq 1$ and

$$\lim_{|x|\to\infty} \sup \phi(x) < \alpha_0,$$

$$\phi(x) > \alpha_1 + \eta \quad \text{for} \quad |x| < L$$

where η and L are positive numbers and $0 < \alpha_0 \leq \alpha \leq \alpha_1 < 1$, α as in Theorem 3.7. Then if L is sufficiently large (depending on η and f) we have for some constants x_0, x_1, K and w $(K, w > 0)$

$$|u(x,t) - U(x - ct - x_0)| \leq Ke^{-wt}, \quad x < 0$$

$$|u(x,t) - U(-x - ct - x_1)| \leq Ke^{-wt}, \quad x > 0$$

Theorem 3.8 establishes the convergence of initial data to two "wave fronts", propagated in opposite directions.

No results on convergence to wave fronts exist for Case 2.

3.3.2.4. Exact solutions and stationary patterns

So far we have been concerned with the existence of solutions to Fisher's equation (2.3) with the function f(u) satisfying one of three general types of conditions. We now look at the existence of solutions to (2.3) in closed form for particular example functions f(u).

- For the example function $f(u) = u(1-u)(u-a)$ in Case 3 (see Figure 2.1), an exact solution to the travelling wave equation (3.8) is available, called the Huxley solution [53]:

$$U(\xi) = [1 + \exp(-\frac{\xi}{\sqrt{2}})]^{-1} \qquad \ldots\ldots (3.9)$$

where the speed c (called the Huxley speed) is given by

$$c = \sqrt{2}\,(\tfrac{1}{2} - a), \quad 0 < a \leqslant \tfrac{1}{2}$$

Here $U(-\infty) = 0$, $U(\infty) = 1$.

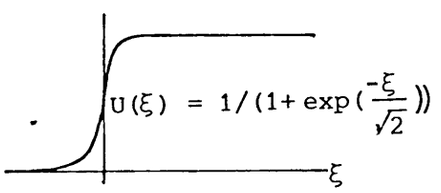

Figure 3.1.

- For the example function $f(u) = u(1-u)$ in Case 1 and $f(u) = u(1-u)(a-u)$ in Case 2 (see Figure 2.1) no travelling wave solutions corresponding to the Huxley solution (3.9) have been obtained as yet.

- Recently Cochran [6] has found an exact formula for the speed in terms of θ, corresponding to the caricature of

f(u) pictured in Figure 3.2. This caricature is a generalization of the cases for which McKean [53] solved Fisher's equation, namely when $\theta = \frac{\pi}{4}$ or $\theta = \frac{\pi}{2}$.

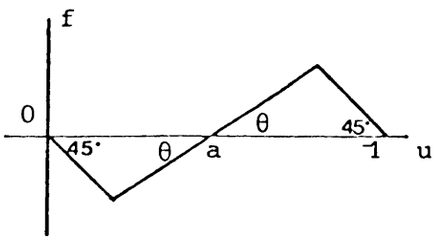

Figure 3.2.

The solutions mentioned above and considered in the preceding paragraphs are all of the travelling wave type. An obvious question arising is: Are there any other types of solutions to equation (2.3)? Results quoted so far (§ 3.3.2.2. and 3.3.2.3.) have mainly been concerning solutions starting from various types of initial data and then converging to a wave front solution travelling with asymptotic speed. We reformulate the question stated above to: Do solutions exist which do not converge to a travelling wave, nor decay to the zero steady state in time? Solutions such as these can be referred to as zero-speed travelling waves or stationary patterns.

We employ a method of Fife [18] to establish the qualitative existence of such solutions. Fife defines stationary patterns as stable, stationary, non-constant, bounded solutions which are not caused by boundary conditions and are defined on the whole of the x-axis.

So any pattern must be the solution of the steady equation

$$\frac{d^2u}{dx^2} + f(u) = 0, \qquad -\infty < x < \infty \qquad \ldots\ldots \quad (3.10)$$

Multiplying (3.10) by $\frac{du}{dx}$ and integrating leads to

$$\frac{1}{2}\left(\frac{du}{dx}\right)^2 + V(u) = E$$

where $V(u) = \int_o^u f(s)ds$ and E is constant. Fife states that if

one draws the graph of the potential V(u) then there is a one-to-one correspondence between the non-constant solutions of (3.10) and horizontal line segments in the (u,V) plane whose finite endpoints lie on the given curve.

The projection of such a segment onto the u-axis is the range of the corresponding solution and the ordinate of the segment is the constant E.

(i) We apply this to our example function of Case 3, $f(u) = u(1-u)(u-a)$, $0 < a \leq \frac{1}{2}$. It follows that $V(u) = -\frac{1}{2}u^2(a - \frac{2}{3}(1+a)u + \frac{1}{2}u^2)$

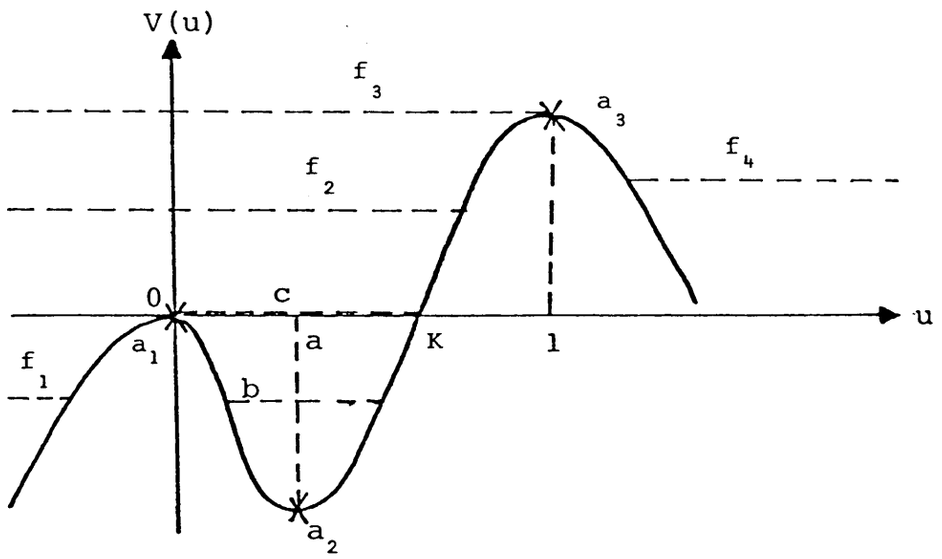

Figure 3.3.: $V(u) = -\frac{1}{2}u^2(a-\frac{2}{3}(1+a)u+\frac{1}{2}u^2)$, $0<a<\frac{1}{2}$

Following Fife [18] we observe the following:

1. $a_1(u=0)$, $a_2(u=a)$ and $a_3(u=1)$ depict constant solutions. As stated before a_1 and a_3 are stable while a_2 is unstable (§ 3.3.2.1.)

2. b depicts a periodic solution, ultimately varing between 0 and K ($\int_0^K f(u)du = 0$).

3. c depicts a solution which has it's supremum at a finite x-value and which goes to zero as $x \to \pm \infty$.

4. f_1, f_2 and f_3 are solutions unbounded from below but bounded from above, f_4 bounded from below but unbounded from above.

Fife proves that every bounded non-constant solution of (3.10) which attains a maximum or minimum at a finite value of x is C^0-unstable. Therefore solutions b, c, f_1, f_2, f_3 and f_4 are all C^0-unstable. In practice this would mean that any of these solutions taken as initial data for the pure initial value problem would evolve in time to one of the stable equilibrium states 0 or 1.

McKean [53] has established the following zero-speed travelling wave solutions to Fisher's equation (in Case 3), corresponding to the stationary patterns described as 2. and 3. respectively.

$$\text{(i)}\quad U(\xi) = 3\left[\sqrt{(2-a)\left(\tfrac{1}{2}-a\right)}\cosh\sqrt{a}\xi + \frac{1}{1+\frac{1}{a}}\right]^{-1},\quad c=0,\ 0<a\leqslant\frac{1}{2} \qquad \ldots\ldots \quad (3.11)$$

((3.11) approximates to (3.9) as $a \uparrow \frac{1}{2}$ when properly translated)

$$\text{(ii)}\quad U(\xi) = \frac{1}{2} + k\ \mathrm{sn}\left(\frac{\xi}{\sqrt{2}}\sqrt{\frac{1}{2}-k^2},\ \frac{k}{\sqrt{\frac{1}{2}-k^2}}\right),\quad 0<k<\frac{1}{2},\ c=0,\ a=\frac{1}{2} \qquad \ldots\ldots \quad (3.12)$$

This forms a one-parameter family of periodic solutions in terms of Jacobi Elliptic functions. McKean also derives similar solutions when $c = 0$, $a < \frac{1}{2}$.

Returning to [18], Fife states that besides the unstable solutions the only nonconstant bounded solutions of (3.10) are the monotone ones, which depend on the existence of two local adjacent maxima having the same height. This special property

of the curve V will, of course, depend on the function f. A slight change in such a function will destroy the property so that monotone solutions such as these are said to be structurally unstable.

For this particular example function we are able to obtain two local adjacent maxima when $a = \frac{1}{2}$

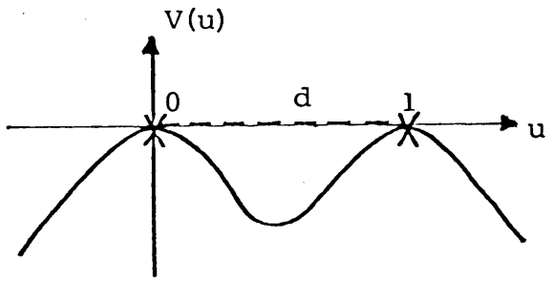

Figure 3.4: $V(u) = -\frac{1}{2}u^2\left(a - \frac{2}{3}(1+a)u + \frac{1}{2}u^2\right)$, $a = \frac{1}{2}$

The dashed line d represents a monotonic increasing (decreasing) solution which takes the value zero (one) at $x = -\infty$ and one (zero) at $x = \infty$. This corresponds to the Huxley solution (3.9) when $a = \frac{1}{2}$, $c = 0$. In practice this solution can be used as initial data and the expected behaviour of not changing shape or position in a time-progressing calculation can be verified numerically (see § 4.4.1.).

An interesting observation is that Aronson and Weinberger state $\int_0^1 f(u)du > 0$ as condition in Case 3 which implies that $a < \frac{1}{2}$ which eliminates the zero-speed solution as a stable rest state. We briefly look at the other two cases:

Case 1 Taking $f(u) = u(1-u)$ as example function leads to

$$V(u) = u^2(\tfrac{1}{2} - \tfrac{1}{3}u).$$

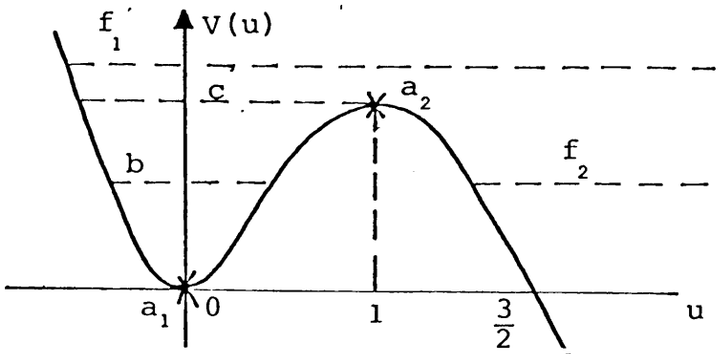

Figure 3.5:
$V(u) = u^2(\frac{1}{2} - \frac{1}{3}u)$

No two adjacent local maxima exist, so that no stable non-constant solution is possible. The constant solutions are $u = 0$ (unstable) and $u = 1$ (stable). The remaining C^0-unstable solutions are periodic solutions (b), unbounded solutions (f_1 and f_2), and solutions attaining a minimum at a finite value of x and approaching it's supremum at $x \to \pm \infty$ (c).

Case 2 Taking $f(u) = u(1-u)(a-u)$ as example function leads to

$$V(u) = \tfrac{1}{2}u^2(a - \tfrac{2}{3}(1+a)u + \tfrac{1}{2}u^2).$$

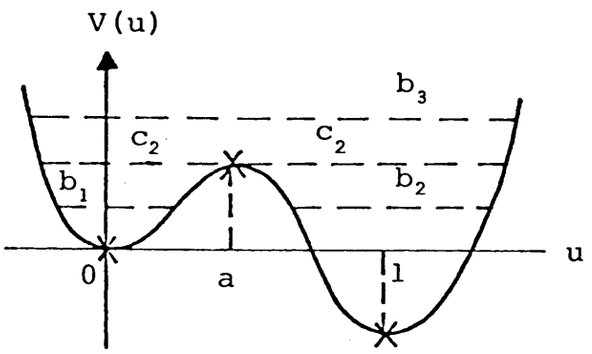

Figure 3.4:
$V(u) = \frac{1}{2}u^2(a - \frac{2}{3}(1+a)u + \frac{1}{2}u^2)$

The constant solutions are $u = 0$, $u = 1$ (both unstable) and $u = a$ (stable). The non-constant solutions are the periodic ones (b_1, b_2, b_3) and two solutions with a supremum at a finite x-value and which tends to a constant value at $x \to \pm \infty$, (c_1 and c_2), C^0-unstable. No two local adjacent maxima exist.

Apart from t-independent solutions to Fisher's equation, results are known to exist for x-independent solutions [10]. These

satisfy the "kinetic equation"

$$\frac{\partial u}{\partial t} = f(u).$$

This will not be discussed as one of the two main components of a reaction-diffusion equation is no longer present.

3.3.3. Simplifications of the Hodgkin-Huxley system

3.3.3.1. Analysis of Nagumo's equation

We now investigate the existence of solutions to the models of the electrical behaviour of the nerve axon, starting with the simplest one, namely that of Nagumo (2.43, 2.44).

This system can be written as a single equation

$$\frac{\partial u}{\partial t} = \frac{\partial^2 u}{\partial x^2} + u(1-u)(u-a) - b\int u\,dt \qquad \ldots\ldots \quad (3.13)$$

where $0 < a < 1$ and $0 < b << 1$.

Being mainly concerned with travelling wave solutions we introduce the co-ordinate

$$\xi = x - ct, \quad c > 0$$

so that equation (3.13) takes the form

$$u''' + cu'' + f_u u' + \frac{b}{c} u = 0, \quad (' = \frac{d}{d\xi}) \qquad \ldots\ldots \quad (3.14)$$

To begin with we will consider results on the existence of solutions to (3.14). Secondly we will consider results concerning the stability of such solutions.

Rewriting (3.14) as a system of three first order differential equations, Hastings [43] first established the existence of a solution satisfying

$$\lim_{|\xi|\to\infty} u(\xi) = 0 \qquad \ldots\ldots \qquad (3.15)$$

This result follows from a discussion of the three-dimensional phase space analysis of this system.

It can be proved [39] that such a solution (a travelling pulse solution) cannot exist unless $0 < a < \frac{1}{2}$. With this restriction the existence of such solutions have been proved subsequently in [42]. See also [4, 9, 77]. (McKean [53] interprets a as representing the amount of novocaine in the nervous system and $a \geqslant \frac{1}{2}$ is supposed to reflect the fact that if too much novocaine is injected into the system the nerves goes "dead". Therefore a plays the role of a doping parameter. This is a physical interpretation of the result mentioned above).

Experimental evidence [45] suggests that there is only one value of c for which a solution to (3.14) satisfying (3.15) exists. It can be proved [41], however, that there are at least two such values of c, say c_* and c^*, such that $0 < c_* < c^*$. Sleeman [79] has shown that the slower pulse with speed c_* is unstable. The faster one with speed c^* is is the stable one which is observed experimentally [41]. The stability of the faster pulse is, however, still unproved. In another study of Sleeman ([80]), it is shown that for the wave speed c sufficiently small, the travelling wave solutions are unstable.

Further qualitative results concerning the relative magnitudes of the constants a, b and c are given in [33] and [79]. These will be discussed in the following paragraph where the full FitzHugh-Nagumo system is discussed and Nagumo's equation as

a special case thereof.

Except for travelling pulse solutions, the existence of a second kind of solutions, periodic solutions, have been established and proved in [9, 40, 42].

It has been proved that the speed c of a periodic solution lies in the interval $0 < c < \sqrt{2}(\frac{1}{2} - a)$ [40]. Maginu [55] shows that the period $L(c)$ is a smooth function of c with one local minimum, and the periodic solutions are unstable for $L'(c) < 0$.

McKean [53] proposed that the cubic polynomial f in (3.13) be replaced by a piecewise linear function, in such a way that one could find exact solutions to the resulting system. One particular caricature which has received the most attention is

$$f_1(u) = \begin{cases} -u, & u \leqslant a \\ a-u, & u > a \end{cases}, \quad 0 < a \leqslant \frac{1}{2}$$

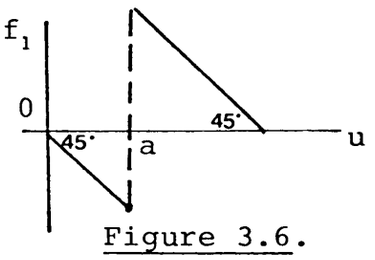

Figure 3.6.

This model has been studied extensively by Rinzel and Keller [74] and Rinzel [70, 72, 73]. Apart from their numerical work which will be discussed in a later paragraph, they also established theoretical results on stability. They show that for certain parameter values two pulse solutions exist with different speeds of propagation. They are able to show that the slower one is unstable and the fast one stable through a linear stability analysis.

They also establish the existence of two periodic waves, representing trains of propagated impulses, for each period greater than some minimum period which depends on the parameters. The slower train is again unstable.

Returning to the original equation (3.14) we mention a conjecture of Hastings [41] on the threshold property. He states that for the boundary condition $u(o,t) = U_o(t)$ the size of $\int_o^T U_o(t)dt$ is crucial. If $U_o(t)$ has sufficiently small compact support and $\int_o^T U_o(t)dt$ is small then the solution will decay to zero. No proof is given. We will discuss the Fitz-Hugh-Nagumo system in the next paragraph for which results on the threshold properly have been proved.

3.3.3.2. Analysis of the FitzHugh-Nagumo system

We now consider the full FitzHugh-Nagumo system as given by (2.41, 2.42):

$$\frac{\partial u}{\partial t} = \frac{\partial^2 u}{\partial x^2} + u(1-u)(u-a) - w$$

$$\frac{\partial w}{\partial t} = b(u - dw) \qquad , d \geqslant 0,\ b > 0,\ 0 < a < 1$$

In the case where $d = 0$ we have, of course, the simpler Nagumo model for which the existence of travelling wave solutions was established by Hastings. By following Hastings' arguments Sleeman [79] establishes the existence of travelling wave solutions for the FitzHugh-Nagumo system.

By setting $\xi = x - ct$, $u(x,t) = \phi(x - ct)$, $w(x,t) = \psi(x - ct)$ we obtain the set of ordinary differential equations:

$$-c\phi' = \phi'' + F(\phi) - \psi \qquad \ldots\ldots \quad (3.16)$$

$$-c\psi' = b(\phi - d\psi) \qquad \text{where } ' \doteq \frac{d}{d\xi} \qquad \ldots\ldots \quad (3.17)$$

$$\text{and } f(\phi) = \phi(1 - \phi)(\phi - a)$$

Sleeman [79] considers a travelling wave solution to the Fitz-Hugh-Nagumo system (2.41, 2.42) as a solution of (3.16, 3.17)

satisfying

$$\lim_{|\xi|\to\infty} \phi(\xi) = \lim_{|\xi|\to\infty} \phi'(\xi) = \lim_{|\xi|\to\infty} \psi(\xi) = 0, \quad \ldots\ldots \quad (3.18)$$

i.e. a pulse solution. The conditions in (3.18) are motivated from the biological background. It represents a nerve in a resting state at the two end points.

Green and Sleeman [33] established some results (later improved by Sleeman [79]) concerning the relative magnitudes of the parameters. The first of these concerns the existence of travelling wave solutions: If $\frac{1}{2} \leqslant a < 1$, $b > 0$, $d \geqslant 0$ then the FitzHugh-Nagumo system (2.41, 2.42) has no bounded non-constant travelling wave solutions, therefore $0 < a < \frac{1}{2}$ is a necessary condition for the existence of travelling wave solutions. We state two more of these results as theorems.

THEOREM 3.9

If $c^2 \geqslant (1-a)^2$ for $0 < a < 1$, $d \geqslant 0$ and $b > 0$ then every bounded travelling wave solution of (3.16, 3.17, 3.18) is identically zero.

A necessary condition for the existence of a travelling wave solution is therefore

$$c^2 < (1-a)^2 \quad \text{for } 0 < a < 1$$

THEOREM 3.10

For any travelling wave solution of the FitzHugh-Nagumo system

$$c^2 > \frac{4b}{(1-a)^2}$$

We thus have an upper as well as a lower bound on the speed of a travelling wave.

From Theorem 3.10 we can derive an upper bound for b, namely

$$b < \frac{(1-a)^4}{4} \qquad \text{for} \quad 0 < a < 1$$

These results are applicable to the simpler Nagumo model (2.41, 2.42) where $d = 0$ without any alteration.
Similarly the results remain unaltered if we consider periodic solutions of the FitzHugh-Nagumo system instead of pulse solutions.

By far the most comprehensive results on the existence and uniqueness of solutions to the FitzHugh-Nagumo system are that of Schonbek [77, 78] and Rauch and Smoller [69]. These results are complicated, we refer the reader to the original text. One particular result which deserves attention is one of Schonbek [77] on the threshold property. Schonbek proves that if the boundary data $u(o,t)$ has finite sup norm and vanishes outside of some interval $[0,T]$ then the solution is bounded for all $t \geqslant 0$, by a constant times the total stimulus $\int_o^T |u(o,t)|dt$. Furthermore, if the total stimulus is sufficiently small, the solution has exponential decay.

To conclude this paragraph we mention two survey articles on the FitzHugh-Nagumo system, namely that of Hadeler [35] and Hastings [41].

3.3.3.3. Analysis of the BVP model (eqs. 2.45, 2.46)

An analysis of the BVP model as such has been performed by FitzHugh [28,29] who also constructed the model. This phase plane analysis, which we referred to in § 2.3.5 when discussing the construction of the model explains the physiological phenomena concerning impulse transmission and illustrates the existence of single pulses or infinite trains of pulses.

The two variables of the BVP model, namely u and w, represent excitability and refractoriness respectively. If the recovery variable w is kept at a constant value, excitation is followed by a plateau action potential of infinite duration. In this case the equation for the uniformly propagated action potential can be solved explicitly. The method is due to A.F. Huxley and the solution is

$$V = V_R + \frac{V_2 - V_R}{2}\left[1 + \tanh \frac{A(V_2 - V_R)}{2}\xi\right]$$

where $V_R = -1.1994$

$V_2 = 1.9857$ ..... (3.19)

$A = 0.3931$

In this case where recovery is omitted the BVP model reduces to a single equation containing only one variable. It is interesting to note the resemblance between this case and the heterozygote inferior case of Fisher's equation, Case 3 (2.8), where the Huxley solution can also be interpreted as "excitation followed by a plateau of infinite duration". In both cases the reaction term is a cubic polynomial in u.

The existence and stability of periodic solutions to the BVP model is studied in [83]. For the stimulus added as an extra,

constant, term to the principal equation (2.45), the stability of the periodic solutions is dependent on the value of I.

No other analytical results exist in the literature except for the phase plane analysis of FitzHugh and the results on the simplified FitzHugh-Nagumo system which have been discussed in the previous paragraph.

3.3.4. The Hodgkin-Huxley system (Appendix B)

The Hodgkin-Huxley system has been obtained empirically and because of it's complexity very few analytical results have been obtained so far, except for the existence of certain types of solutions, namely pulse and periodic travelling wave solutions.

A study to be mentioned at the outset is that of Casten, Cohen and Lagerstrom [5]. Another useful survey, covering subsequent development and extensions of the theory behind the Hodgkin-Huxley equations is that of Evans [16].

As in the case of the BVP model, FitzHugh [29] also studies a modified version of the Hodgkin-Huxley model, which he calls the "Vm-reduced" system. The four variables V, m, h and n of the Hodgkin-Huxley system can be grouped into two classes: The fast variables V and m and the slow variables h and n. If h and n are kept at constant values (say at their resting state values), instead of being allowed to change slowly according to their differential equations, no recovery follows the excitation of the nerve. The pulse solution to the system is replaced by a wave front solution, which means that the potential remains at a constant value for an infinite period after excitation, instead of returning to the rest potential.

FitzHugh [29] draws these conclusions from a phase plane analysis. The full Hodgkin-Huxley system would require a phase space analysis which is far more complicated to study.

R.E. Plant [68] studies the space-clamped Hodgkin-Huxley model with the aid of yet another approximation. The approximation to the four-dimensional system is obtained by assuming that the fast variables V and m are described by algebraic rather than differential equations. Using this approach, known properties of the solution of the Hodgkin-Huxley equations, such as the threshold property, and repeated oscillation under constant current stimulus are successfully modelled.

The most comprehensive results concerning this system are those of G.A. Carpenter [4] who studies the existence of pulse and periodic solutions using a phase space analysis. The set of reaction-diffusion equations is arranged as consisting of a principal differential equation coupled with ℓ "slow" and m "fast" equations. In the Hodgkin-Huxley system $\ell = 2$ and $m = 1$. The principal, slow and fast equations are studied separately and then pieced together to form true solutions of the system. General conditions are given for the existence of pulse solutions, finite wave trains and periodic solutions. The results are too complicated and general to state here and the reader is referred to the original paper. Further results on the existence of periodic solutions is given in [84].

We conclude this paragraph by mentioning two more studies - that of Hassard [38] in which the existence of unstable periodic solutions is shown for small current stimuli and that of Sabah and Sprangler [76] in which the complex frequency-current-

voltage relation for the membrane is studied by linearizing the Hodgkin-Huxley equations. The interested reader is referred to these papers.

3.4. Numerical treatment

3.4.1. Introduction

In this discussion on computational results for the reaction-diffusion models of impulse propagation in the nerve, an outline is given of various numerical studies available in the literature. These studies are discussed briefly, with emphasis on the purpose and methods behind the studies, pointing to aspects which require investigation in the present numerical study.

3.4.2. Fisher's equation (2.3)

Although various theoretical results on the behaviour of solutions to Fisher's equation exist in the literature (§3.3.2), numerical results are, by comparison, rather scarce.

Following the construction of the model in 1937, Fisher [27] carried out a few computations to illustrate that the model was plausible. The computations were carried out by transforming the partial differential equation (2.3) to an ordinary differential equation, making use of the fact that $\frac{\partial p}{\partial t} = - v \frac{\partial p}{\partial x}$ when looking for a solution representing "a wave of stationary form advancing with velocity v". The equation was then integrated numerically for certain parameter values of p by means of expansions in terms of p. Fisher tabulated the form of the wave, so as to show, for different values of the density of the mutant

gene, the value of the gradient of gene ratio and the position at which this value occurs relative to the "centre" of the wave (the point in advance of which there are as many mutant genes as there are parent genes behind it).

A significant observation of Fisher, which has been proved subsequently (Theorem 3.5) is: "It appears that the actual velocity of advance must be the minimum compatible with the differential equation".

It is clear that very little computational work on this very interesting model exists. One of the purposes of the present study is therefore to carry out computations on Fisher's equation and to compare the computed results with the behaviour predicted by existing theorems and thus possibly obtaining a better understanding of the behaviour of the model.

3.4.3. Nagumo's equation and the FitzHugh-Nagumo system (equations (2.43, 2.44) and (2.41, 2.42), respectively).

The most comprehensive results on Nagumo's equation, theoretically as well as numerically are due to Rinzel and Keller [74].

Following McKean [53] the authors studied a slightly modified version of the original equation, namely where the non-linear reaction function $f(u) = u(1-u)(u-a)$ in (2.43) is replaced by the Heaviside step-function

$$f_1(u) = \begin{cases} -u, & u \leqslant a \\ a-u, & u > a, \end{cases} \qquad 0 < a \leqslant \frac{1}{2} \quad \ldots (3.20)$$

(See Fig. 3.6)

For this simplified Nagumo model they determined all periodic

and pulse travelling wave solutions. For certain parameter values there are two different pulse-shaped waves with different propagation speeds. These speeds are plotted as a function of the parameter a for various positive values of b (where a and b are the parameters in equations (3.20) and (2.44), respectively). Similarly curves are obtained for the pulse height and pulse width as a function of a for various values of b.

In the case of wave trains Rinzel and Keller give numerically determined curves for the propagation speed as a function of it's period and for the maximum amplitude as a function of the period.

The travelling wave solutions to Rinzel and Keller's version of Nagumo's equation is obtained by introducing the travelling wave co-ordinate $z = x + ct$ and then reducing the system to a single equation

$$V_c''' - cV_c'' - V_c' - \frac{b}{c} V_c = 0 , \qquad b > 0,\ c > 0$$

with appropriate initial and boundary conditions. The resulting initial boundary value problem is solved numerically by making use of a transcendental equation relating a, b and c and which had previously been obtained by McKean [53].

For the FitzHugh-Nagumo system (2.41, 2.42) Rinzel [71] obtained numerical results concerning periodic solutions by introducing the co-ordinate $z = \lambda x - \omega t$ and transforming the partial differential equations to ordinary differential equations (λ is the wavelength, ω the impulse frequency and $c = \frac{\omega}{\lambda}$ the speed of propagation). When the speed c is not known in advance, as

is the case here, a shooting technique is usually used. Rinzel replaces this technique with an alternative, described in [71], and determines a dispersion relation (ω against λ) for the family of periodic solutions.

Rinzel also solves the set of partial differential equations (2.41, 2.42) using an implicit Crank-Nicolson scheme and describes the stimulus-response properties of a uniform nerve model with a steadily maintained stimulus at a fixed location. For an appropriate range of stimuli repetitive firing occurs.

The intension of the present investigation is to study Nagumo's equation and the FitzHugh-Nagumo system using a Finite Element scheme. No modifications will be made to the original partial differential equations and the study will be extended to include an investigation of the influence of initial and boundary conditions on the initiation of pulse and periodic solutions.

3.4.4. The BVP model (equations 2.45, 2.46)

Very few studies on the numerical solution of the BVP equations have appeared in the literature. Two computer studies were carried out by FitzHugh, who also constructed the model [29, 30]. In the first of these he gives a motion picture description of impulse propagation using computer animation. The purpose was to help one visualize the changing state of an excitable membrane. The method is described as "an elementary finite step numerical approximation method". In the second of these studies a numerical method to solve the BVP equations is described in which the partial differential equations are transformed to ordinary differential equations, representing travelling wave equations. The system has solutions for two velocities -

presumably representing the stable and unstable travelling wave solutions.

Both these studies are unsatisfactory from the computational point of view. The first provide neither method nor numerical results and in the second case an iteration on the speed is needed because it is not known in advance. A direct solution of the partial differential equations would provide the speed as a result of the computations.

A particular study of importance is that of R.M. Muira [61] which is by far the most significant as far as numerical work on this model is concerned. In this paper only the stable solitary wave solution to the BVP equations is computed with the aim of finding an accurate method for computing the speed.

Three methods are used. In two of these the travelling wave co-ordinate $\xi = x - ct$ is used to transform the partial differential equations (2.45, 2.46) into a system of ordinary differential equations. The third method consists of solving the original partial differential equations directly by means of Lees' [52] modified Crank-Nicolson Finite Difference scheme in which the non-linear terms are evaluated using extrapolated values of the solution. This semi-implicit scheme is conditionally stable. The solitary wave emerges as long-time solution for sufficiently large stimulus. The speed of the wave is obtained from the calculated results.

A particular feature of Muira's calculations on the BVP model is that the stimulus is not modelled as a boundary condition but added to the right-hand side of the principal equation

(2.45) as an extra term.

Another feature of this paper is the "wave integrals" which are derived to determine the closeness of the computed solution to the exact solution. Although the BVP model does not have conserved integrals of motions as do some non-linear evolution equations such as the Korteweg-de Vries equation, integral expressions can be defined which must take on prescribed values when the solution is a solitary travelling wave. [For a single pulse integration is carried out over the whole of the ξ-axis, for periodic solutions only over one period].

We intend to construct a Finite Element scheme for solving the BVP model and to compare our results on the asymptotic speed of propagation to that of Muira.

One final study which should be mentioned is that of Copeland [13] which is a guide to the programs used by Muira [61]. The study concerns itself with programming aspects and efficiency of implimentation.

3.4.5. The Hodgkin-Huxley system (Appendix B)

The first computations on the Hodgkin-Huxley system were carried out using a desk calculator and are described in the original paper by Hodgkin and Huxley [45]. They solved the system in both the space-clamped case (in which the action potential is the same at every point of the axon) as well as in the case of a propagated action potential.

In the first case a numerical solution to a set of four or-

dinary differential equations is required. The principal equation is given by (2.17) and the three subsidary equations by (2.13, 2.15, 2.16). Hodgkin and Huxley solved this set of first-order ordinary differential equations using Hartree's [37] iterative integration method.

In the second case the principal equation is a partial differential equation ((1) of Appendix B). Hodgkin and Huxley avoided solving the partial differential equation directly by making use of the assumption that during steady propagation the curve of the potential V against time at any one position is similar in shape to that of V against distance at any particular instant.

It follows that $\frac{\partial^2 V}{\partial x^2} = \frac{1}{\theta^2}\frac{\partial^2 V}{\partial t}$ where θ is the velocity of conduction.

Hence the principal equation ((1) of Appendix B) reduces to

$$\frac{a}{2R\theta^2}\frac{d^2V}{dt^2} = C_m\frac{dV}{dt} + \bar{g}_K n^4(V-V_K) + \bar{g}_{Na} m^3h(V-V_{Na}) + \bar{g}_\ell(V-V_\ell) \quad \ldots\ldots (3.21)$$

with the subsidary equations remaining unchanged. The fact that θ is not known in advance requires the implimentation of a shooting method which is described in [45].

Good qualitative as well as quantitive agreement was found with experiment for both the space-clamped case and the propagated action potential at temperatures 6,3°C and 18,5°C. Other aspects in which they found good agreement with experimental evidence were the velocity of conduction (18,8 m/sec

calculated, 21,2 m/sec experimentally at temperature 18,5°C), the time course of impedance changes, net fluxes of potassium and sodium per impulse, absolute refractory period and recovery of excitability during the relative refractory period. The value of threshold to short current pulses, subthreshold responses and subthreshold oscillations during a long rectangular pulse are other aspects also studied.

Computations with a desk calculator are not only tedious but also time-consuming. The obvious answer to this is the digital computer and the first paper to be published on digital computer solutions of the Hodgkin-Huxley system was that of Cole, Antosiewicz and Rabinowitz [8] which appeared in 1955. Only the space-clamped action potential is studied with the principal equation (2.17) modified to allow for a total current varying with time:

$$I(t) = C_m \frac{dV}{dt} + \bar{g}_K\, n^4 (V - V_K) + \bar{g}_{Na}\, m^3 h (V - V_{Na}) + \bar{g}_\ell (V - V_\ell).$$

The subsidary equations (2.13, 2.15, 2.16) remain unchanged. The initial values of m, n and h are obtained by substituting V=0 into the subsidary equations and setting $\frac{dm}{dt} = \frac{dn}{dt} = \frac{dh}{dt} = 0$. These conditions imply that the axon is in a resting state before excitation.

Cole et al carried out integrations with the following three types of functions I(t):

(i) $I(t) = I_0, \quad t > 0, \quad I_0$ constant

(ii) $I(t) = I_0, \quad 0 < t \leqslant T$

(iii) $I(t) = \frac{It}{T}, \quad 0 < t < T, \quad I$ constant

$0, \quad t > T.$

The set of ordinary differential equations is solved using a fourth-order Runge-Kutta method. The threshold strength and duration curve was established. Repetitive firing was obtained for condition (i) above and furthermore the behaviour of the theoretical axon near threshold as well as the response to steadily rising currents were investigated.

The above calculations were only for the space-clamped case. We intend to investigate the effect of similar types of boundary conditions for the original Hodgkin-Huxley system.

In 1959 R. FitzHugh and H.A. Antosiewicz [31] extended the work of Cole et al [8] to account for a propagated action potential, in which all variables of state are functions of the space-variable x as well as the time-variable t. Again the relation

$$\frac{\partial^2 V}{\partial x^2} = \frac{1}{\theta^2}\frac{\partial^2 V}{\partial t^2}$$

is used to obtain an ordinary differential equation as principal equation:

$$V'' = K[V' + \frac{1}{C_m}(\bar{g}_K n^4 (V - V_K) + \bar{g}_{Na} m^3 h (V - V_{Na}) + \bar{g}_\ell (V - V_\ell)]$$

where

$$K = \frac{2R\theta^2 C_m}{a}$$

K is not known in advance because of it's dependence on θ as in the Hodgkin-Huxley case and must therefore be calculated by using a shooting method. The wave form desired is one in which V approaches zero as $t \to \pm \infty$. If an incorrect value of K is used in the calculation, V eventually becomes very large and diverge to $\pm \infty$. A single value of K is obtained for every temperature value. These calculations render single

pulses but fail to produce two or more successive propagated action potentials.

In all the numerical studies up to 1959 the Hodgkin-Huxley system was simplified to a system of ordinary differential equations and solved as such.

In 1966 Cooley and Dodge [11] were the first to endeavour solving the non-linear partial differential equation with the associated subsidary equations of Appendix B directly. They integrated the partial differential equation by using a Finite Difference scheme.

Their choice of initial conditions correspond to an axon in the steady state at the resting potential. The axon is then stimulated by a constant current stimulus of infinite duration at one end of the axon. This stimulus is added as an extra term to the right-hand side of the principal equation.

Cooley and Dodge carried out computations to determine the threshold strength and duration curve. They obtained repetitive firing in response to a maintained stimulus and compared their results with previous solutions to the space-clamped axon. The effect of temperature on the threshold intensity of a short stimulus and on the rheobase was also determined for a series of temperature values.

With the Finite Element scheme which is to be constructed in this study for solving the Hodgkin-Huxley system, one will be able to solve the system directly, as in the case of Cooley and Dodge [11]. This will enable us to compare the Finite Element scheme and Finite Difference schemes as applied

to this system.

In addition we intend to investigate the initiation of pulses for various types of boundary conditions.

A particular boundary condition, simulating a constant current of infinite duration, has been investigated by Stein [81] who constructed a frequency-current curve for a temperature of 6.3°C which shows that the frequency of pulses in a train is dependent on the strength of the current. Stein concentrated on the effect of alterations to the Hodgkin-Huxley system such as steadying potassium or leakage current densities. He also touches upon the matter of applying two stimuli sequentially with the hope of triggering two pulses and conjectures that this is dependent on the absolute refractory period. We feel that these two aspects have not been investigated to full extent, especially the question of repetitive stimuli giving rise to repetitive firing. The matter of a one-to-one correspondence between stimuli and firing will be investigated in Chapter 5 and a minimum time-lapse between stimuli will be established to ensure one-to-one correspondence. The method used by Stein is an implicit Finite Difference scheme; similar to one which had previously been used in [67] where the initiation of action potentials was investigated.

A recent study of Miller and Rinzel [57] deals with the phenomenon that not all pulses in a train seem to be travelling at the same speed. In general, pulse speeds and interspike intervals will not remain constant during propagation. This is a very interesting matter and a very recent branch of investigation which will thus also enjoy our attention in the present study.

CHAPTER 4

A FINITE ELEMENT STUDY OF FISHER'S EQUATION

4.1. Introduction

In this chapter we concern ourselves with the numerical solution of Fisher's equation (2.3). Fisher's equation is solved for particular functions $f(u)$ using the Crank-Nicolson-Galerkin method. The qualitative behaviour of the numerical solutions are then compared with the theoretical results quoted in the preceding chapter, concentrating on three aspects namely the asymptotic speed of propagation of a travelling wave, results on stability and convergence to wave fronts.

Cases 1 and 3 of Fisher's equation will be discussed in greater detail than Case 2 because of the similarity in behaviour of solutions of Case 2 to that of Case 1.

4.2. The Finite Element method for Fisher's equation

We need the following definitions:

Let Ω be a bounded domain in $\mathbb{R}^m$, $m \geq 1$,

$x = (x_1, x_2, \ldots, x_m) \in \Omega$, $dx = dx_1 \ldots dx_m$.

The Sobolev space H^1 is defined by

$$H^1(\Omega) = \{w \mid w \in L^2(\Omega), \frac{\partial w}{\partial x_i} \in L^2(\Omega), \ i=1,\ldots,m\}$$

and $$\|w\|_{H^1(\Omega)} = [\|w\|^2_{L^2(\Omega)} + \sum_{i=1}^{n} \|\frac{\partial w}{\partial x_i}\|^2_{L^2(\Omega)}]^{\frac{1}{2}}$$

where $L^2(\Omega)$ is the space of square integrable functions on Ω, that is, the space of functions which are measurable and such

that

$$\|w\|_{L^2(\Omega)} = [\int_\Omega w^2 \, dx]^{\frac{1}{2}} < \infty.$$

It is well-known that $L^2(\Omega)$ is a Hilbert space with respect to the inner product

$$(f,g) = \int_\Omega f(x)\, g(x)\, dx .$$

Also of interest is the space $H_0^1(\Omega)$, the subspace of $H^1(\Omega)$ consisting of those functions which vanish on $\partial\Omega$, the boundary of Ω.

The solution of Fisher's equation (2.3):

$$\frac{\partial u}{\partial t} = \frac{\partial^2 u}{\partial x^2} + f(u)$$

is based on the continuous time Galerkin method ([17]) where the weak solution $u \in H^1$ $(m = 1)$ satisfies

$$(\frac{\partial u}{\partial t}, v) = (\frac{\partial^2 u}{\partial x^2}, v) + (f,v) \quad \forall\ v \in H^1 \qquad \ldots\ldots (4.1)$$

with $(\ ,\ )$ denoting the L_2 inner product.

If we approximate u by $U \in K_N$, where $K_N = \text{span}\ \{\phi_1, \ldots, \phi_N\}$, a finite dimensional subspace of H^1, and

$$U(x,t) = \sum_{i=1}^{N} U_i(t)\phi_i(x),$$

then (4.1) becomes, after integration by parts,

$$(\frac{\partial U}{\partial t}, \phi_j) + (\frac{\partial U}{\partial x}, \phi_j') = (f,\phi_j) + [\frac{\partial U}{\partial x}\, \phi_j]_{\partial\Omega} \qquad \ldots\ldots (4.2)$$

$$j = 1, 2, \ldots, N$$

where a dash denotes differentiation with respect to x, and

$[\frac{\partial U}{\partial x}\,\phi_j]_{\partial\Omega}$ is a boundary term which is necessarily zero as consequence of our choice of basis functions unless possibly when $j = 1, N$. For homogeneous Dirichlet boundary conditions equation (4.2) applies only for $j = 2,3,\ldots,N-1$ and for homogeneous Neumann conditions, the boundary terms vanish for $j=1,N$. For boundary conditions other than the two types mentioned above, the terms $[\frac{\partial U}{\partial x}\,\phi_j]$, $j = 1,N$ are not zero and is represented by b_1 and b_N respectively, $b_i = 0$, $2 \leqslant i \leqslant N-1$.

Evaluation of (4.2) leads to the system of ordinary differential equations

$$M\,\dot{\underline{\alpha}} + S\,\underline{\alpha} = F(\underline{\alpha}) + \underline{b} \qquad \ldots\ldots \qquad (4.3)$$

where $M = ((\phi_i,\phi_j))$, $S = ((\phi_i',\phi_j'))$, $\underline{\alpha} = (U_1, U_2, \ldots, U_N)^T$, $\underline{b} = (b_1,0,0,\ldots,0,b_N)^T$ and a dot denotes differentiation with respect to time.

The matrices M and S are known as the mass and stiffness matrices respectively. Equation (4.3) represents the semi-discrete Galerkin method, and to obtain approximate solutions to this set of ordinary differential equations the time variable t is discritised. If k is an interval in time and m a positive integer, we put

$$\begin{aligned} t &= mk \\ \dot{\underline{\alpha}} &= \frac{1}{k}(\underline{\alpha}^{m+1} - \underline{\alpha}^{m}), \quad m = 0, 1, 2,.. \\ \underline{\alpha} &= \frac{1}{2}(\underline{\alpha}^{m+1} + \underline{\alpha}^{m}), \quad m = 0, 1, 2, .. \end{aligned} \qquad \ldots\ldots \qquad (4.4)$$

in (4.3) where $\underline{\alpha}^m$ is an approximation to $\alpha(mk)$.

This leads to the Crank-Nicolson-Galerkin (C.N.G.) method which is second order correct in time. It requires the solution of a

system of non-linear algebraic equations at each time step:

$$\sum_{i=1}^{N} \left[\left(\frac{\alpha_i^{m+1} - \alpha_i^m}{k} \right) (\phi_i, \phi_j) + \left(\frac{\alpha_i^{m+1} + \alpha_i^m}{2} \right) (\phi_i', \phi_j') \right]$$

$$- \left(f\left(\sum_{i=1}^{N} \frac{\alpha_i^m + \alpha_i^{m+1}}{2} \phi_i \right), \phi_j \right) - b_j = 0 \qquad \ldots\ldots (4.5)$$

$$j = 1, \ldots, N$$

$$m = 0, 1, 2, \ldots$$

This is solved by Newton's iteration method ([49]):

If the system to be solved is

$$\underline{f}(\underline{X}) = 0$$

one iteration consists of solving

$$J(\underline{X}^{\nu})(\underline{X}^{\nu} - \underline{X}^{\nu+1}) = f(\underline{X}^{\nu})$$

for $(\underline{X}^{\nu} - \underline{X}^{\nu+1})$ where $J(\underline{X})$ is the Jacobian matrix $\frac{\partial J(\underline{X})}{\partial \underline{X}}$.

The iteration terminates when $|f(\underline{X}^{\nu}) - f(\underline{X}^{\nu+1})| < \varepsilon$ where $\varepsilon = 10^{-5}$.

In the examples considered in this study, three iterations per time step are required for convergence.

As basis function $\{\phi_i\}_{i=1,\ldots,N}$ we choose piece-wise linears (hat functions) depicted in Figure 4.1.

The resulting linear tridiagonal system is solved using Gaussian elimination [49]. (See Appendix D).

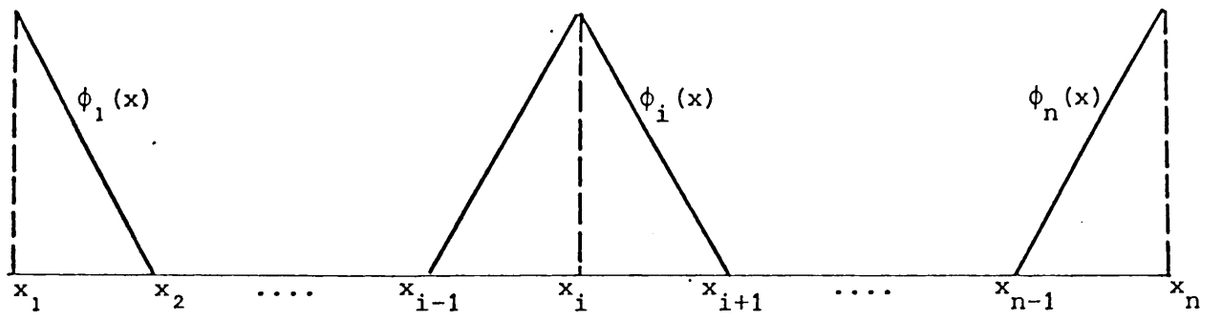

Figure 4.1: Graph of $\phi_1(x), \phi_n(x)$, $2 \leq \phi_i(x) \leq n-1$.

4.3. Solution to Fisher's equation for $f(u) = u(1-u)$

4.3.1. Wave front solutions

We recall from equation (3.8) that

$$U'' + cU' + f(U) = 0 , \qquad c > 0 \qquad (\xi = x - ct)$$

is the relevant equation to solve when looking for travelling wave solutions to Fisher's equation, travelling to the right. For a wave travelling to the left the corresponding equation is

$$U'' - cU' + f(U) = 0 , \qquad c > 0 \qquad (\xi = x + ct) \qquad \ldots\ldots (4.6)$$

If $f(U) = U(1-U)$ (the example function for case 1 of Fisher's equation), a solution in closed form is not available to (3.8) or (4.6) (§ 3.3.2.4) so that we resort to numerical techniques.

Equation (4.6) is solved numerically using a "search technique". We rewrite (4.6) as a first order system

$$\begin{aligned} U' &= W \\ W' &= cU' + U^2 - U \end{aligned} \qquad \ldots\ldots (4.7)$$

The initial conditions are

$$\begin{aligned} U &= 0,99 \\ W &= 0,01 \quad \text{at} \quad \xi = \chi \end{aligned} \qquad \ldots\ldots (4.8)$$

where χ is an arbitrary point somewhere to the right of the origin of the ξ-axis. We note that

$$\left.\begin{aligned} U &= 1 \\ W &= 0 \end{aligned}\right\} \qquad \ldots\ldots \quad (4.9)$$

is a solution to (4.7) which signifies biologically that all of the population consists of one type of individuals. In (4.8) we consider a slight disturbance from this condition with the hope of obtaining a solution different from (4.9).

The numerical procedure used is Hamming's Predictor-corrector method ([51]) with Runge-Kutta fourth order method ([51]) to provide the required additional starting values [For details of these methods see Appendix D]. It is clear from these methods that using (4.9) as initial conditions at $\xi = \chi$, no other solution than that given by (4.9) will be generated.

A calculation is carried out starting at $\xi = \chi$ and proceeding to the left on a grid with spacing $h = 0{,}1$.

The initial values are then changed to

$$\begin{aligned} U &= 0{,}999 \\ W &= 0{,}001 \end{aligned}$$

and another calculation is carried out. The initial point is moved to the right until the two calculations "coincide" as $\xi \to -\infty$. This process is repeated once more.

The results of the calculations are as follows:
In agreement with a result of Rothe [75] which has been given in Theorem 3.5 (§ 3.3.2.2) solutions are found for values of c greater than some minimal value c^*. In our case $c^* = 2$.

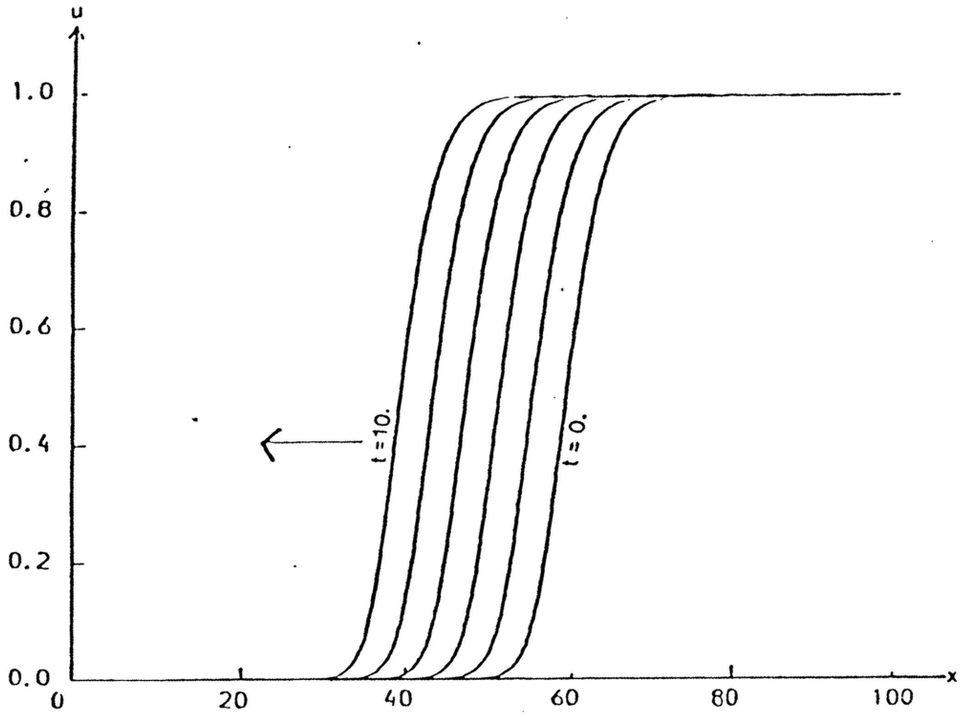

Figure 4.2: Solution of Fisher's equation, $f(u) = u(1-u)$, with $u(x,0)$ obtained from solving Eq.(4.6) for $c = 2$.

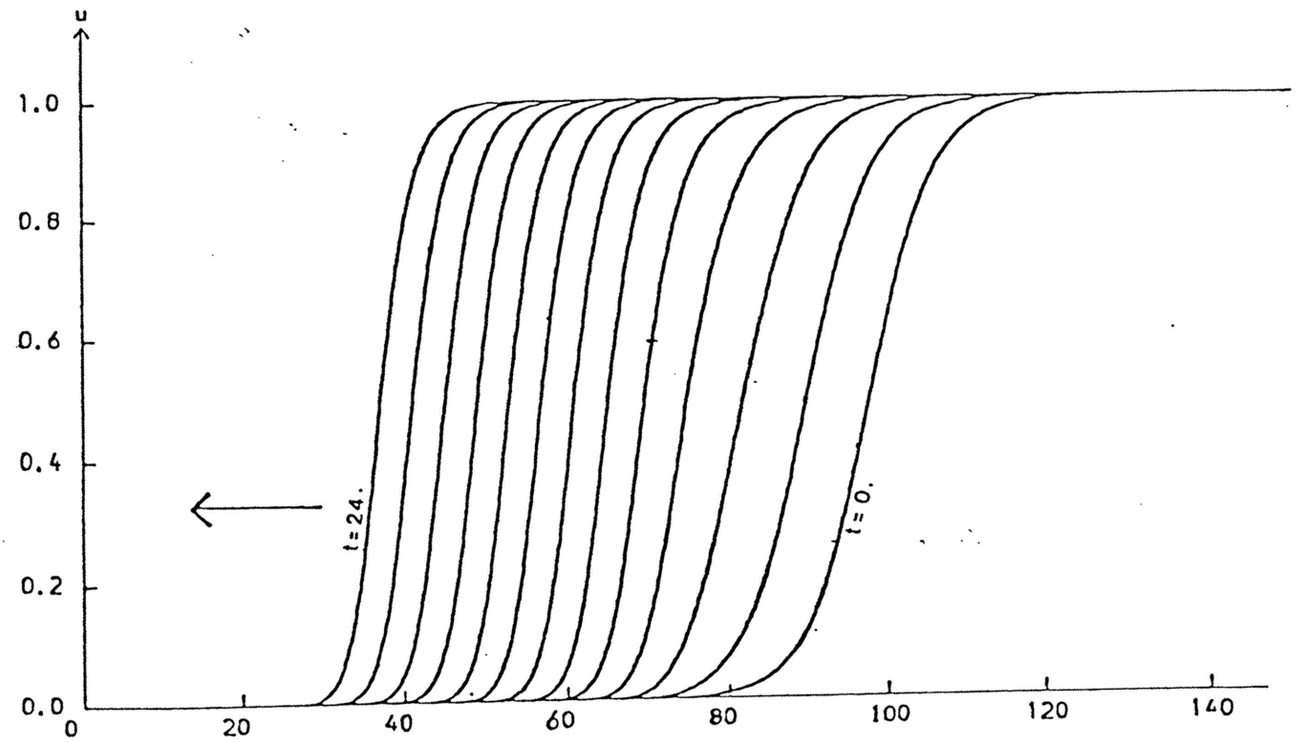

Figure 4.3: Solution of Fisher's equation, $f(u) = u(1-u)$, with $u(x,0)$ obtained from solving Eq.(4.6) for $c = 4$.

For values less than $c^* = 2$. oscillations occur in the solution. The solutions obtained for $c = 2$ and $c = 4$ are shown in the graphs for $t = 0$ in Figures 4.2 and 4.3 respectively. These are wave front solutions which satisfy $U(-\infty) = 0$, $U(\infty) = 1$.

The value of $c^* = 2$ corresponds to $\sqrt{4f'(0)}$ which Aronson and Weinberger [1] give as a lower bound for the speed of any possible travelling wave solution.

The discussion on stationary patterns (§ 3.3.2.4) showed that no non-constant zero-speed travelling wave solutions exist for Fisher's equation with $f(u) = u(1-u)$. This again, correlates with the fact that equation (4.6) has no solutions for $c < c^*$.

4.3.2. Time-progressing solutions

Fisher's equation (2.3) with $f(u) = u(1-u)$ is solved using the Crank-Nicolson-Galerkin method as described in § 4.2. The mesh size $h = 0{,}5$ and time-step $k = 0{,}5$.

4.3.2.1. The asymptotic speed of propagation

(1) The initial data $\underline{\alpha}(0)$ for the first time-progressing calculation is the solution obtained numerically from solving the system (4.7) for $c = 2$. The boundary conditions are $u(0,t) = 0$ and $u(100,t) = 1$.

In this case the initial data is transmitted with the asymptotic speed approximating 2 moving to the left and remaining unaltered in shape (see Figure 4.2).

(2) The initial data $\underline{\alpha}(0)$ for the second time-progressing calculation is the solution obtained numerically from solving the system (4.7) for $c = 4$. The boundary conditions are

the same as in (1).

In this case the profile changes rapidly to assume the shape of the initial data for the case $c = 2$. The speed initially 4 converges to the asymptotic speed $c^* = 2$ (obtained from following $u = 0,5$ in time). (See Figure 4.3).

We can conclude, therefore, that although the ordinary differential equation (4.6) has solutions for values $c \geqslant c^* = 2$ representing wave fronts, the only wave front solution obtainable from a time-progressing solution of Fisher's equation, as in this study, is the front travelling with asymptotic speed c^*. To cover both the cases of waves travelling to the left and to the right one could say that travelling wave solutions exist only if $|c| \geqslant c^*$ where the speed c is positive if the wave is travelling in one direction, negative in the other.

4.3.2.2. Results on stability

We refer back to Theorems 3.1(1) and 3.2 in which it is stated that the only stable equilibrium state for both the pure initial value problem and the initial-boundary value problem in Case 1 is $u \equiv 1$.

We use various examples of initial and boundary data to verify this for the example function $f(u) = u(1 - u)$. Results are as follows: Any non-zero rectangular pulse (or stimulus) taken as initial data, however small the dimensions, evolves in time to converge to the stable equilibrium state $u \equiv 1$. This can also be verified by starting with initial data $u \equiv 1$ everywhere, except for a finite x-interval where $u \neq 1$. The disturbance is eliminated rapidly and the solution converges to $u \equiv 1$ as time

Solutions of Fisher's equation, f(u) = u(1-u), using various types of initial and boundary data as indicated:

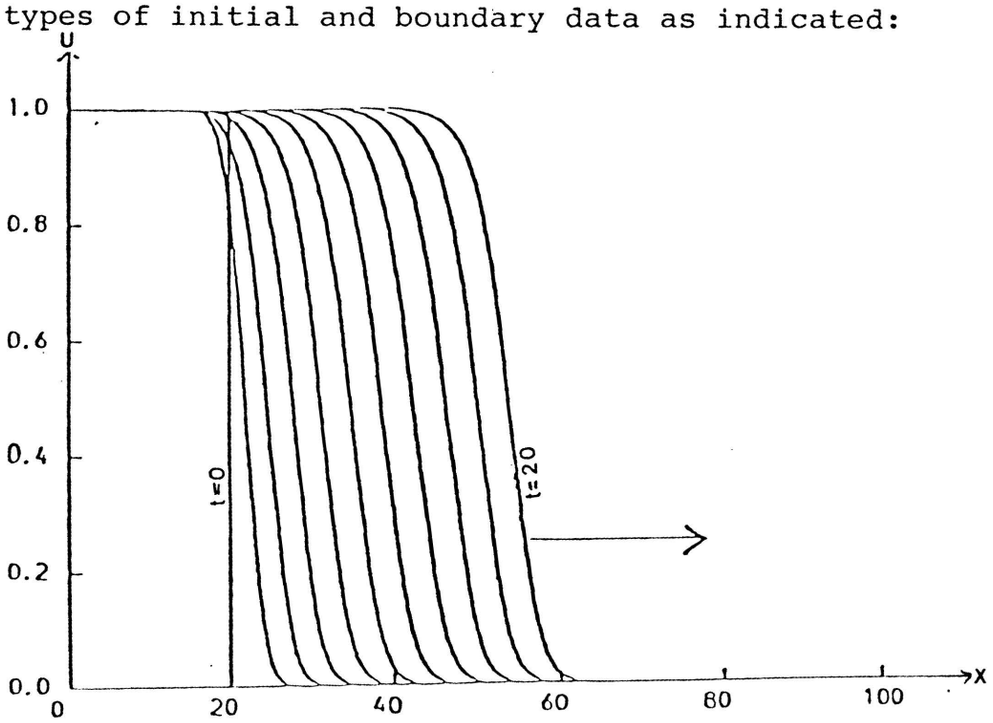

Figure 4.4.

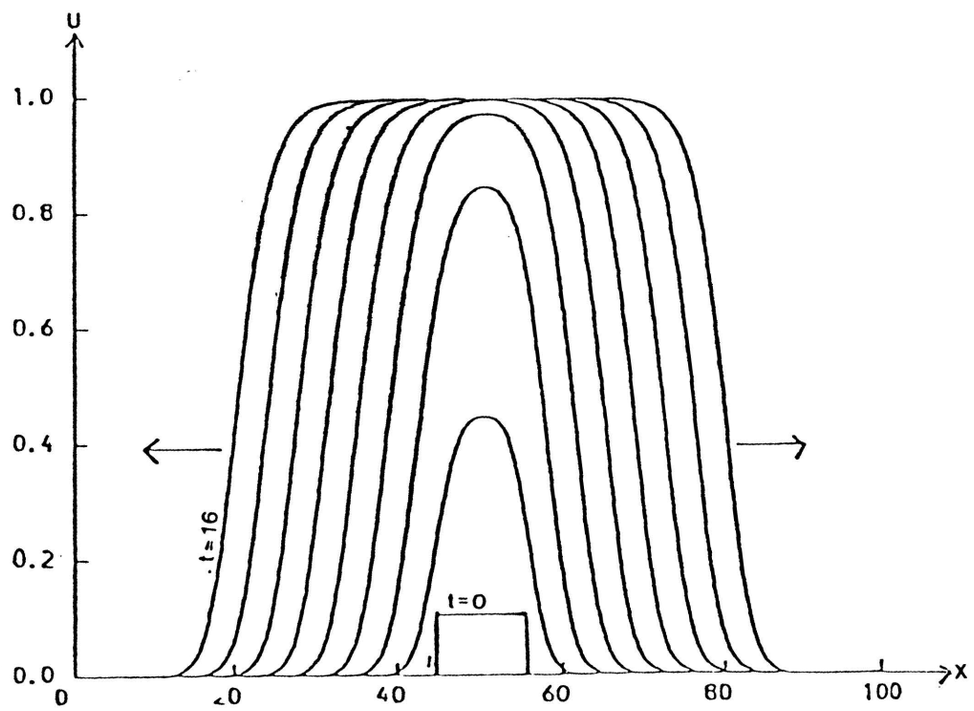

Figure 4.5.

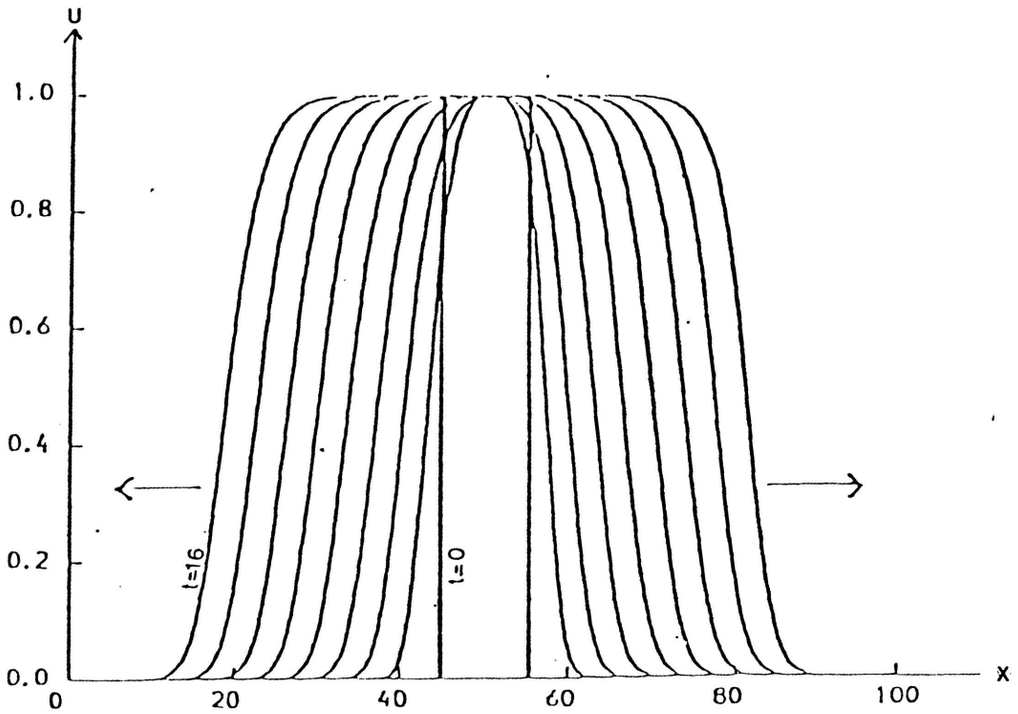

Figure 4.6.

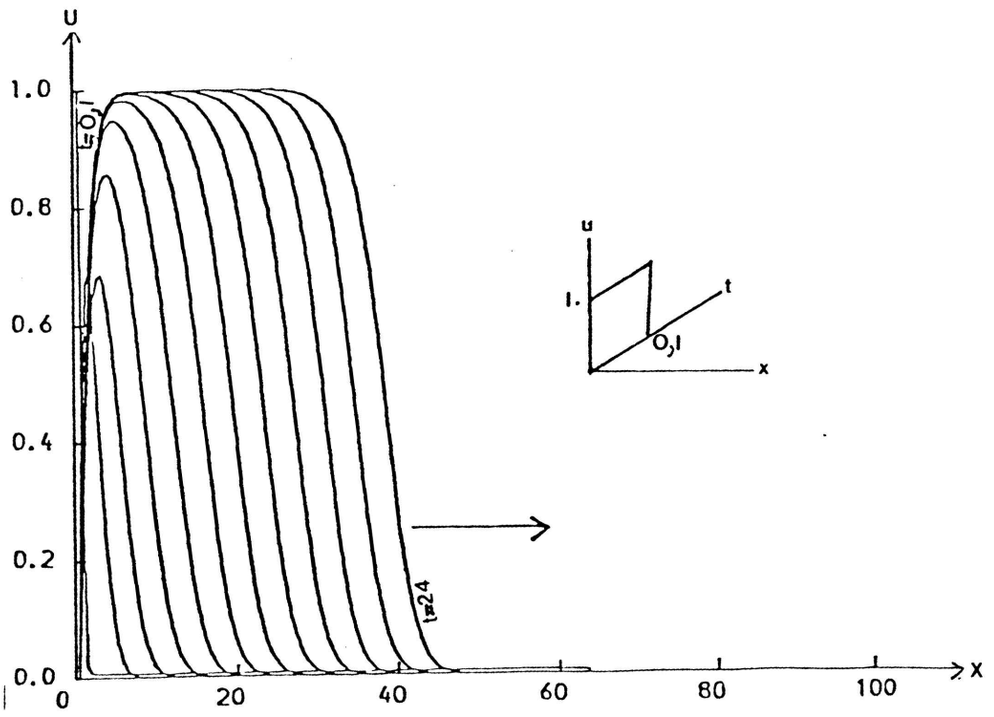

Figure 4.7.

progresses.

Similar results hold for the initial-boundary value problem. A rectangular pulse, applied for however small a duration of time, grows to unity and is propagated away from the boundary verifying the fact that $u \equiv 1$ is the only stable equilibrium state. (See Figures 4.4. - 4.7)

4.3.2.3. Convergence to wave fronts

(1) Consider the results depicted in Figures 4.4 - 4.7.

If any rectangular stimulus is taken as initial data the height grows to one and the data evolves into two wave fronts travelling in opposite directions, one with speed rapidly converging to 2 and the other to -2. The shape of the two wave fronts propagating away from each other converges rapidly to the shape of the solution $U(\xi)$ to the travelling wave equation for $c = 2$ and to $U(-\xi)$ respectively.

(2) In the case of a rectangular stimulus as boundary data such as

$$u(o,t) = \begin{cases} \beta & \text{for } t \leqslant T \\ 0 & \text{for } t > T \end{cases} \quad , \; 0 < \beta \leqslant 1, \; T > 0$$

we obtain the following boundary layer pattern for $t >> T$:

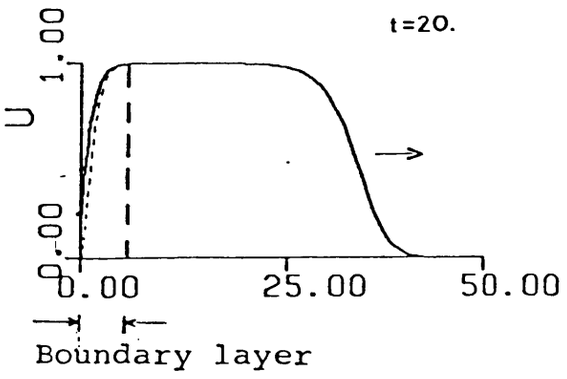

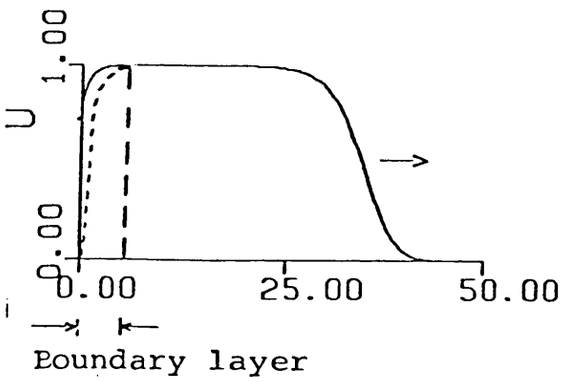

The boundary condition for $t > T$ seems to be inappropriate because the solution obtained is inconsistent from the physical point of view. The population densities are kept at a fixed value on the left-hand boundary which can be interpreted as an external force keeping the population densities fixed. More appropriate would probably be $\frac{\partial u}{\partial x}(0,t) = 0$ for $t > T$ in which case the value of $u(0,t)$ is expected to grow to one and remain at one for $t > T$. (See § 5.2.1 or 5.5.2.2).

For the boundary condition $u(0,t) = 1$, $t \geqslant 0$ a wave front starts propagating away from the boundary with asymptotic speed c^*. The speed converging from below had a value of 2,082 at $t = 28$.

(3) An interesting case is obtained if we exceed the restriction $0 \leqslant u(x,t) \leqslant 1$ and take a rectangular stimulus with height 2, as initial data. The height is rapidly reduced to 1. and the wave fronts are propagated to the left and the right with shape and speed according to the travelling wave solution for the asymptotic speed $c^* = 2$. (See Figure 4.9).

4.4. Solutions to Fisher's equation for $f(u) = u(1-u)(u-a)$

The relevant equation to solve when looking for travelling wave solutions is, in this case, given by

$$U'' + cU' + U(1-U)(U-a) = 0 \qquad c > 0 \quad \ldots\ldots \quad (4.10)$$

where $\xi = x - ct$, the wave travelling to the right. We recall from § 3.3.2.4 that an exact solution to (4.10) exists, namely the Huxley solution, given by equation (3.9):

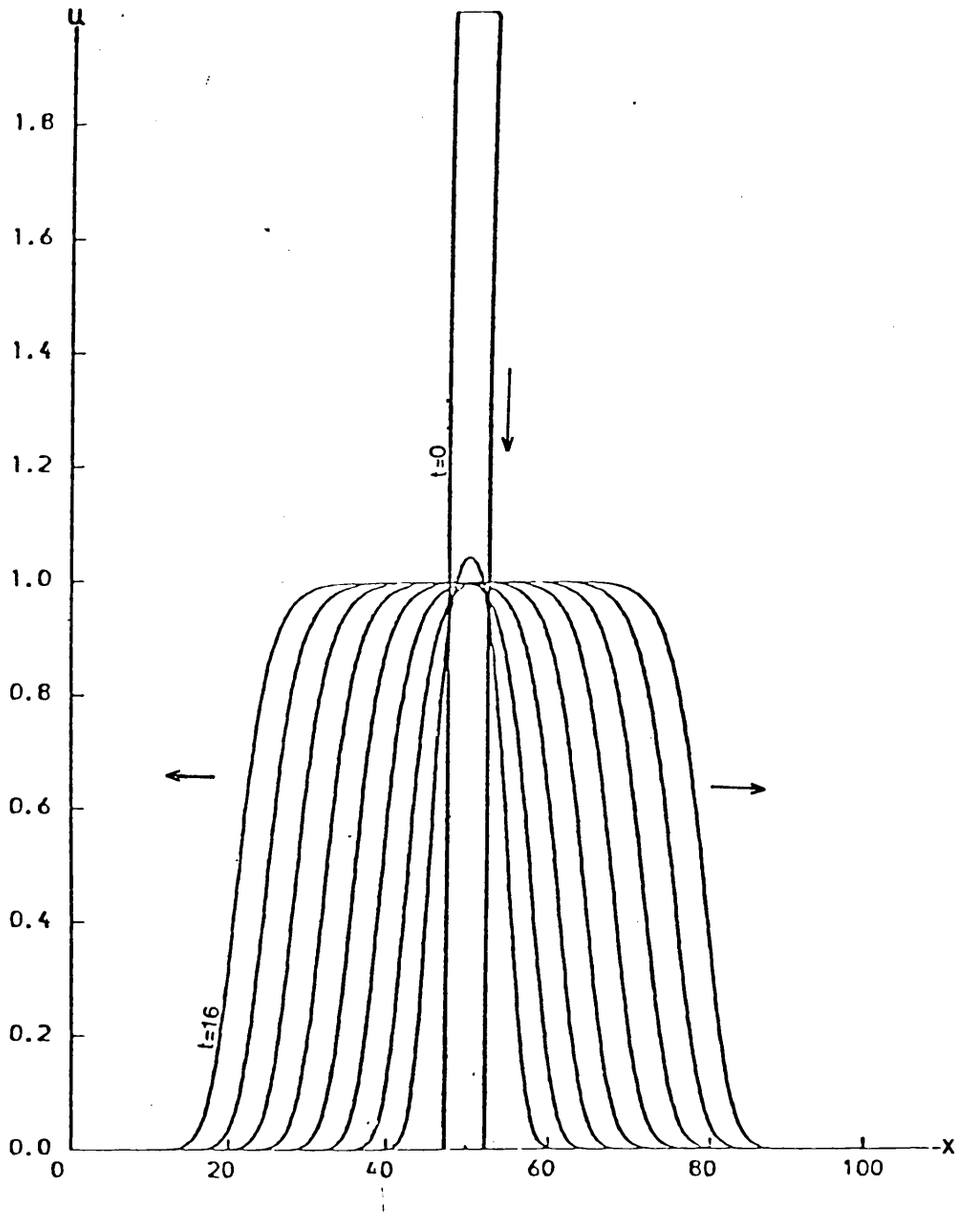

Figure 4.9: Solution of Fisher's equation, f(u) = u(1-u), with initial data as indicated.

$$U(\xi) = 1/\,(1 + \exp(-\xi/\sqrt{2})) \qquad \ldots\ldots \quad (4.11)$$

where $c = \sqrt{2}(\frac{1}{2} - a), \qquad 0 < a \leqslant \frac{1}{2}$ $\ldots\ldots$ (4.12)

We also recall the result of Rothe, given as Theorem 3.6 (§ 3.3.2.2), which states that for a particular function f only one velocity c^* exists, admitting wave front solutions, which is verified in this study.

We solve Fisher's equation as a partial differential equation using the Crank-Nicolson-Galerkin method for various initial and boundary conditions.

4.4.1. The asymptotic speed of propagation

(1) We first take the Huxley solution, given in (4.11), as initial data for $a = \frac{1}{4}$. The wave front is propagated to the left, the shape of the front remaining unchanged and the speed c being approximately the Huxley speed. For $a = \frac{1}{4}$ and $h = k = 0{,}5$ the computed speed was found to be 0,3544. The exact speed is 0,3535.

The interesting case is of course when $a = \frac{1}{2}$ which had been mentioned in connection with stationary patterns (§ 3.3.2.4) and which represents a zero-speed travelling wave.

In this case our calculations show that the wave front remains absolutely fixed and the speed is therefore zero. Even more interesting is the fact that a step function as initial data, e.g. $u(x,0) = 0$ if $x < 0$, $u(x,0) = 1$ if $x \geqslant 0$ changes shape as time develops until it assumes the values of the exact solution with the point $u = 0{,}5$ remaining stationary. (Note that when $a = \frac{1}{2}$ $1 - u$ is a solution

of Fisher's equation if u is a solution, which implies that a vertical line through u = 0,5 divides the solutions into symmetrical parts).

4.4.2. Results on stability

We recall the discussions on the threshold property exhibited in this case (following Theorems 3.1 and 3.2 of § 3.3.2.2). These imply that any initial or boundary data either dies away rapidly or grows to unity, with no intermediate possibilities. This conclusion is verified for initial data by the results depicted in Figures 4.10 and 4.11.

We first take a rectangular pulse as initial data and determine the dimensions of such a pulse which would be sufficient to trigger a travelling wave (or travellings waves as is the case). This gives rise to a threshold curve which we establish for $a = \frac{1}{4}$. (See Figure 4.12). Any rectangular distribution of which the dimensions fall within the shaded region will evolve into a travelling wave.

Note that according to Theorem 3.8 (§ 3.3.2.3) the height of the initial distribution should exceed the value of a. In this case where $a = \frac{1}{4}$ it corresponds to our findings.

Similarly we take a rectangular distribution as boundary data at $x = 0$ with zero initial data, $u(x,0) \equiv 0$, $x > 0$, and solve the problem in the quarter plane $x \geq 0$, $t \geq 0$. The solution, again, either dies away or grows to unity as t increases. (See Figure 4.13 and 4.14). A threshold curve for this is given in Figure 4.15. A stimulus of which the dimensions fall within the shaded area will produce a wave whereas one outside would not.

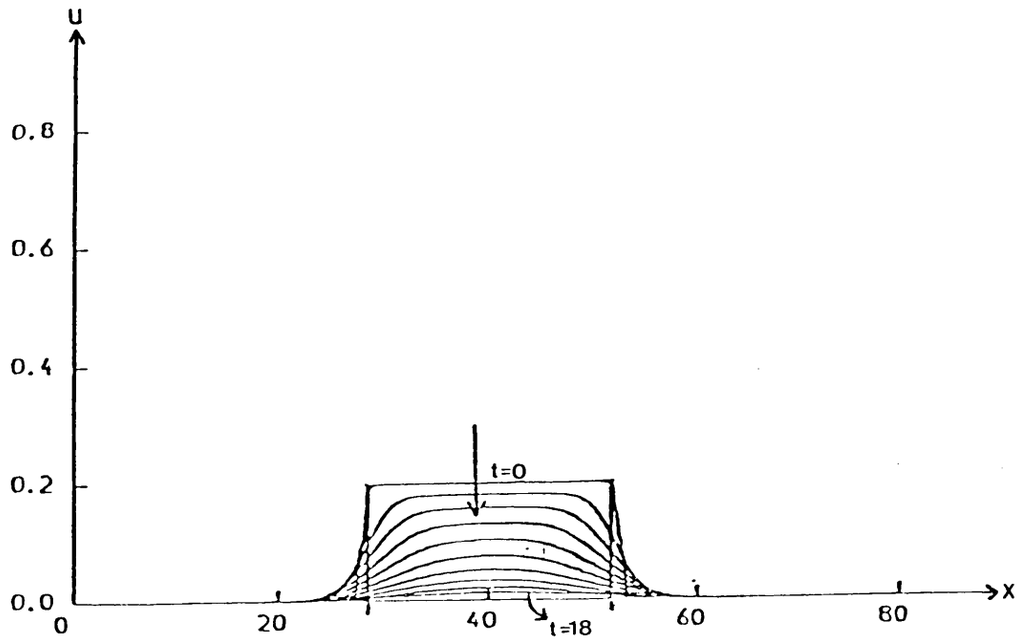

Figure 4.10: Solution of Fisher's equation with $f(u) = u(1-u)(u-a)$ using sub-threshold initial data.

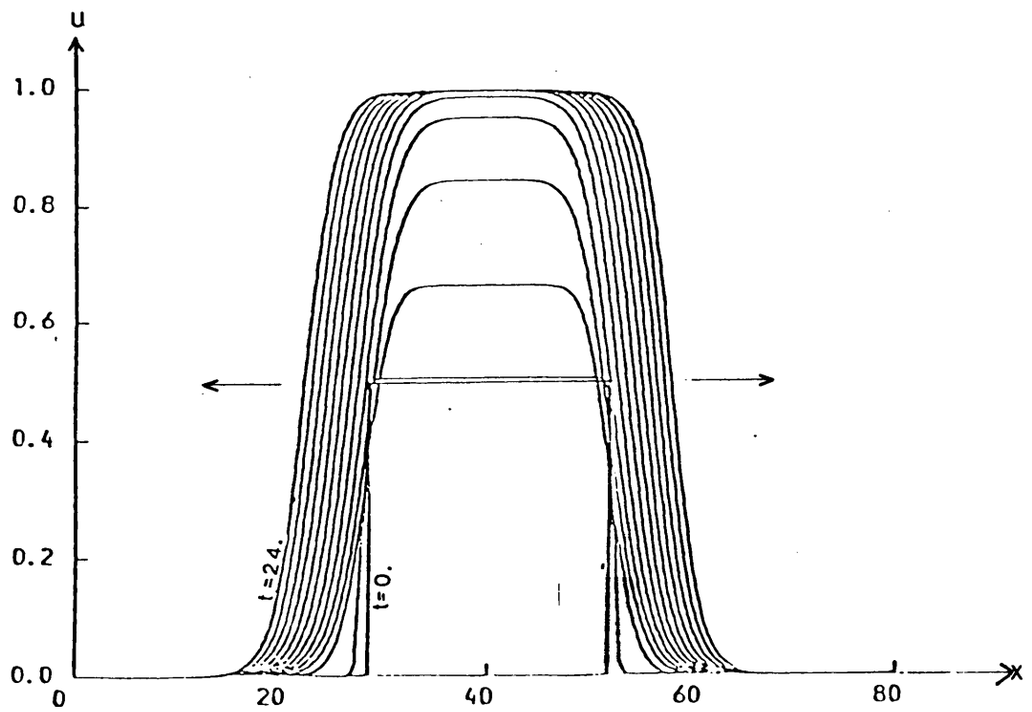

Figure 4.11: Solution of Fisher's equation with $f(u) = u(1-u)(u-a)$ using super-threshold initial data.

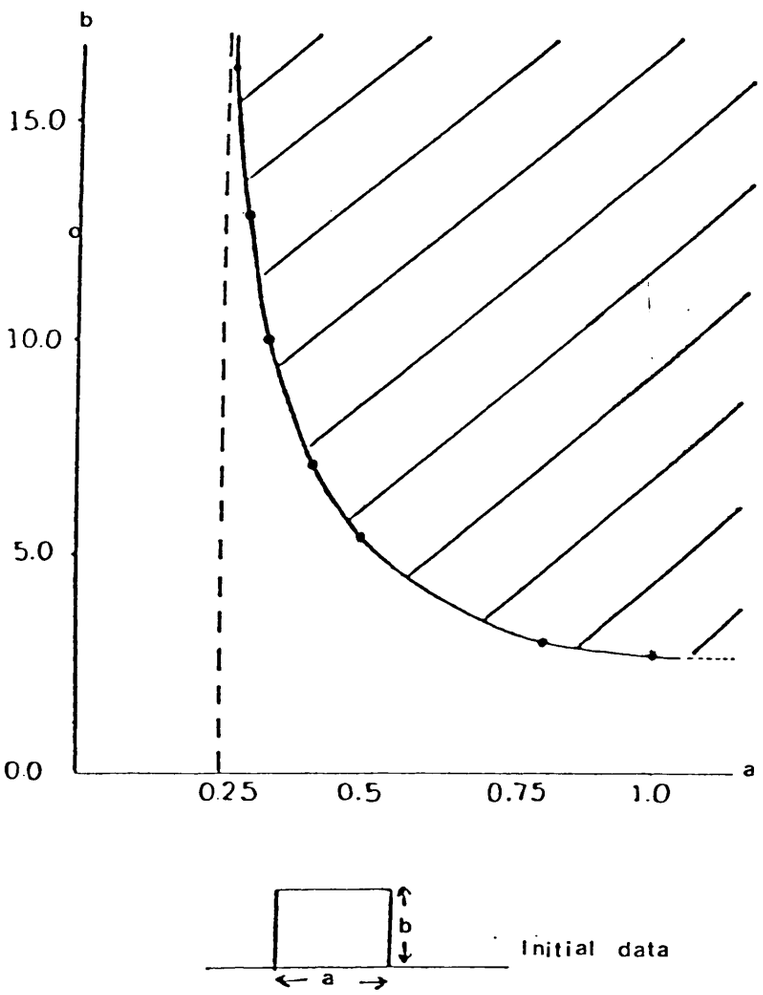

Figure 4.12: Threshold strength curve for the pure initial value problem associated with Fisher's equation with $f(u) = u(1-u)(u-\alpha)$, $\alpha = \frac{1}{4}$.

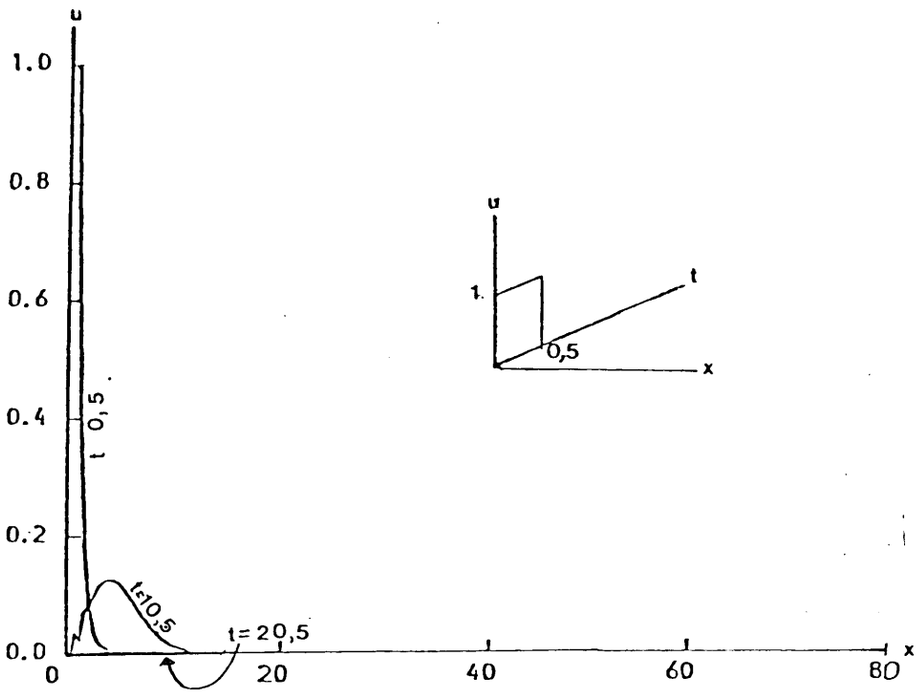

Figure 4.13: Solution of Fisher's equation with $f(u) = u(1-u)(u-a)$ using sub-threshold boundary data.

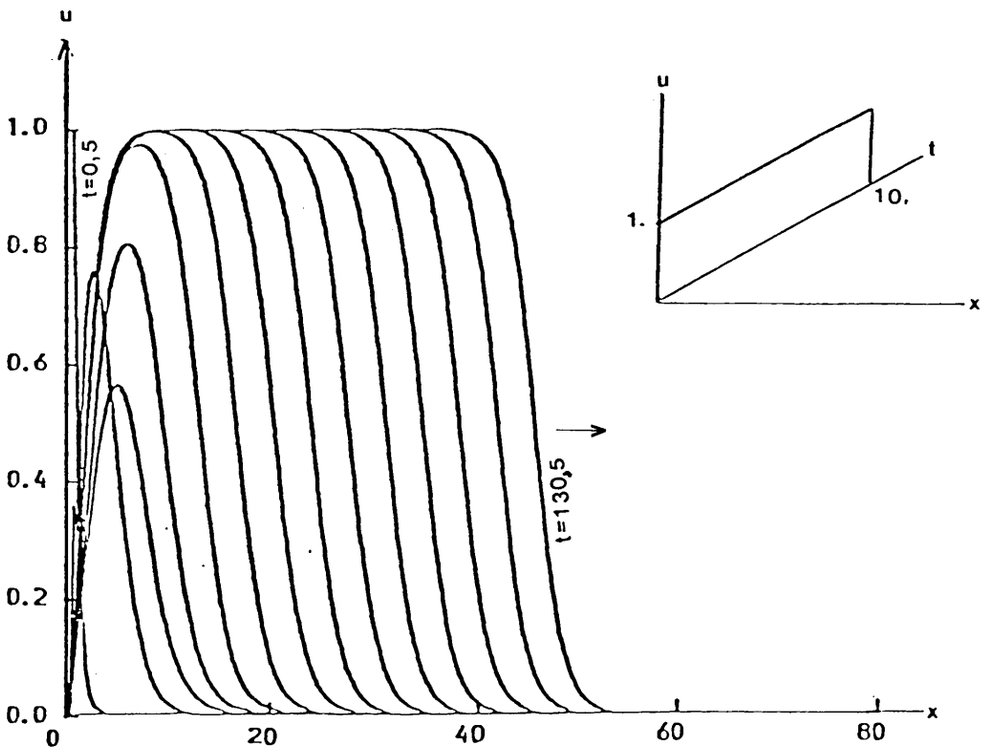

Figure 4.14: Solution of Fisher's equation with $f(u) = u(1-u)(u-a)$ using super-threshold boundary data.

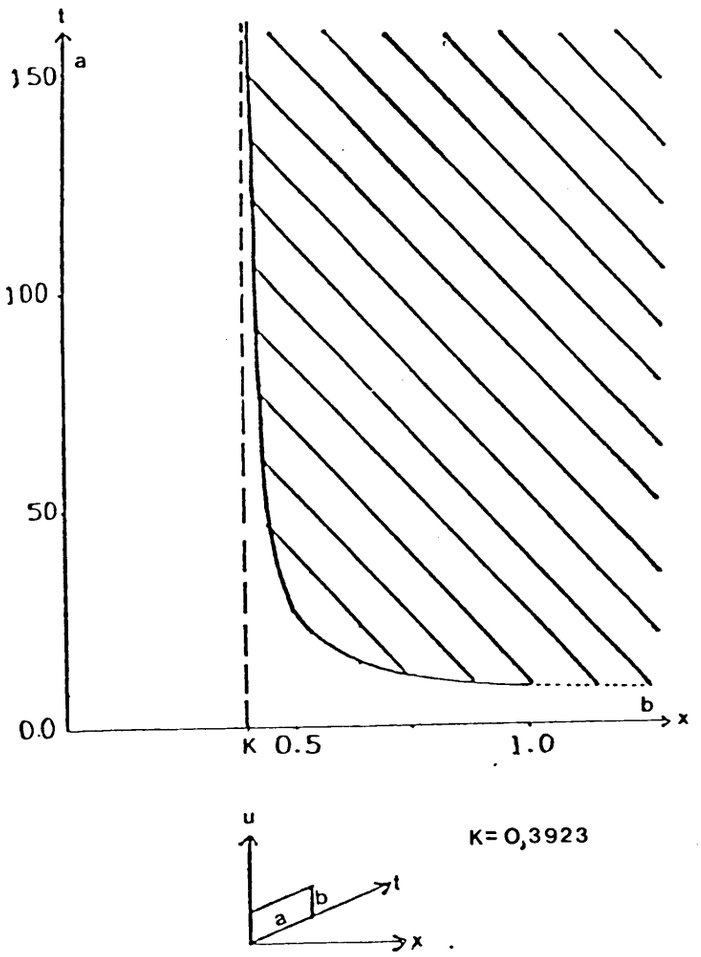

Figure 4.15: Threshold strength and duration curve for the initial-boundary, value problem associated with Fisher's equation, $f(u) = u(1-u)(u-\alpha)$, $\alpha = \frac{1}{4}$.

Note that the height of a rectangular stimulus on the boundary, according to Theorem 3.3 should exceed K where K is such that $\int_0^K f(u)du = 0$.

For $a = \frac{1}{4}$ and $f(u) = u\ (1-u)(u-a)$ and $a = \frac{1}{4}$,

$$K = 0{,}3923$$

which is shown in Figure 4.15 as a lower bound for the height of the rectangular boundary distribution. This corresponds to our findings.

4.4.3. Convergence to wave fronts

We recall Theorems 3.7 and 3.8 (§ 3.3.2.3) concerning the convergence to a travelling wave front from monotone initial data and concerning the convergence to two wave fronts travelling in opposite directions from initial data obeying the threshold conditions.

Our experiments indicate the following:

(1) A rectangular initial distribution with dimensions within the shaded region of Figure 4.11 grows to one and is then propagated to the left and the right. The shapes of the wave fronts are those of the Huxley solution $U(\xi)$ and $U(-\xi)$ with speeds $c_1 = \sqrt{2}(\frac{1}{2} - a)$ and $c_2 = -c_1$ respectively.

(2) For boundary data $u(0,t) = a_o$, either of the following situations occur for large t:

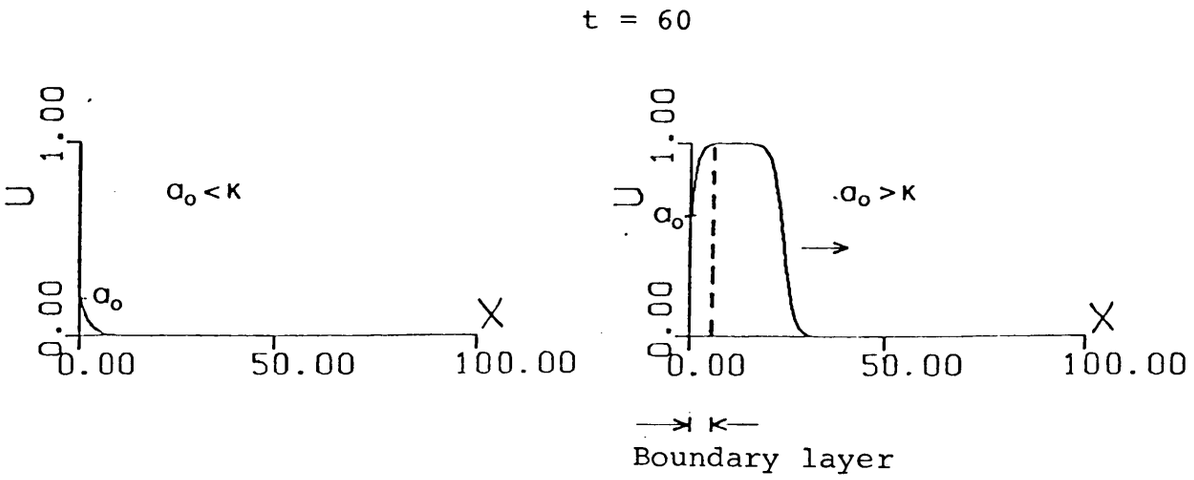

Figure 4.16

(K is defined as before)

In both cases boundary layers form on the left-hand boundary. If $a_o = 1$ a front obeying the shape and speed of the Huxley solution propagates away from the boundary.

(3) If we exceed the condition $0 \leq u(x,t) \leq 1$ as in the previous case and use a rectangular initial distribution with height 2, the height is rapidly reduced to 1 and propagated to the left and right according to the Huxley formula.

(4) If we insert Dirichlet boundary conditions on both the left- and right-hand boundaries,

with $u(x,0) = 0$, $0 < x < L$,

values of $u(0,t)$ and $u(L,t)$ exceeding the threshold value a, lead to two wave fronts being generated at the respective boundaries, one travelling to the right, the other to the left with shape and speed obeying the Huxley formula. On collision the two fronts do not eliminate each other. In the region of the collision the value of the solution u increases from zero to one until the

stable equilibrium state of unity is reached eventually throughout the interval on the X-axis, except close to the boundary where a boundary layer could form due to the Dirichlet boundary conditions.

The outcome of various possible boundary conditions are indicated in Figure 4.17.

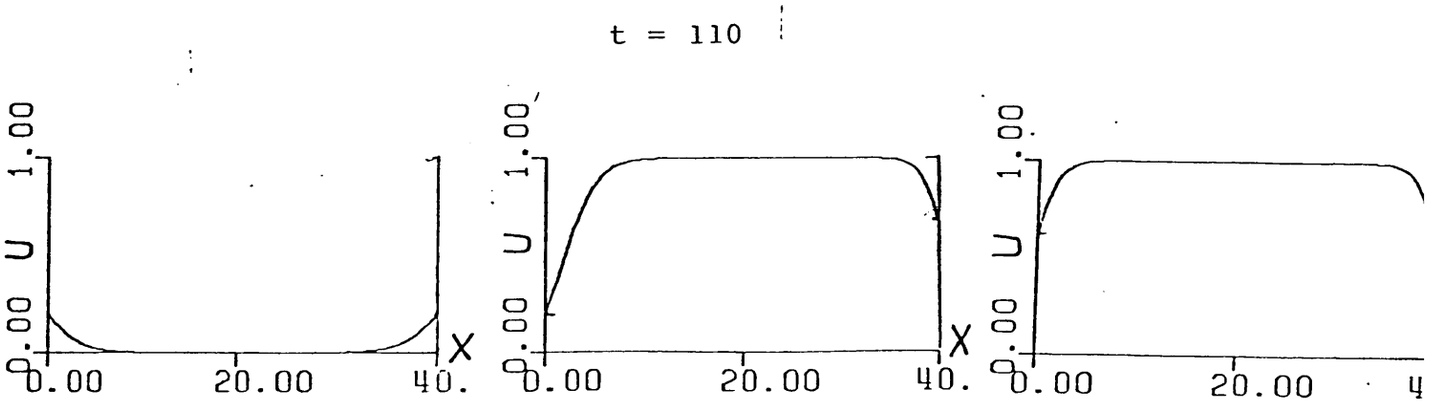

Figure 4.17.

Thus if the value of either u(0,t) or u(L,t) exceeds the value of a then u(x,t) would attain the value 1 throughout the interval except close to the boundaries.

4.5. Solution of Fisher's equation for f(u) = u(1-u)(a-u)

We will discuss this particular case of Fisher's equation briefly. The behaviour of solutions in this case is essentially the same as in the case of a quadratic f, case 1.

The ordinary differential equation (3.8) with f(U) = U(1-U)(a-U), which is the equation which need be solved when looking for travelling wave solutions, has no exact solutions existing in literature.

We solve, numerically, the partial differential equation

$$\frac{\partial u}{\partial t} = \frac{\partial^2 u}{\partial x^2} + u(1-u)(a-u) \qquad \ldots\ldots \quad (4.13)$$

to verify the theoretical results on stability, the asymptotic speed of propagation and the existence of wave fronts as discussed in Chapter 3.

We refer back to Theorems 3.1(2), 3.4 and the remark following Theorem 3.2. Summarizing these results: The only stable equilibrium state in this case is $u \equiv a$ and furthermore there exists a travelling wave front solution $U = q^*(x-c^*t)$ of (3.8) such that

$$\lim_{\xi \to -\infty} q^*(\xi) = a$$

where c^* is the asymptotic speed of propagation.

The Crank-Nicolson-Galerkin method was used to solve (4.13) in order to verify the theoretical results mentioned above.

(1) Various rectangular initial distributions were used to verify the results on <u>stability</u>. The results to this were similar to that of Case 1. Any non-zero disturbance increases or decreases to the value of a and is then propagated in two opposite directions. In the case of boundary data a boundary layer forms if the height of the boundary data differs from the value of a. Close to the boundary a travelling front with height equal to a starts propagating away from the boundary. The situation is depicted in Figure 4.18.

(2) Another point of interest is the asymptotic speed of propa-

gation. For $a = 0,75$ the speed was calculated from the numerical solutions as 1,748 and for $a = 0,25$ it was 0,9676. These correspond well to the values of $2\sqrt{f'(0)} = 1,732$ for $a = 0,25$ and $2\sqrt{f'(0)} = 1,000$ respectively. This, again, correlates to the behaviour of solutions in Case 1 where the asymptotic speed $c^* = \sqrt{4f'(0)}$. [1]

(3) According to Aronson and Weinberger [1] travelling wave solutions exist for all $c \geqslant c^*$ if $f'(0) > 0$ (as is the case). Of these, however, only the solution for $c = c^*$ would be obtained in a time-progressing calculation as had been verified for Case 1 (§ 4.3.2.1).

(4) A final point to be made is that the behaviour described in (1) and (2) was obtained for various sample values of a between 0 and 1. Even values of a less than ½ gave the same results. Apparently no restriction on a is necessary as in case 3 . (see § 2.3.4 of Chapter 2 on this matter).

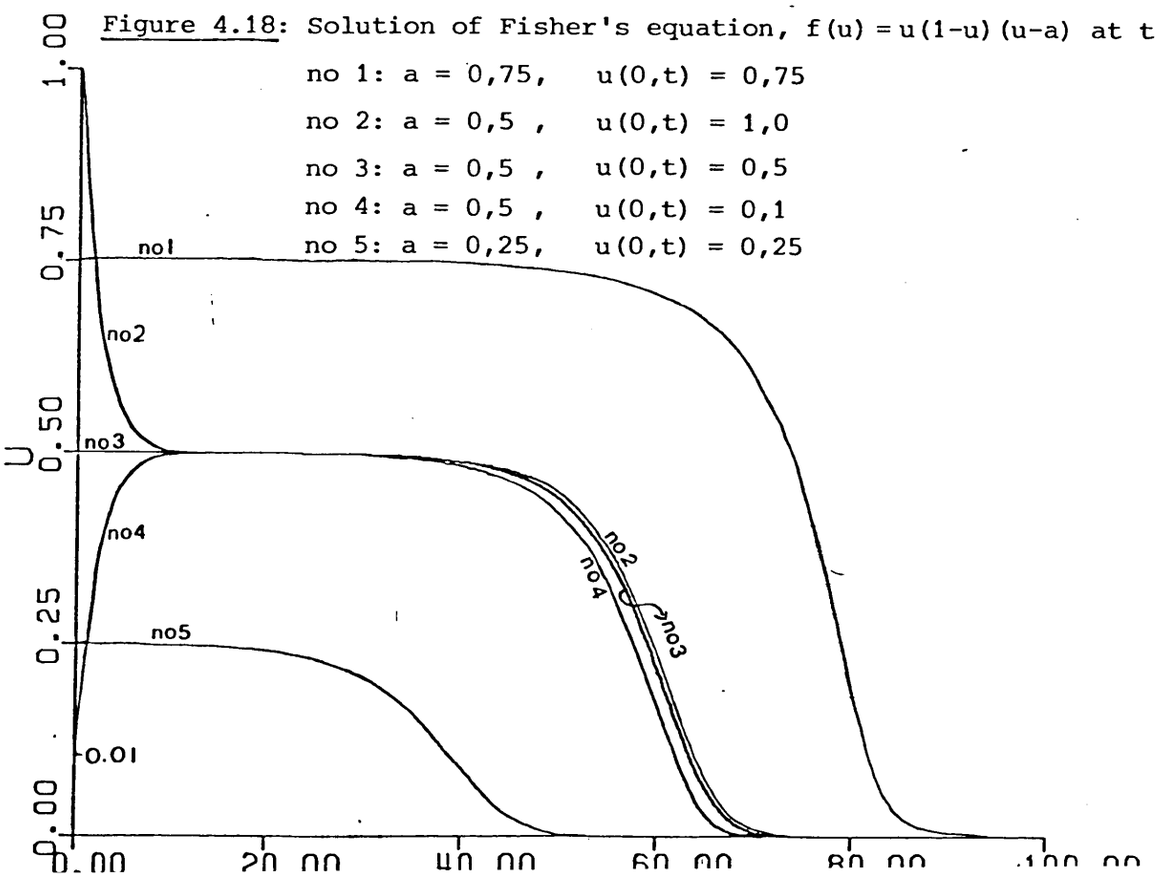

Figure 4.18: Solution of Fisher's equation, $f(u) = u(1-u)(u-a)$ at $t = 50$:
no 1: a = 0,75, u(0,t) = 0,75
no 2: a = 0,5 , u(0,t) = 1,0
no 3: a = 0,5 , u(0,t) = 0,5
no 4: a = 0,5 , u(0,t) = 0,1
no 5: a = 0,25, u(0,t) = 0,25

4.6. A drift term added to Fisher's equation

When discussing the construction of Fisher's model of population genetics (§ 2.2.2 of Chapter 2) it was pointed out that complicating factors such as unequal increase in population in opposite directions were ignored for the sake of simplicity. In this paragraph we will touch upon this matter in order to illustrate how such a complicating factor affects the numerical method to be used. The example we look at is the one discussed in § 2.2.2 where a term involving a first space derivative (called the drift term) is added to Fisher's equation.

The relevant equation is

$$\frac{\partial u}{\partial t} = \frac{\partial^2 u}{\partial x^2} - m\frac{\partial u}{\partial x} + u(1-u)(u-a) \qquad \ldots\ldots \quad (4.14)$$

where the constant $m > 0$ and $0 < a \leqslant \frac{1}{2}$.

If, once again, we look for travelling waves moving to the left and follow the derivation of equation (3.8) we get

$$U'' + (c-m)U' + U(1-U)(U-a) = 0 \ , \quad ' = \frac{d}{d\xi} \qquad \ldots\ldots \quad (4.15)$$

Equation (4.15) has the Huxley solution (see § 3.3,2.4)

$$U(\xi) = [1 + \exp(-\frac{\xi}{\sqrt{2}})]^{-1}$$

provided that $c - m = \sqrt{2}(\frac{1}{2} - a)$ $\qquad \ldots\ldots \quad (4.16)$

and so the velocity of the wave front travelling to the left is

$$c = \sqrt{2}(\tfrac{1}{2} - a) + m \qquad \text{where} \quad m > 0, \quad 0 < a \leqslant \tfrac{1}{2} \quad \ldots(4.17)$$

and the velocity of the front travelling to the right is

$$c = -\sqrt{2}(\tfrac{1}{2} - a) + m \qquad \ldots\ldots \quad (4.18)$$

Starting with a rectangular initial distribution, sufficiently large to produce a travelling wave, the solution is propagated to the left and right with speeds approximately as given by (4.17) and (4.18). This implies that the population increases at different rates in opposite directions as had been conjectured in § 2.2.2.

The main problem, however, in handling the drift term arises in the numerical solution of the partial differential equation (4.14) for arbitrary initial and boundary conditions. Experience gained in solving (4.14) without the reaction term has shown that both Finite Difference and Finite Element methods give rise to large oscillations in the numerical solution if m has a significantly large modulus value. The interested reader is referred to [47] for methods (including "upwinding") of treating this malaise. To illustrate the point we show in Figure 4.19 a C.N.G. solution of (4.14) with increasing time for $m = 20$, $a = 0,25$, $u(0,t) = 1$, $u(100,t) = 0$, grid spacing $h = 0,5$, time-step $k = 0,1$. In Figure 4.20 we show a C.N.G. solution of (4.14) for $m = 50$, $u(x,0) = 1$, $160 \leqslant x \leqslant 220$, $k = 0,1$. The offending oscillations are clearly visible.

4.7. Discussion of the numerical solutions

In all the calculations of which the results have been described in paragraphs 4.3.2, 4.4, 4.5 and 4.6 Fisher's equation was solved using the Crank-Nicolson-Galerkin method with $h = k = 0,5$ and $a = \frac{1}{4}$ unless otherwise stated. The test and trial functions used were piece-wise linears.

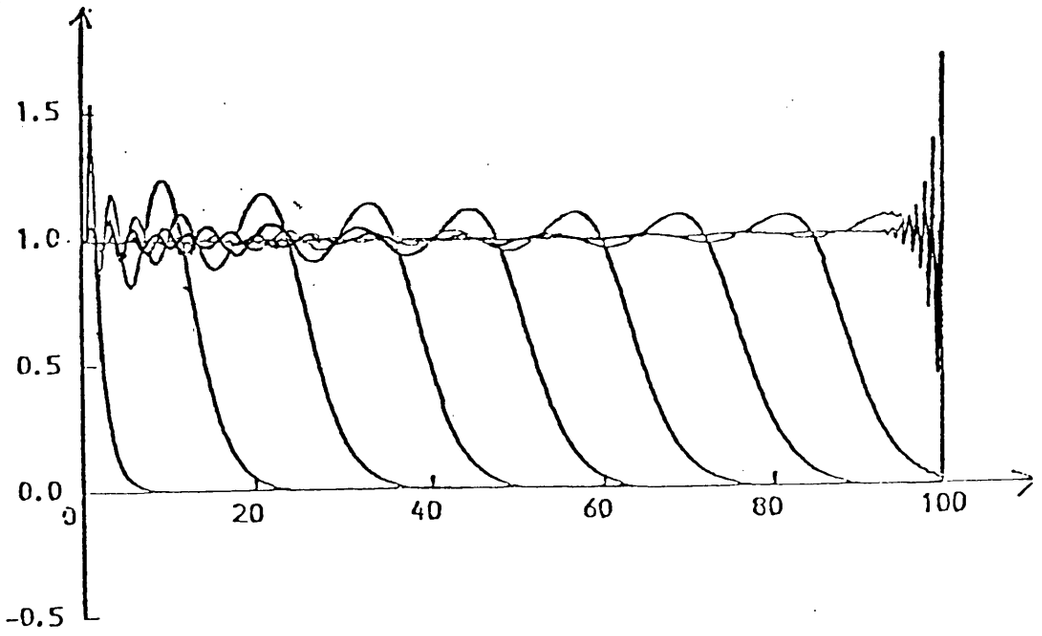

Figure 4.19: Solution of $\frac{\partial u}{\partial t} = \frac{\partial^2 u}{\partial x^2} - m\frac{\partial u}{\partial x} + u(1-u)(u-a)$, $M = 20$, $a = 0{,}25$, $k = 0{,}1$, $u(0,t) = 1$, $u(100,t) = 0$ depicted at various stages up to where a fixed pattern has formed.

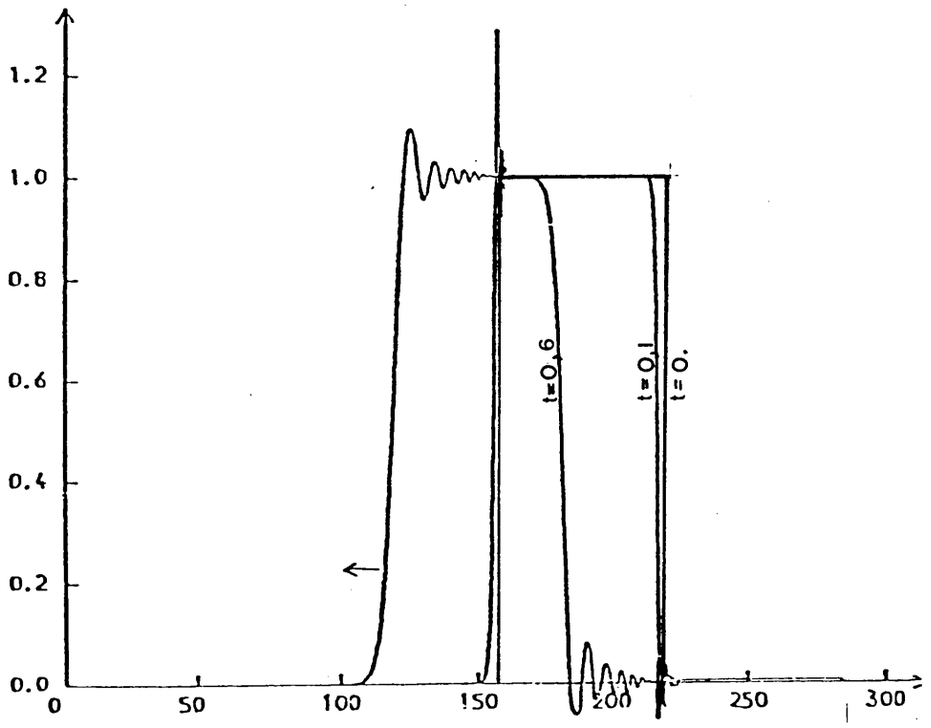

Figure 4.20: Solution of $\frac{\partial u}{\partial t} = \frac{\partial^2 u}{\partial x^2} - m\frac{\partial u}{\partial x} + u(1-u)(u-a)$, $m = 50$, $a = 0{,}25$ and $k = 0{,}1$.

The question arises: What criterion may be used to obtain a meaningful comparison between the results of one numerical method and that of another? Probably the best answer to this would be to compare the computed propagation speeds yielded by the different methods. A conjecture which had to be rejected was that the numerical method would affect the accuracy with which the equilibrium state $u = 1,00$ would be attained. Experiments showed, however, that the value of 1,0000 is reached exactly with no approximation error whatsoever.

The rather coarse mesh and the linear basis functions rendered good results contrary to expectations. For $k = h = 0,5$ in case 3 where $f(u) = u(1-u)(u-a)$, $a = \frac{1}{4}$ we obtained the value $c = 0,3543795$, when the actual speed should be $\sqrt{2}(\frac{1}{2} - a) = 0,3535533...$ Decreasing the time step to $k = 0,1$ changed the speed very little (10^{-3}).

Another change which gave no improvement was to substitute equation (4.4):

$$\underline{\alpha} = \frac{1}{2}(\underline{\alpha}^{m+1} + \underline{\alpha}^{m}), \qquad m = 0,1,2, \ldots$$

of the C.N.G. method with

$$\underline{\alpha} = s\,\underline{\alpha}^{m+1} + (1-s)\underline{\alpha}^{m}, \qquad m = 0,1,2, \ldots$$

where different values of s were tried, $0 < s < 1$.

For $s = 0,6$ the speed is $c = 0,3554$ and for $s = 0,75$ the speed is $c = 0,3571$, both worse than for $s = 0,5$.

For $s = 0,45$ the speed improves to $c = 0,3538$ but slight oscillations in the solution make their appearance. The

maximum height of the wave front which had stayed fixed at 1,000000 suddenly had oscillations to the order of 10^{-2}.

When employing the Crank-Nicolson-Galerkin method we used piece-wise linear basis functions. One would expect to obtain better results (for speed for example) when using quadratic basis functions. This is impractical, however, because the non-linear reaction term makes employing rather tedious. For $f(u) = u(1-u)$ the term (u^2, ϕ_i) produces more than three times the number of terms to be calculated when ϕ_i is a quadratic basis function than when ϕ_i is linear.
For a term such as (u^3, ϕ_i) which is obtained when $f(u) = u(1-u)(u-a)$ the situation would even be worse.

An exact measurement of the speed has been studied by Muira [61] for the BVP model. Our method was to follow a fixed point on the wave front ($u = 0,5$) and then interpolate (using cubic polynomials) to find the distance it had travelled for a certain lapse of time. As the wave settles to a fixed shape the speed converges to a fixed value. This method which is far less complicated that the one Muira used gave satisfactory results and employment of a more intricate method was considered unnecessary.

CHAPTER 5

A FINITE ELEMENT STUDY OF THE HODGKIN-HUXLEY EQUATIONS

5.1. Introduction

In this chapter the models of impulse propagation in the nerve are studied numerically. We first investigate the three simpler models, namely Nagumo's, FitzHugh-Nagumo's and the BVP model. A Finite Element scheme is constructed by means of which it is possible to investigate aspects such as the qualitative behaviour of solutions and the asymptotic speed of propagation of travelling pulses, emerging as long-time solutions for sufficiently large stimuli. Another aspect to which considerable attention is paid is the boundary data necessary to generate a single pulse or a train of pulses.

The Hodgkin-Huxley system is studied in greater detail than the three simpler models. We employ the Finite Element method once again and investigate the effect of various types of boundary data on the solutions. Of particular interest are the results obtained for repetitive stimulation (such as periodic boundary data). In this case not only the initiation of pulse and train solutions will be discussed but also the speeds of individual pulses in a train which need not necessarily be the same for all pulses.

5.2. Solution of Nagumo's equation

5.2.1. Numerical procedure

Nagumo's equations are given by (2.43, 2.44):

$$\frac{\partial u}{\partial t} = \frac{\partial^2 u}{\partial x^2} + u(1-u)(u-a) - w$$

$$\frac{\partial w}{\partial t} = bu \qquad , \quad b > 0, \quad 0 < a < 1$$

We note that equation (2.43) differs from Fisher's equation (2.3) with $f(u) = u(1-u)(u-a)$ only in the last term of (2.43) with the variable w making it's appearance, which is then connected to the variable u through equation (2.44). We intend following basically the same procedure as for solving Fisher's equation described in § 4.2.

Our solution is based on the continuous time Galerkin Method where the weak solution $u \in H^1$, $w \in H^1$ satisfy

$$(\frac{\partial u}{\partial t}, v) = (\frac{\partial^2 u}{\partial x^2}, v) + (f,v) - (w,v) \quad \forall\ v \in H^1 \qquad \ldots\ldots (5.1)$$

and $$\frac{\partial w}{\partial t} = b\,u \qquad \ldots\ldots (5.2)$$

We approximate u and w by $U \in K_N$ and $W \in K_N$, respectively, where $K_N = \text{span}\{\phi_1, \ldots, \phi_N\}$, a finite-dimensional subspace of H^1,

$$U(x,t) = \sum_{i=1}^{N} U_i(t)\phi_i(x)$$

$$W(x,t) = \sum_{i=1}^{N} W_i(t)\,\phi_i(x)$$

where ϕ_i, $1 \leqslant i \leqslant N$ are basis functions and $U_i(t)$, $W_i(t)$, $1 \leqslant i \leqslant N$, are time dependent coefficients.

We first deal with the simpler equation (5.2) which reduces to a first order differential equation

$$\sum_{i=1}^{N} \dot{W}_i(t)\phi_i(x) = b \sum_{i=1}^{N} U_i(t)\phi_i(x) \qquad \ldots\ldots (5.3)$$

Using the Trapezoidal rule formula, we obtain

$$\frac{1}{k}\,(\tilde{W}_i^{m+1} - \tilde{W}_i^m) = \frac{b}{2}(\tilde{U}_i^{m+1} + \tilde{U}_i^m), \qquad 1 \leqslant i \leqslant N, \qquad \ldots\ldots \quad (5.4)$$

$$m = 0,1,2, \ldots$$

where k is the time-increment as before, $\tilde{W}_i^m$ an approximation to $w(x_i, km)$.

Equation (5.1) becomes, after integration by parts

$$(\frac{\partial U}{\partial t}, \phi_j) + (\frac{\partial U}{\partial x}, \phi_j') = (f, \phi_j) - (W, \phi_j) + [\frac{\partial U}{\partial x}\,\phi_j]_{\partial\Omega}, \qquad j = 1,2,\ldots,N$$

$$\ldots\ldots \quad (5.5)$$

where $[\frac{\partial U}{\partial x}\,\phi_j]_{\partial\Omega}$ is a boundary term which is zero unless possibly when $j = 1, N$. For conditions other than homogeneous Dirichlet or Neumann conditions, the boundary terms are not zero and are taken to be b_1 and b_N respectively.

Evaluation of (5.5) leads to the system of ordinary differential equations

$$M\dot{\underline{\alpha}} + S\underline{\alpha} = F(\underline{\alpha}) - M\underline{\gamma} + \underline{b}$$

where $M = ((\phi_i, \phi_j))$, $S = ((\phi_i', \phi_j'))$, $\underline{\alpha} = (U_1, \ldots, U_N)^T$

$$\underline{\gamma} = (W_1, \ldots, W_N)^T \qquad \text{and} \qquad \underline{b} = (b_1, 0, \ldots, 0, b_N)^T$$

Using the Crank-Nicolson Method to discretise in time we obtain:

$$\sum_{i=1}^{N} [\frac{1}{k}(U_i^{m+1} - U_i^m)(\phi_i, \phi_j) + \frac{1}{2}(U_i^{m+1} + U_i^m)(\phi_i', \phi_j')]$$

$$-(f(\sum_{i=1}^{N} \frac{1}{2}(U_i^{m+1} + U_i^m)\phi_i), \phi_j) + \sum_{i=1}^{N} \frac{1}{2}(W_i^{m+1} + W_i^m)(\phi_i, \phi_j) - b_j = 0 \quad \ldots(5.6)$$

$$j = 1, \ldots, N$$

where $f(u) = u(1-u)(u-a)$ and $b_j = 0$ unless possibly when $j = 1,N$.

Solving for W_i^{m+1} in (5.4) and inserting this relation in (5.6) changes the relevant term to

$$\sum_{i=1}^{N} \left(\frac{kb}{4}(U_i^{m+1} + U_i^m) + W_i^m\right)(\phi_i, \phi_j) \qquad \ldots\ldots (5.7)$$

We then solve the set of non-linear algebraic equations (5.6) at each time step using Newton's method [49] as outlined in § 4.2. The solution is required in the semi-infinite strip $[0 \leqslant x \leqslant L] \times [t \geqslant 0]$. As basis function $\phi_i(x)$, $1 \leqslant i \leqslant N$, we choose piece-wise linear functions, once more, depicted in Figure 4.1. In all calculations $k = h = 0{,}5$ with initial conditions given by:

$$u(x,0) = 0 \quad , \quad x > 0$$
$$w(x,0) = 0 \quad , \quad x \geqslant 0$$

The choice of initial conditions is motivated from the physical nature of the nerve. The nerve is initially in a state of rest and is then stimulated at the one end for a certain duration of time. We assume the stimulated end to be the left-hand end. The stimulus can be modelled as either a Neumann or a Dirichlet boundary condition at $x = 0$. This will be discussed in the next paragraph. At the other end of the nerve, that is, the right-hand boundary of the problem, $x = L$, we use either of the following:

$$\text{(i)} \quad u(L,t) = 0 \quad , \quad t \geqslant 0 \qquad \ldots\ldots (5.9)$$

$$\text{(ii)} \quad \frac{\partial u}{\partial x}(L,t) = 0 \quad , \quad t \geqslant 0 \qquad \ldots\ldots (5.10)$$

The first of these is used for L large compared to the distance an initiated pulse travels before termination (for example when we investigate the initiation of a pulse and not

the long-time behaviour).

The second condition is used for all other calculations, that is, when a pulse does reach the right-hand boundary. It is supposed to "let go" the pulse across the boundary without changing the speed close to the boundary. More appropriate is the travelling wave condition

$$c\,\frac{\partial u}{\partial x}(L,t) + \frac{\partial u}{\partial t}(L,t) = 0$$

but this requires the speed c to be known in advance and was not used in this study.

5.5.2. Results

We are primarily interested in the initiation of either a single pulse or a train of pulses. These may arise as a result of different prescribed boundary conditions at $x = 0$. The following types were investigated:

$$1. \qquad u(0,t) = \begin{cases} I & \text{for } 0 \leqslant t \leqslant T \\ 0 & \text{for } t > T \end{cases}, \quad I \text{ constant.}$$

The calculations show that a single travelling pulse is obtained provided I and T exceed certain threshold values. For a finite L and condition (5.10) the time-progressing solution approaches the zero steady state as $t \to \infty$, whether a pulse had been triggered or not. The threshold values for the initiation of a pulse depend on both a and b as do the shape of the pulse and the speed of propagation.

In particular for $b = 0{,}0025$, $I = 1{,}0$, a travelling pulse is obtained for values of a in the range $0 \leqslant a \leqslant 0{,}265$. For $a = 0{,}1$ and $b = 0{,}0025$ a particular set of threshold values

are I = 1,0 and T = 3,97, approximately. The threshold increases with increasing a.

The shape of the pulse, for various values of a, is shown in Figure 5.1. Note that the shape of the pulse for a = 0,0 is remarkably different from that for a = 0,25. All these figures are plotted for t = 120. A feature to be noted is the remarkably flat "roofs" of the pulses for smaller values of a.

Although the qualitative behaviour of this model is in agreement with that of the original Hodgkin-Huxley model, the shape of the pulses for smaller values of a differs from the shape of the experimental, as well as calculated, action potential curve (see Figure 2.5 (Ch 2) and 5.15 (Ch 5)). This does not come as a surprise because, as has been pointed out in it's construction (§ 2.3.5), the model was intended to simulate qualitative rather than quantitative behaviour in the nerve.

The speed and height curves for a range of values of a and b for the travelling pulse is shown in Figures 5.3 and 5.4 respectively. The "knees" of these curves are extremely difficult to calculate. The possible lower parts of each of these curves which turns and stretches back from the "knees" to the c-axis represent the speeds of the unstable solutions of which the existence had been discussed in § 3.3.3.1. In Figure 5.2 we show a proposed speed diagram of McKean [53] for Nagumo's equation. The resemblance to the present computed

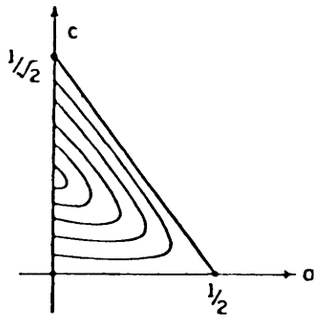

Figure 5.2.
[From McKean [53]]

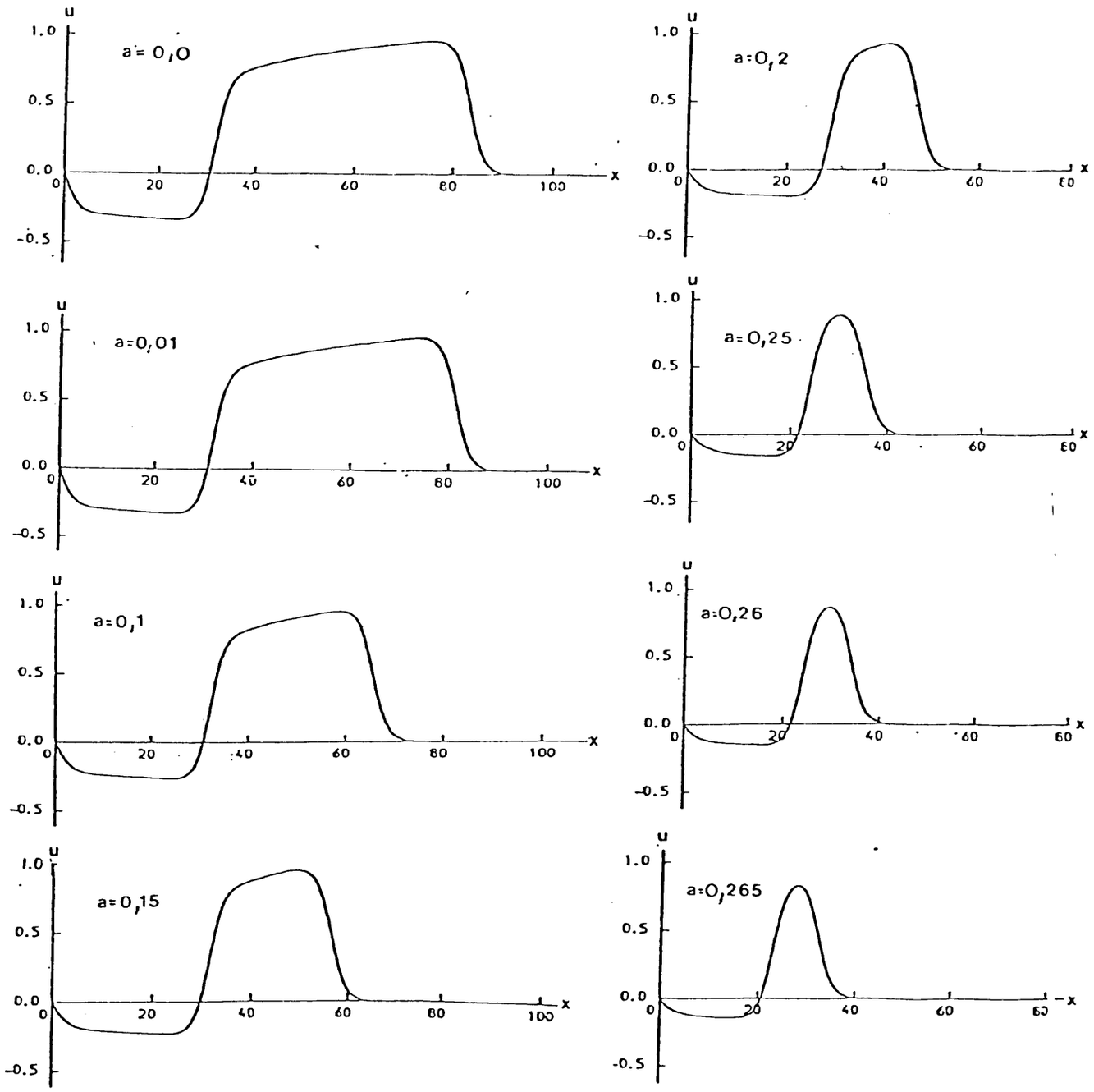

Figure 5.1: Solution of Nagumo's equation for b = 0,0025, a as indicated and t = 120.

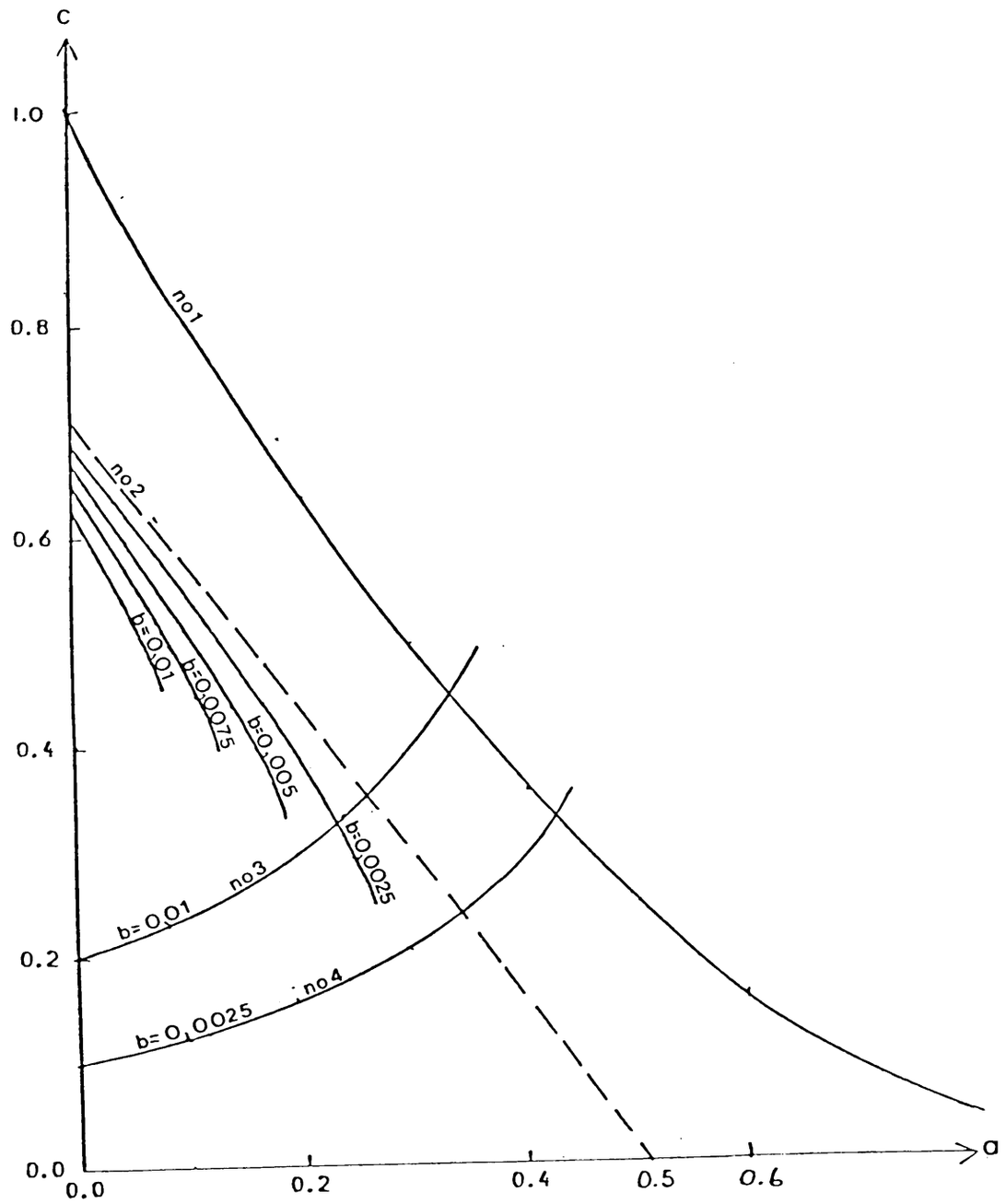

Figure 5.3: Speed curves of Nagumo's equation for various values of b. Bounds on the speed, determined by Sleeman [79] are indicated:

no 1: $c = (1-a)^2$, upper bound for c

no 2: Huxley speed $c = \sqrt{2}(\frac{1}{2} - a)$, $b = 0$

no 3, no 4: $C = \frac{2\sqrt{b}}{(1-a)}$, lower bound for c.

speed diagram as far as the upper parts of the speeds are concerned is clear.

Rinzel and Keller obtained the upper as well as lower parts of the speed curves for their simplified model (Fig. 3.5) by solving the ordinary differential equation (3.14) to find travelling wave solutions. From a time-progressing solution such as ours it is possible only to obtain results for the stable travelling pulse and thus the upper parts of the speed diagram.

One clear advantage of our calculations over that of Rinzel and Keller for their simplified model is to be noted in the speed diagram. Their choice of the Heavi-side function as reaction-term has the effect that the speed of the faster, stable pulse

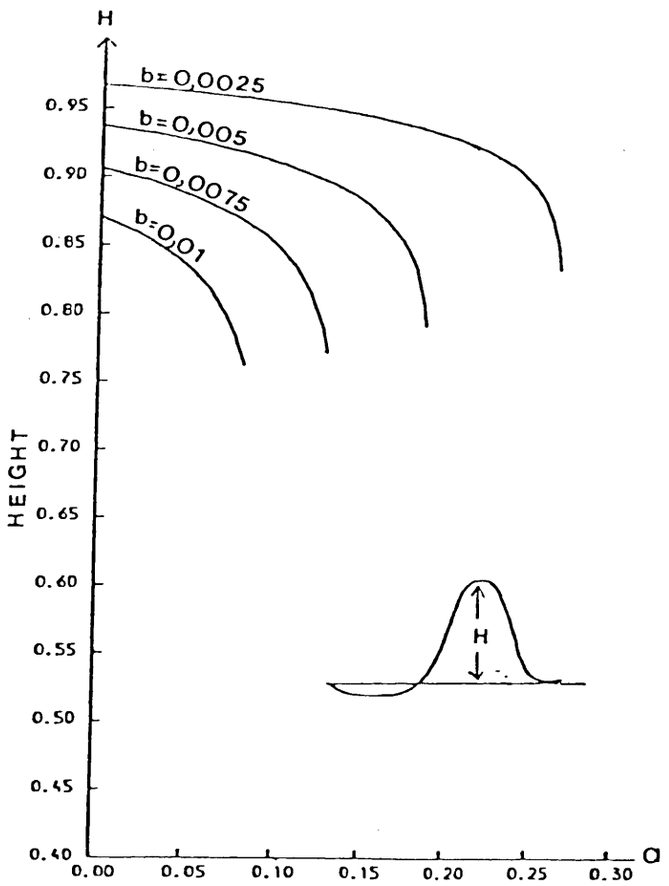

Figure 5.4: Height curves for Nagumo's equation for various values of b.

tends to infinity as $a \to 0$. The speed contours are so steeply inclined close to $a = 0$ that for $a < 0{,}15$ it is nearly impossible to determine the speed.

In Figure 5.3 we also indicate the upper and lower bounds for the speed given by Sleeman [79] and quoted in § 3.3.3.2. The bound on the value of b was particularly useful in finding appropriate values for a and b. The straight line $c = \sqrt{2}(\frac{1}{2} - a)$ represents $b = 0$. This is the Huxley speed which was discussed in connection with Fisher's equation (§ 3.3.2.4 eq. (3.9)).

2. $u(0,t) = I$, $t \geqslant 0$, I constant

For this boundary condition, which represents a constant stimulus of infinite duration, the expected train of pulses is not obtained. A single travelling pulse is produced which tails to a boundary layer at $x = 0$. (See Figure 5.5). One would expect repetitive firing under infinite stimulation (experimental evidence of this was described in § 2.3.3) but this boundary condition fails to provide it. The value of I (provided the value exceeds threshold) has no influence on this phenomenon, increasing the strength of the stimulus still produces no second pulse.

3. $$u(o,t) = \begin{cases} I & , \; n(T_1 + T_2) \leqslant t \leqslant n(T_1 + T_2) + T_1 \\ 0 & , \; n(T_1 + T_2) + T_1 < t < (n+1)(T_1 + T_2) \end{cases}$$

$$n = 0,1,2, \ldots$$

This boundary condition represents repetitive stimulation. It was found that careful tuning of T_1 and T_2 results in a <u>train</u> of travelling pulses being fired. For example of $a = 0{,}075$ and

Solutions of Nagumo's equation with conditions on left-hand boundary as indicated: (a = 0,075, b = 0,01).

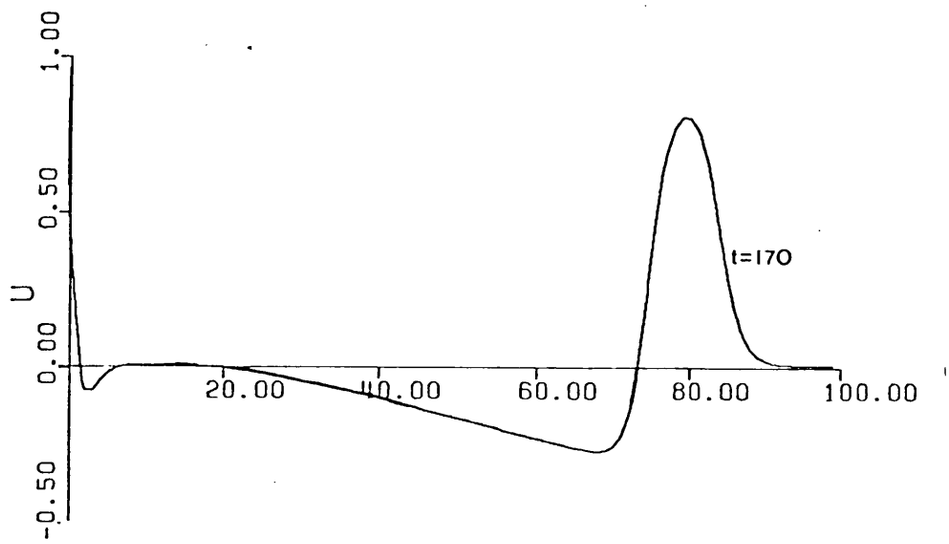

Figure 5.5: u (0,t) = 1 , t ⩾ 0.
Single pulse tailing to a boundary layer.

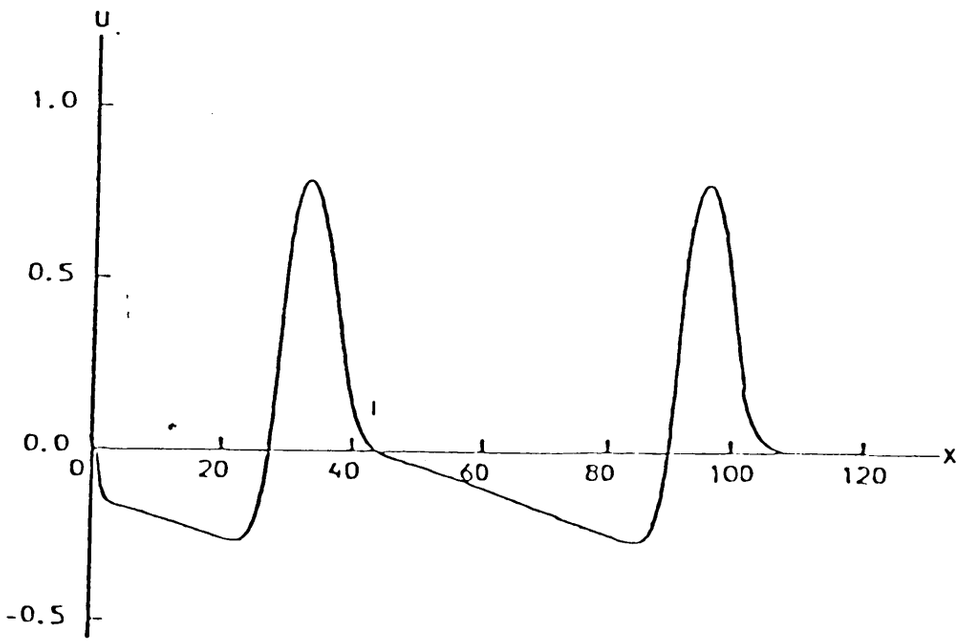

Figure 5.6: Repetitive stimulation causing repetitive firing as described in 3. of § 5.2.2.

$b = 0,01$, $I = 1,0$ a train of pulses for $T_1 = 20$, $T_2 = 110$ is obtained. The first two pulses are shown in Figure 5.6 for $t = 200$. One expects this phenomenon to be related to the concept of an absolute refractory period in the sense that T_2 should exceed the duration of the absolute refractory period following excitation of the nerve. We recall from § 2.3.1.2 that during this period no stimulus, however strong, will be able to produce a second pulse.

Increasing the value of I above 1,0 has no influence on the speed or the height of a travelling pulse.

From the application of the above three Dirichlet boundary conditions we see that repetitive stimulation was the only way of obtaining repetitive firing. We now discuss the case where a Neumann boundary condition is prescribed.

4. $$\frac{\partial u}{\partial x}(0,t) = I = -\frac{1}{2} I^*, \quad t > 0, \quad I \text{ constant}, \quad I^* > 0$$
$$u(x,0) = 0, \quad x \geqslant 0.$$

The reason for the relation $I = -\frac{1}{2} I^*$ will become clear in the next paragraph where restrictions on I^* are discussed.

This Neumann boundary condition is applied to a range of values of I, a and b. The experiments indicate that this boundary condition produces only a single pulse whereafter it settles to a boundary layer which steadies down as depicted in Figure 5.7.

Thus, again, the infinite current fails to produce repetitive firing (a wave-train).
This observation is in agreement with the following comment of Rinzel [71]:

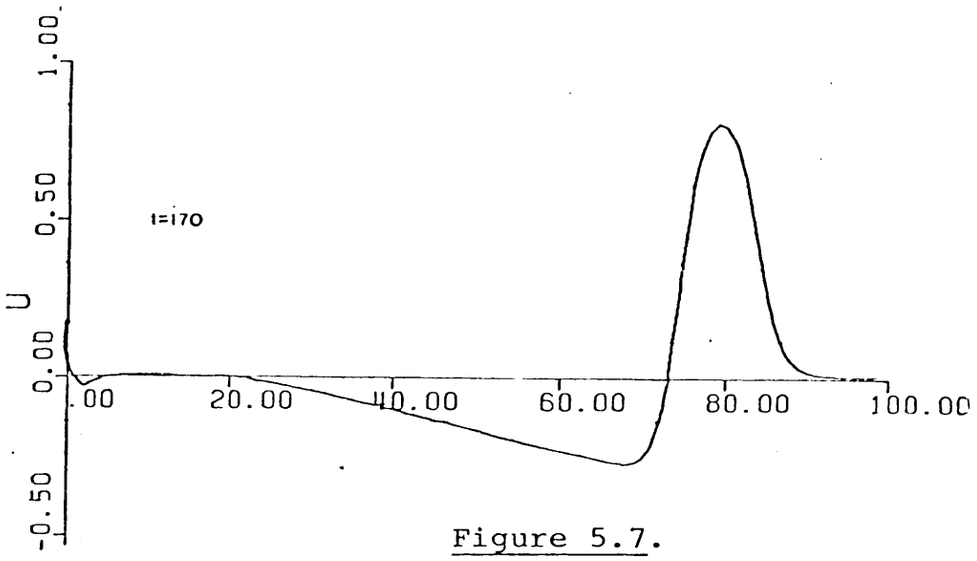

Figure 5.7.

"On the other hand d = 0 (Nagumo's Equation) is apparently inappropriate for repetitive firing under constant current stimulation. Numerical experiments, with a simplified FitzHugh-Nagumo equation, for a point stimulated cable indicate that steady repetitive firing is not achieved for constant I^* but that the solution after an initial transient approaches a t-independent steady state as $t \to \infty$".

The steady state which Rinzel refers to above is either zero for all values of x (if $I^* = 0$) or a monotone decreasing state which is non-zero close to the left-hand boundary (if $I^* \neq 0$). This coincides with our findings for this particular boundary condition.

5.3. Solution of the FitzHugh-Nagumo system

5.3.1. Numerical Procedure

The FitzHugh-Nagumo system is given by (2.41, 2.42):

$$\frac{\partial u}{\partial t} = \frac{\partial^2 u}{\partial x^2} + u(1-u)(u-a) - w$$

$$\frac{\partial w}{\partial t} = b(u - dw), \qquad b > 0, \quad d \geq 0, \quad a \in (0,1)$$

The approximation scheme used in this case is similar to that applied to Nagumo's equation. The differences are outlined:

The second equation (2.42) is approximated by an implicit Finite Difference scheme, corresponding to (5.7)

$$\frac{1}{k}(W_i^{m+1} - W_i^m) = \frac{b}{2}\left[(U_i^{m+1} + U_i^m) - d(W_i^{m+1} + W_i^m)\right] \quad \ldots\ldots (5.11)$$

Solving (5.11) for W_i^{m+1} renders

$$W_i^{m+1} = \frac{kb}{2+kbd}(U_i^{m+1} + U_i^m) + \frac{2-kbd}{2+kbd} W_i^m \quad \ldots\ldots (5.12)$$

Inserting (5.12) in (5.6) gives the C.N.G. scheme:

$$\sum_{j=1}^{N}\left[\frac{1}{k}(U_i^{m+1} - U_i^m)(\phi_i,\phi_j) + \frac{1}{2}(U_i^{m+1} + U_i^m)(\phi_i',\phi_j')\right]$$

$$-\left(f\left(\sum_{i=1}^{N}\frac{1}{2}(U_i^{m+1} + U_i^m)\phi_i\right),\phi_j\right) + \sum_{i=1}^{N}\left(\frac{kb}{4+2kbd}(U_i^{m+1} + U_i^m) + \frac{2}{2+kbd} W_i^m\right)(\phi_i,\phi_j)$$

$$- b_j = 0$$

$$j = 1,2, \ldots, N$$

In all our calculations $k = h = 0,5$ again and the initial condition as well as the boundary condition on the right-hand boundary were the same as for Nagumo's equation. The basis functions are piece-wise linears as depicted in Figure 4.1.

5.3.2. Results

For the Dirichlet conditions on the left hand boundary:

1. $u(0,t) = \begin{cases} I & \text{for } 0 \leqslant t \leqslant T, \quad I \text{ constant} \\ 0 & \text{for } t > T \end{cases}$

2. $u(0,t) = I, \quad t \geqslant 0, \quad I \text{ constant}$

and 3. $$u(0,t) = \begin{cases} I, & n(T_1 + T_2) \leqslant t \leqslant n(T_1 + T_2) + T_1 \\ 0, & n(T_1 + T_2) + T_1 < t < (n+1)(T_1 + T_2) \end{cases}$$

$$n = 0,1,2, \ldots.$$

The results are qualitatively the same as for Nagumo's model. In the first case a single pulse (Figure 5.8) is obtained for sufficient stimulus after which the zero steady state is reached eventually. In the second case a single pulse is fired which tails to a boundary layer (Figure 5.9), provided the stimulus strength is above threshold. Once again no train of pulses is produced. A stimulus below threshold fails to trigger a pulse, a boundary layer forms on the left-hand boundary which steadies down to an equilibrium state. A stimulus exceeding the value 1,0 has no influence on the height or speed of the pulse, as can be seen in Figure 5.10 where $u(0,t) = 2, \quad t > 0$.

Parameters a and b were given values which are feasible for the simpler Nagumo equations, and for parameter d the value 2,54 was used. The third boundary condition produced repetitive firing for the same values as for Nagumo's equation (See Figure 5.11).

The only interesting case was the Neumann boundary condition:

4. $$\frac{\partial u}{\partial x}(0,t) = I = -\frac{1}{2} I^*, \quad t > 0, \quad I \text{ constant}, \quad I^* > 0$$

$$u(x,0) = 0, \quad x \geqslant 0.$$

We recall that this condition failed to produce repetitive firing for the simpler Nagumo model. It is obtained, however, for the full FitzHugh-Nagumo system (See Figure 5.12).

The choice of parameter values to get this phenomenon is very critical. A particular set which does the trick is a = 0,139, b = 0,008, d = 2,54 and $I^* = 0,6$. The wave train is shown in Figure 5.10. The relative magnitudes are in agreement with the results of Green and Sleeman [33] discussed in § 3.3.3.2.

Numerical experiments carried out by Rinzel and Keller [74] and Rinzel [71] suggest that for values a, b and c for which repetitive firing occur, I^* must lie in one of two ranges $I_1 < I^* < I_2$ or $I_3 < I^* < I_4$, $(I_2 < I_3)$. The value of $I^* = 0,6$ presumably lie in the upper range, the lower range representing unstable solutions.

Finally two interesting features of the model are observed. The first of these occurs when triggering two pulses simultaneously from the left- and right-hand boundaries respectively, one travelling to the right, the other to the left. On collision the two pulses eliminate each other and as time progresses the zero steady state is reached. Hodgkin [45] states that nerves can conduct impulses in both directions and the velocity is independent of the direction in which it is travelling. This is in correlation with our findings. Our calculations also indicate that two such pulses cannot "pass through" each other, that is, soliton behaviour is not obtained.

The second case is when the nerve is stimulated at a point near the centre of the nerve. A stimulus, sufficiently strong, grows in height, splits into two to produce two pulses, one propagated to the left, the other to the right.

Solution of the FitzHugh-Nagumo system for $a = 0,139$, $b = 2,54$ and conditions on the left-hand boundary as indicated:

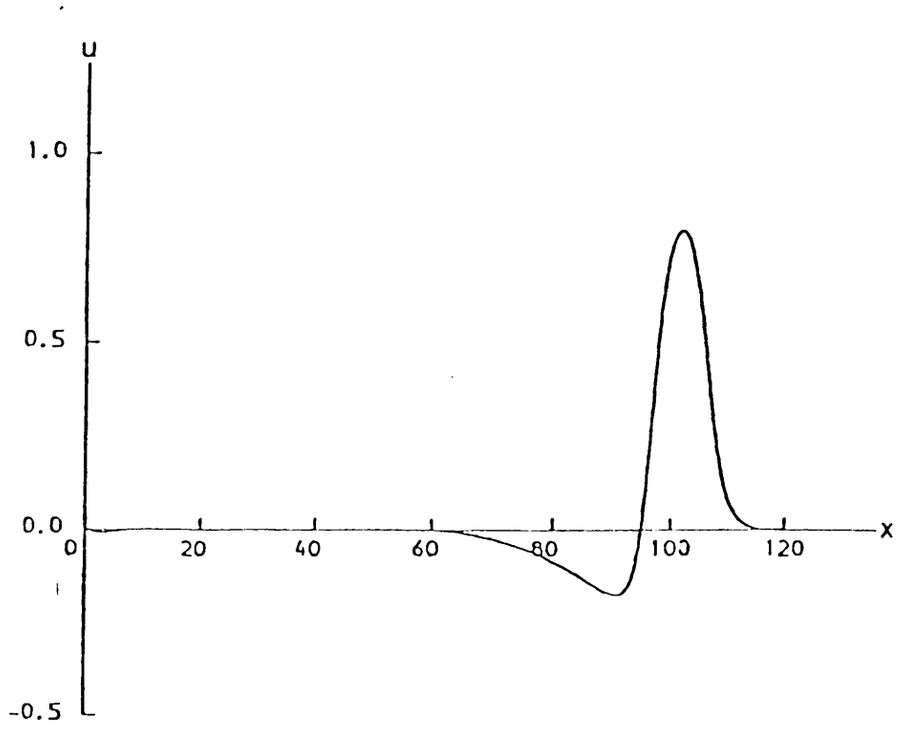

Figure 5.8: $u(0,t) = 1 \quad , \quad 0 \leqslant t < 20$
$= 0 \quad , \quad t \geqslant 0$

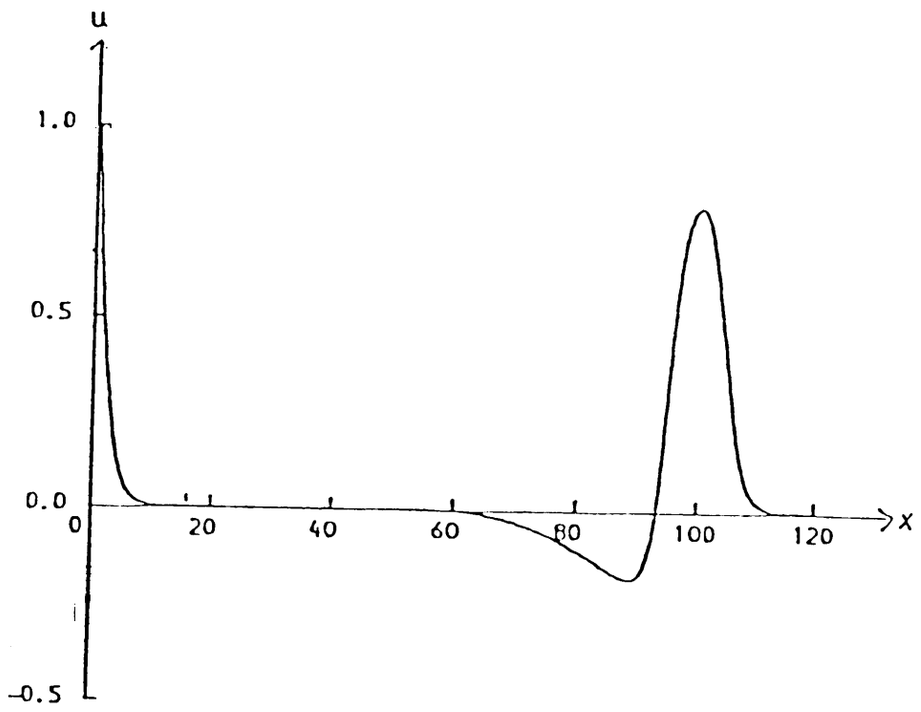

Figure 5.9: $u(0,t) = 1 \quad , \quad t \geqslant 0.$

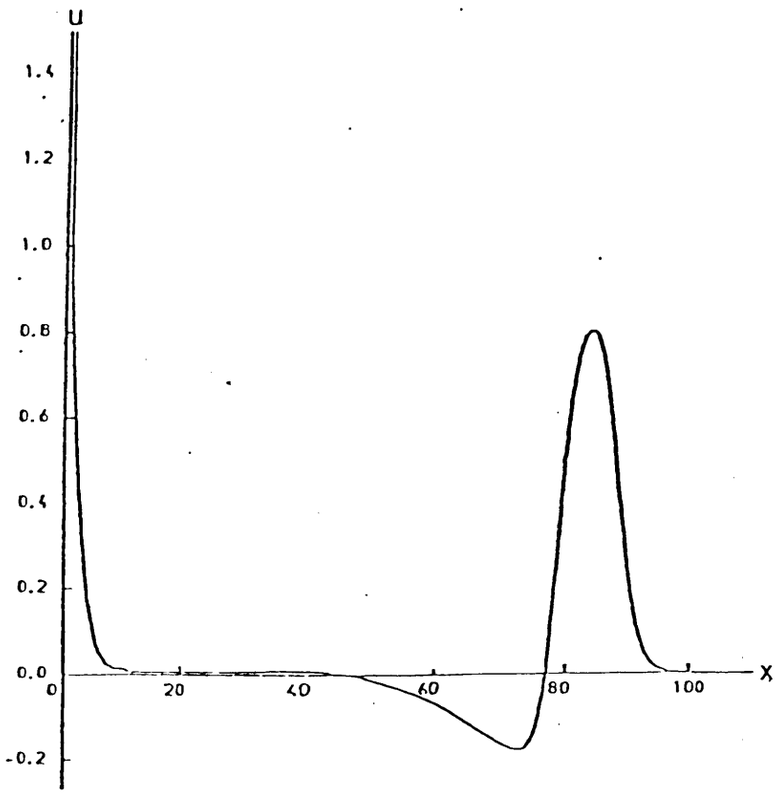

Figure 5.10: $u(0,t) = 2, \quad t \geqslant 0$

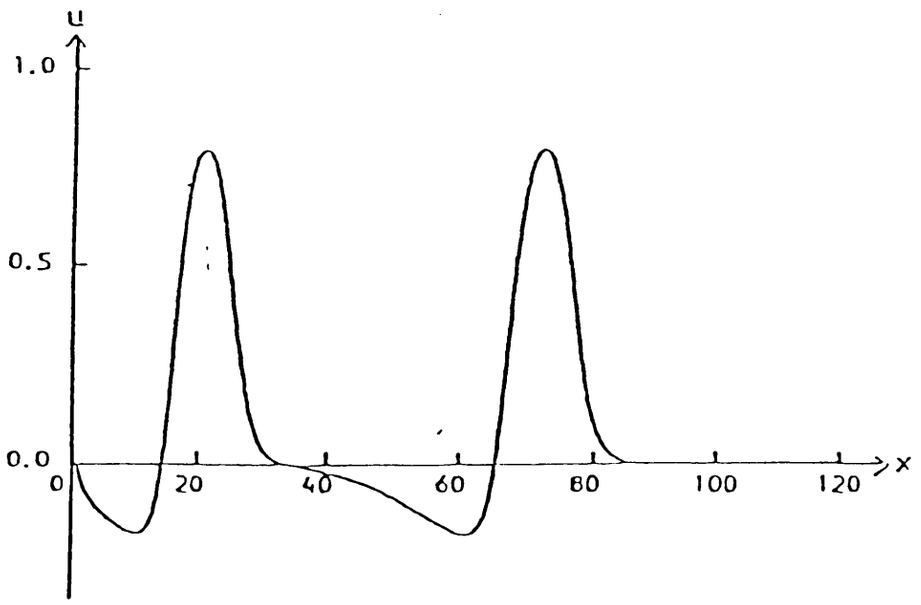

Figure 5.11: Repetitive firing obtained from repetitive stimulation, conditions as in 3. of § 5.2.2.

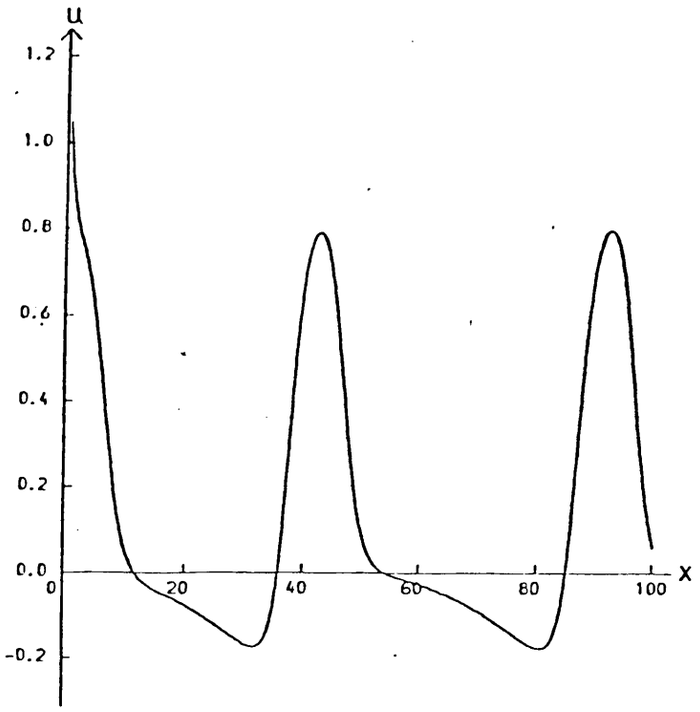

Figure 5.12: Repetitive firing obtained for the Neumann condition 4. of § 5.3.2.

5.4. Solution of the BVP model

5.4.1. Numerical procedure

The BVP equations are given by (2.45, 2.46).

$$\frac{\partial u}{\partial t} = \frac{\partial^2 u}{\partial x^2} + u - \frac{1}{3}u^3 - w$$

$$\frac{\partial w}{\partial t} = \phi(u + a - bw)$$

$$1 - \frac{2b}{3} < a < 2,\ 0 < b < 1,\ b < \frac{1}{\phi^2}$$

We will discuss this model only briefly because of it's similarity to the Nagumo and FitzHugh-Nagumo models which were discussed in the previous two paragraphs.

In the latter two models the stimulus to excitation is modelled by the specification of an appropriate boundary condition.

Another way of applying a stimulus is by adding an extra term, representing the stimulus, to the right-hand side of the principal equation. This method is employed in the BVP model of Muira [61] (see also § 5.5.2.1).

Here it is decided to follow Muira's formulation in which (2.46) becomes

$$\frac{\partial u}{\partial t} = \frac{\partial^2 u}{\partial x^2} + u - \frac{1}{3}u^3 - w + S$$

where the stimulus-term is given by

$$S(x,t) = S_o \exp(\frac{-x^2}{x_o^2}), \qquad 0 \leqslant x \leqslant \ell, \quad 0 \leqslant t \leqslant t_o$$

The boundary conditions are

$$\frac{\partial u}{\partial x}(0,t) = 0, \qquad u(L,t) = 0, \quad t \geqslant 0$$

and the initial conditions are

$$u(x,0) = u_R, \qquad w(x,0) = w_R$$

where (u_R, w_R) is the unique resting state corresponding to the given values of the constants and determined from (2.45, 2.46) by setting $\frac{\partial u}{\partial t} = \frac{\partial w}{\partial t} = 0$.

These values of the constants are

$$u_R = -1,199408035 , \qquad w_R = -0,0624260044$$

$$\Phi = 0,08 , \quad a = 0,7 , \quad b = 0,8 , \quad \ell = 3,0,$$

$$t_o = 0,5 , \quad x_o^2 = 0,1 , \quad S_o = 15 \text{ and } L = 50$$

Whereas Muira uses a Finite Difference scheme we employ the

Crank-Nicolson-Galerkin method as formulated for the Nagumo and FitzHugh-Nagumo systems.

We approximate, once again, u and w by

$$U(x,t) = \sum_{i=1}^{N} U_i(t)\phi_i(x) \quad \text{and} \quad W(x,t) = \sum_{i=1}^{N} W_i(t)\phi_i(x)$$

respectively. We give the changes in the C.N.G. scheme outlined in § 5.2.1:

The second equation (2.46) is solved implicitly by:

$$\frac{W_i^{m+1} - W_i^m}{k} = \Phi\left(\frac{U_i^{m+1} + U_i^m}{2} - b\,\frac{W_i^{m+1} + W_i^m}{2} + a\right)$$

which implies that

$$W_i^{m+1} = \frac{2 - b\,k\,\Phi}{2 + b\,k\,\Phi}\,W_i^m + \frac{\Phi\,k}{2 + k\,b\,\Phi}\,\frac{U_i^{m+1} + U_i^m}{2} + \frac{2\,\Phi\,k\,a}{2 + k\,b\,\Phi} \qquad \ldots\ldots \quad (5.13)$$

The scheme corresponding to (5.6) is

$$\sum_{i=1}^{N}\left[\frac{1}{k}(U_i^{m+1} - U_i^m)(\phi_i,\phi_j) + \frac{1}{2}(U_i^{m+1} + U_i^m)(\phi_i',\phi_j')\right]$$

$$- \left(f\left(\sum_{i=1}^{N}\frac{1}{2}(U_i^{m+1} + U_i^m)\phi_i\right),\phi_j\right) + \sum_{i=1}^{N}\frac{W_i^{m+1} + W_i^m}{2}(\phi_i,\phi_j) - (S,\phi_j) = 0$$

$$j = 1,2,\ldots,N \qquad \ldots\ldots \quad (5.14)$$

where W_i^{m+1} is given by (5.13) and

$$f(u) = u - \frac{1}{3}u^3$$

5.4.2. Results

For the given boundary conditions a single pulse is produced. Figures 5.13a and 5.13b show the two variables u and w at different stages.

Muira [61] uses various methods to find an accurate value for the speed of propagation. By solving the travelling wave equations (a system of ordinary differential equations obtained by introducing the variable $\xi = x - ct$) and using "wave integrals" Muira establishes the value $c = 0,811765$ as an accurate approximation for the speed in this case.

For a time-progressing calculation such as ours the speed is obtained after the pulse has settled down. Muira uses a Crank-Nicolson Finite-Difference scheme with $\Delta t = 0,008$ and $\Delta x = 0,0625$ and obtains a value of $c = 0,81288$ for the speed at $t = 44$.

Using a coarser grid-size $h = 0,5$ our calculations for the speed at $t = 44$ is 0,84522 for a time-step $k = 0,5$. Reducing the time-step to $k = 0,1$ the speed is 0,82601. Further reducing of the time-step to $k = 0,05$ reduces the speed to 0,82211. It is clear that a smaller time-step gives a better approximation to the speed.

Figure 5.14 depicts the solution of the reduced BVP-system where the variable w in (2.45, 2.46) is kept at it's resting value instead of being allowed to vary according to the differential equation 2.46. The solution in closed form which is available in this case (§ 3.3.3.3) is also depicted.

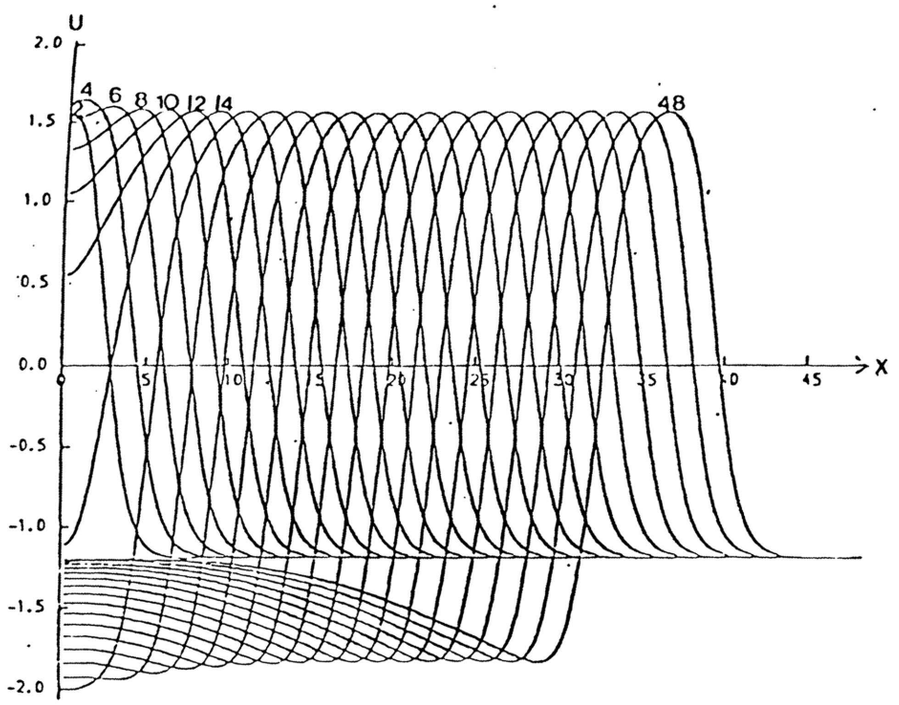

Figure 5.13a: Solution of the BVP model showing U at various stages.

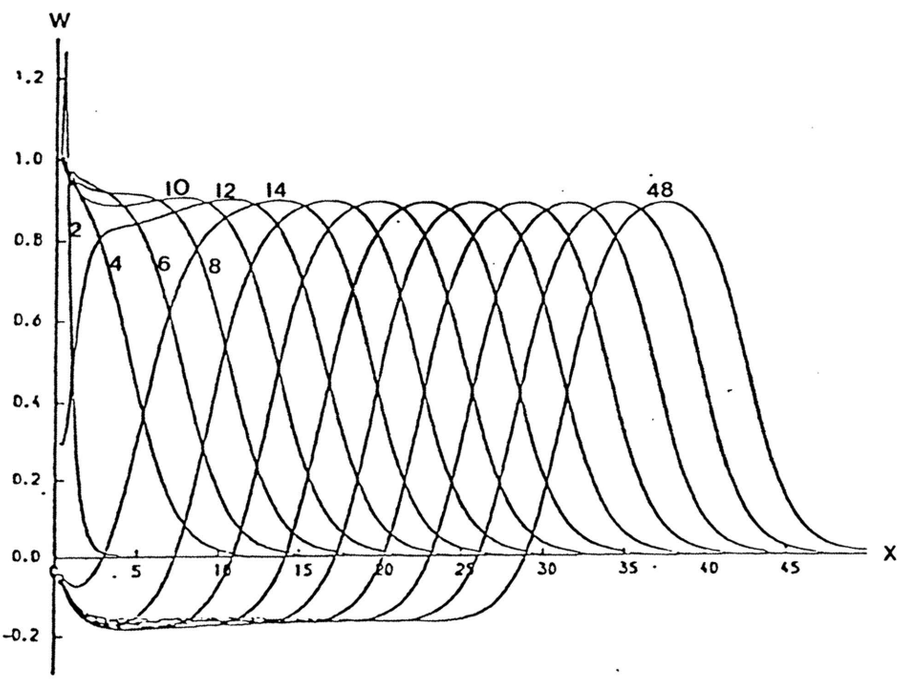

Figure 5.13b: The corresponding changes in the recovery variable W

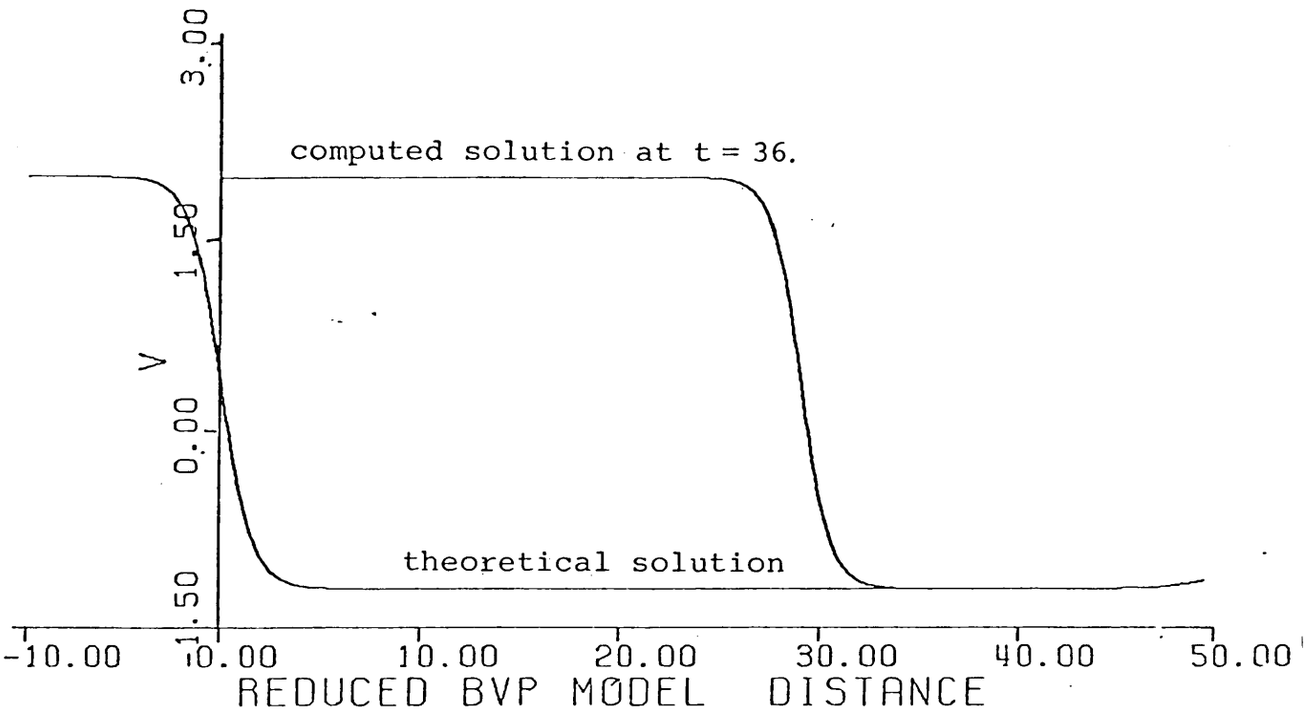

Figure 5.14: Solution of the BVP reduced system.

5.5. Numerical solution of the Hodgkin-Huxley system

5.5.1. Numerical procedure

We recall the governing equations of the Hodgkin-Huxley system from Appendix B:

$$\frac{a}{2R}\frac{\partial^2 V}{\partial x^2} = C_m \frac{\partial V}{\partial t} + \bar{g}_K\, n^4 (V - V_K) + \bar{g}_{Na}\, m^3 h (V - V_{Na}) + \bar{g}_\ell (V - V_\ell) \qquad \ldots\ldots \quad (5.15)$$

$$\frac{\partial n}{\partial t} = \phi(\alpha_n(1-n) - \beta_n n)$$

$$\frac{\partial m}{\partial t} = \phi(\alpha_m(1-m) - \beta_m m) \qquad \ldots\ldots \quad (5.16)$$

$$\frac{\partial h}{\partial t} = \phi(\alpha_h(1-h) - \beta_h h)$$

where $\phi(T) = 3^{(T-6,3)/10}$, T temperature, and the variables V, n, m and h are functions of both x and t. The functions α_n, α_m, α_h, β_n, β_m and β_h are dependent only on V(and therefore implicitly an x and t), the exact form of these together with the values of the constants a, R, C_m, $\bar{g}_K$, $\bar{g}_{Na}$, $\bar{g}_\ell$, V_K, V_{Na} and V_ℓ are given in Appendix B.

In order to use a Crank-Nicolson-Galerkin scheme similar to that used for the other models we define the following approximations:

$$V(x,t) \doteq \sum_{i=1}^{N} V_i(t)\phi_i(x)$$

$$n^4(x,t) \doteq \sum_{i=1}^{N} n_i^4(t)\ \phi_i(x)$$

$$m^3(x,t) \doteq \sum_{i=1}^{N} m_i^3(t)\ \phi_i(x)$$

$$h(x,t) \doteq \sum_{i=1}^{N} h_i(t)\ \phi_i(x)$$

where $\phi_i(x)$, $i = 1, \ldots, N$ are basis functions.
We refer the reader to § 5.2.1 where details concerning the C.N.G. method is described.

The procedure for solving the Hodgkin-Huxley system at every time-instant is outlined:

I A first approximation for n_i^{m+1}, m_i^{m+1} and h_i^{m+1} (where n_i^m approximates $n(x_i, mt)$ etc) is obtained by using Euler forward differences:

$$n_i^{m+1} = n_i^m + k\dot{n}_i^m$$

$$m_i^{m+1} = m_i^m + k\dot{m}_i^m$$

$$h_i^{m+1} = h_i^m + k\dot{h}_i^m \quad , \quad i = 1,2,\ldots,N) \qquad \ldots\ldots (5.17)$$

The last terms in the three equations (5.17) are calculated from the right-hand sides of the subsidary equations (5.16) by using V_i^m, $i=1,\ldots,N$

These approximated values for n_i^{m+1}, m_i^{m+1} and h_i^{m+1} are then used in II to obtain V_i^{m+1}, $i=1,\ldots, N$.

II. The C.N.G. formula for solving the principal equation is

$$\sum_{i=1}^{N} \frac{C_m}{k}(V_i^{m+1} - V_i^m)(\phi_i,\phi_j) + \frac{a}{2R}\cdot\frac{1}{2}(V_i^{m+1} + V_i^m)(\phi_i',\phi_j')]$$

$$+ \frac{1}{2}(f^m + f^{m+1}) - b_j = 0, \qquad j=1,\ldots,N \qquad \ldots\ldots (5.18)$$

where b_j as before and

$$f^m = \bar{g}_K\Big(\sum_{i=1}^{N}(n_i^m)^4\phi_i\Big)\Big(\sum_{i=1}^{N} V_i^m\,\phi_i - V_K\Big)$$

$$+ \bar{g}_{Na}\Big(\sum_{i=1}^{N}(m_i^m)^3\phi_i\Big)\Big(\sum_{i=1}^{N} h_i^m\,\phi_i\Big)\Big(\sum_{i=1}^{N} V_i^m\,\phi_i - V_{Na}\Big)$$

$$+ \bar{g}_\ell\Big(\sum_{i=1}^{N} V_i^m\,\phi_i - V_\ell\Big)$$

The resulting set of linear equations is solved by using Gaussian elimination [49], if the basis functions ϕ_i are piece-wise linears.

III. The values obtained for V_i^{m+1}, $i = 1, \ldots, N$ are now used to recalculate n_i^{m+1}, m_i^{m+1} and h_i^{m+1} from the Trapezoidal rule formulas

$$n_i^{m+1} = n_i^m + \frac{k}{2}(\dot{n}_i^m + \dot{n}_i^{m+1})$$

$$m_i^{m+1} = m_i^m + \frac{k}{2}(\dot{m}_i^m + \dot{m}_i^{m+1})$$

$$h_i^{m+1} = h_i^m + \frac{k}{2}(\dot{h}_i^m + \dot{h}_i^{m+1}) \qquad \ldots\ldots \quad (5.19)$$

A return step to II gives a second approximation to V_i^{m+1}, $i = 1, \ldots, m$. This is compared to the first approximation and if the maximum difference exceeds 10^{-4} another calculation of III and a return step to II is required. In our calculations not more than two return steps to II were required to achieve the necessary accuracy.

Unless otherwise stated, we use time-step $k = 0.01$ and mesh size $h = 0,05$. The corresponding initial and boundary conditions are described in what follows.

5.5.2. Results

5.5.2.1. Initiation of single and periodic pulse solutions

In this section the intention is to investigate the numerical solution of (5.15, 5.16) for various types of boundary data using the C.N.G. scheme described in § 5.5.1. We are interested in the initiation and propagation of single as well as periodic pulse solutions.

Before discussing the initial and different types of boundary

data in detail, we pause to discuss the shape of a single pulse or train of pulses and the asymptotic speed of propagation as obtained from the present calculations.

Figure 5.15a shows the shape of an action potential over a distance of 10 cm at t = 3,5 msec. Figures 5.15b and 5.15c show the corresponding changes in the variables n, m and h and the conductances g_{Na} and g_K, respectively. (For initiation of this pulse condition 5, described subsequently, was used on the left hand-boundary).

Figure 5.15a can be seen to duplicate the experimentally obtained curve of Hodgkin and Huxley far better than do the solutions of the other models (see Figures 2.5, 5.1, 5.8 and 5.13).

Figure 5.15b shows that the fast variable m reaches it's maximum rapidly and follows a nearly horizontal path before decreasing rapidly to a value below the original value, whereafter it increases slowly again to the original value. The slow variables n and h are recovery variables and their turning points are reached after that of V and m.

From Figure 5.15c it can be seen that the rapid rise in potential is due, almost entirely, to sodium conductance. As the sodium conductance decreases the potassium conductance increases to dominate the situation whereafter it decreases once more to the original value.

Figure 5.16a shows the behaviour of solutions to the Vm-reduced system. The slow variables n and h are kept at their resting state values. Excitation is not followed by recovery. The

Solution of the Hodgkin-Huxley system: Single travelling pulse.

at t = 3,5 msec

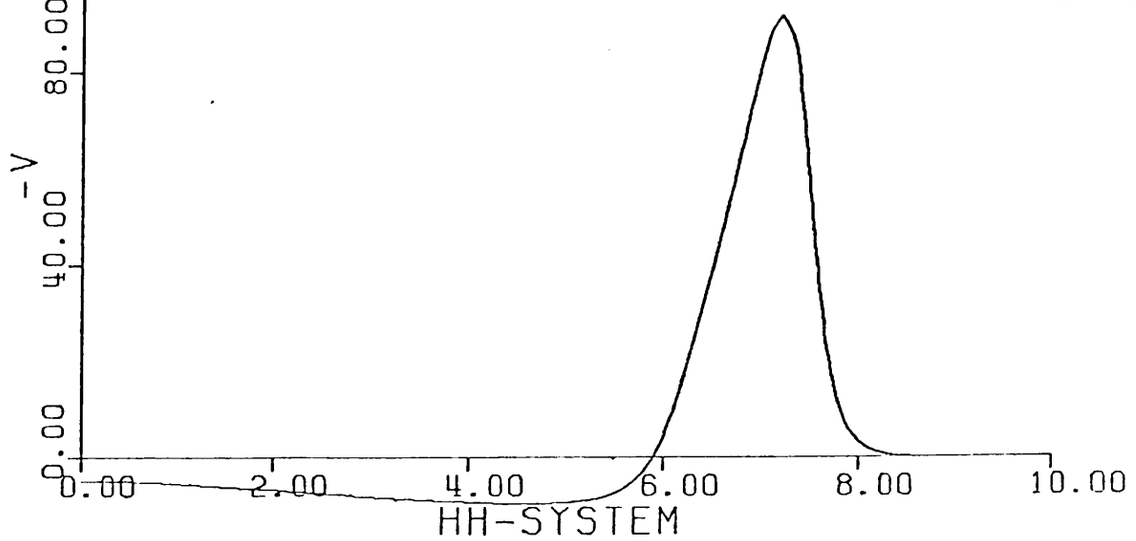

Figure 5.15a

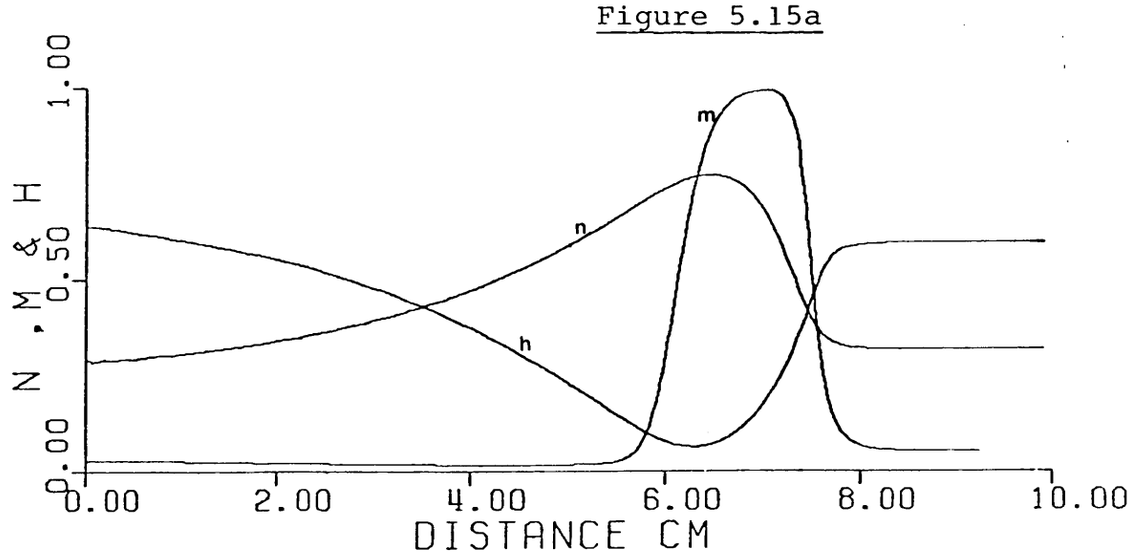

Figure 5.15b

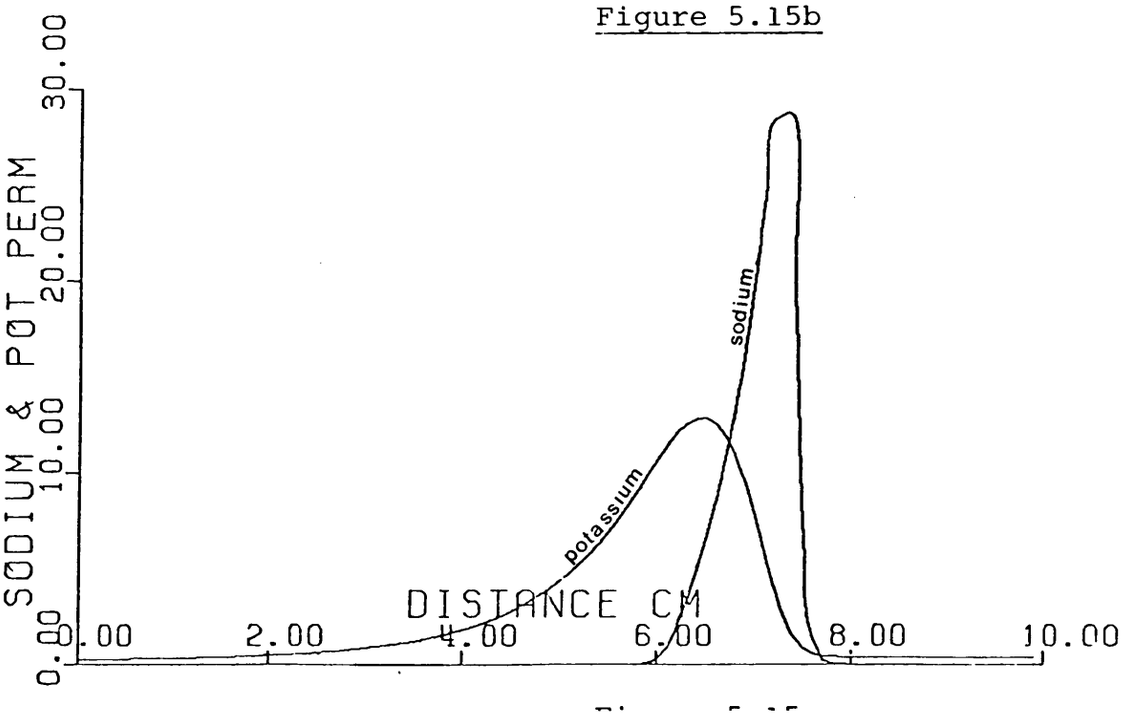

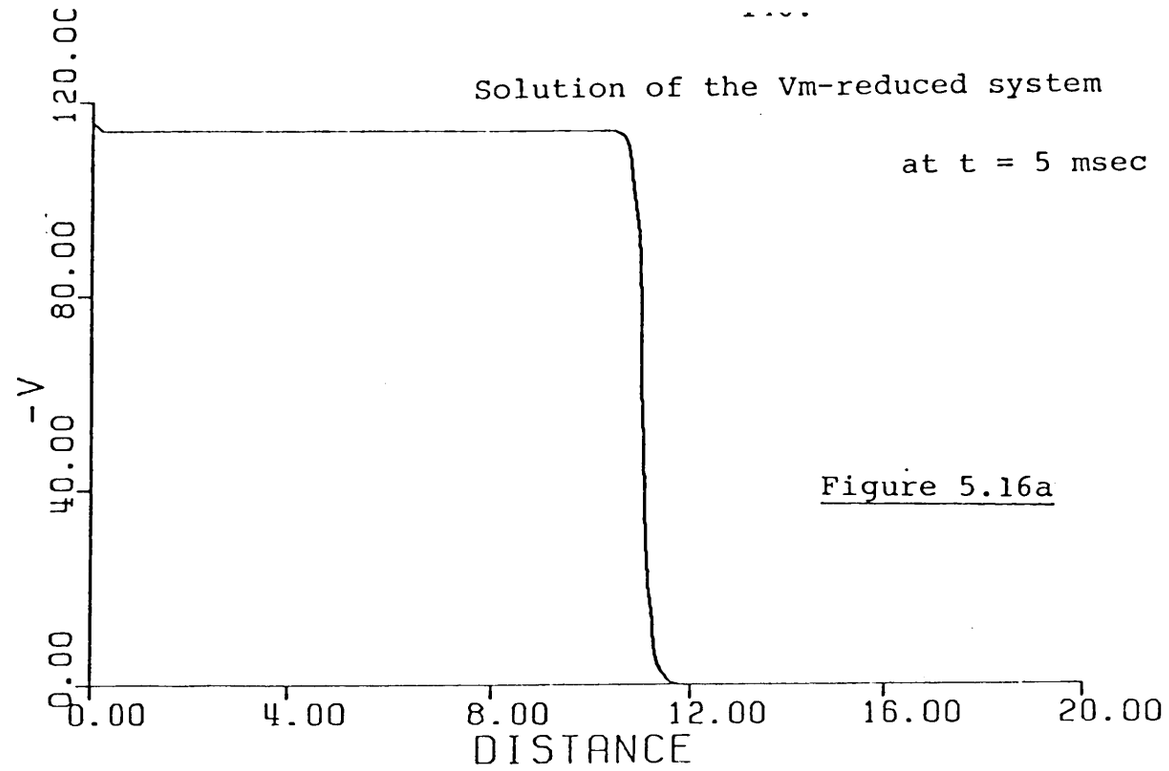

Figure 5.16a

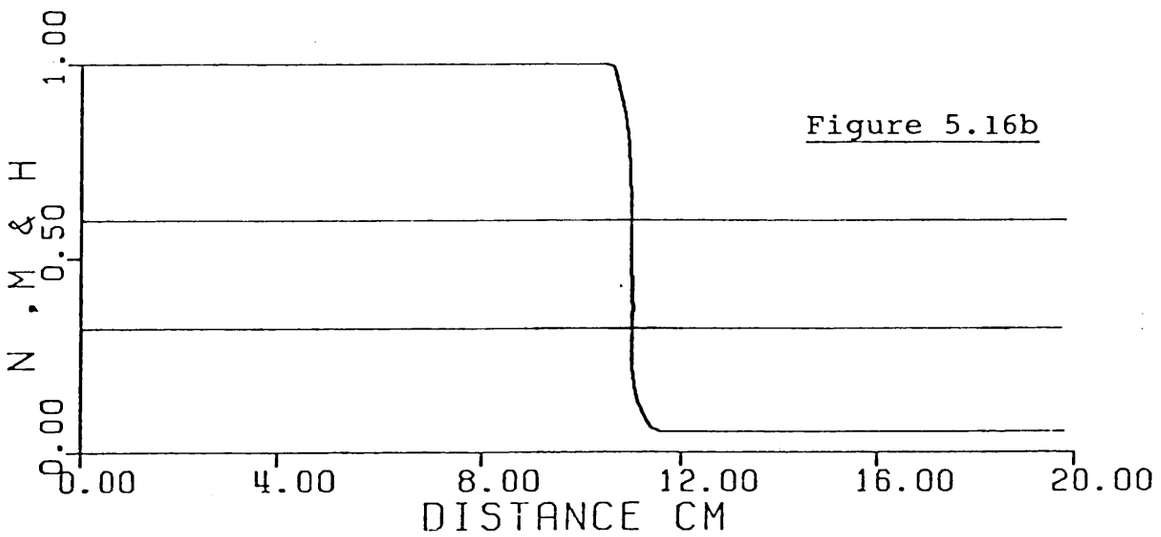

Figure 5.16b

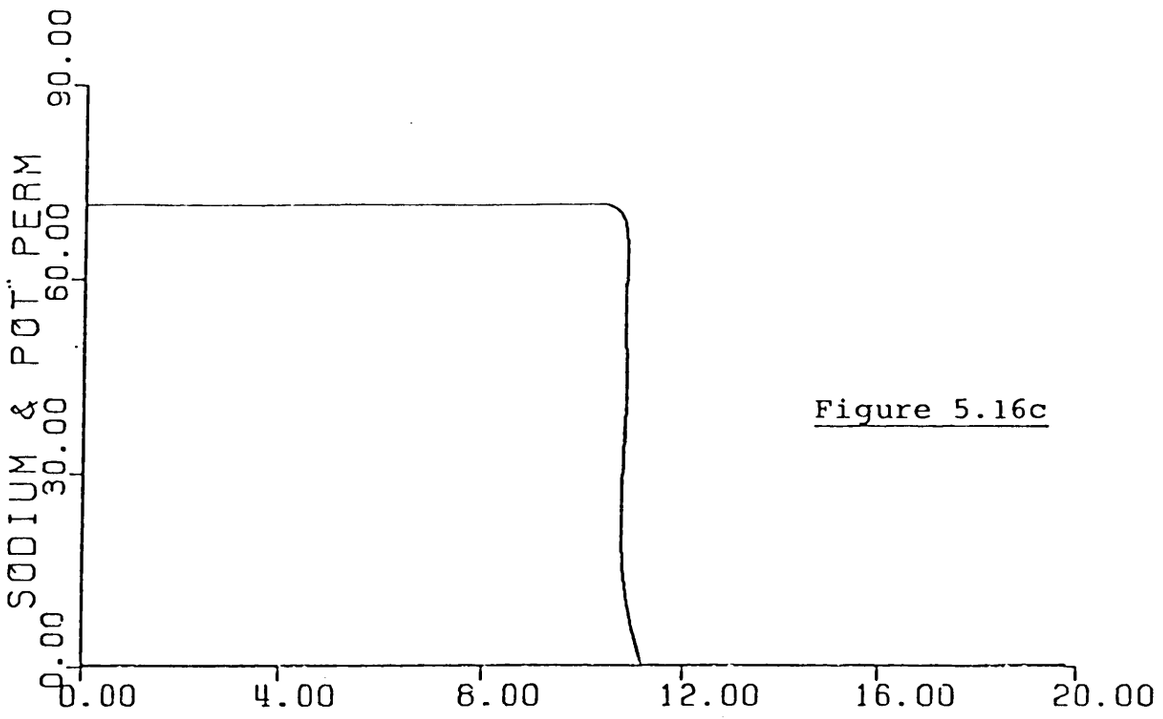

Figure 5.16c

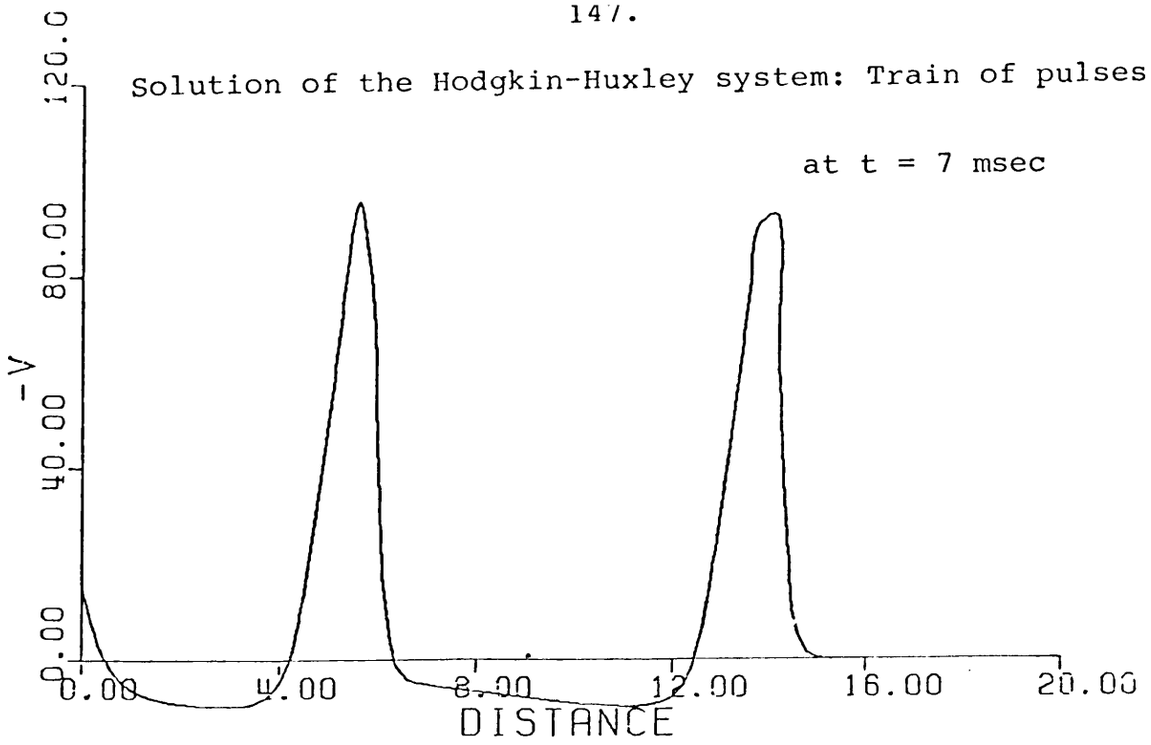

Figure 5.17a

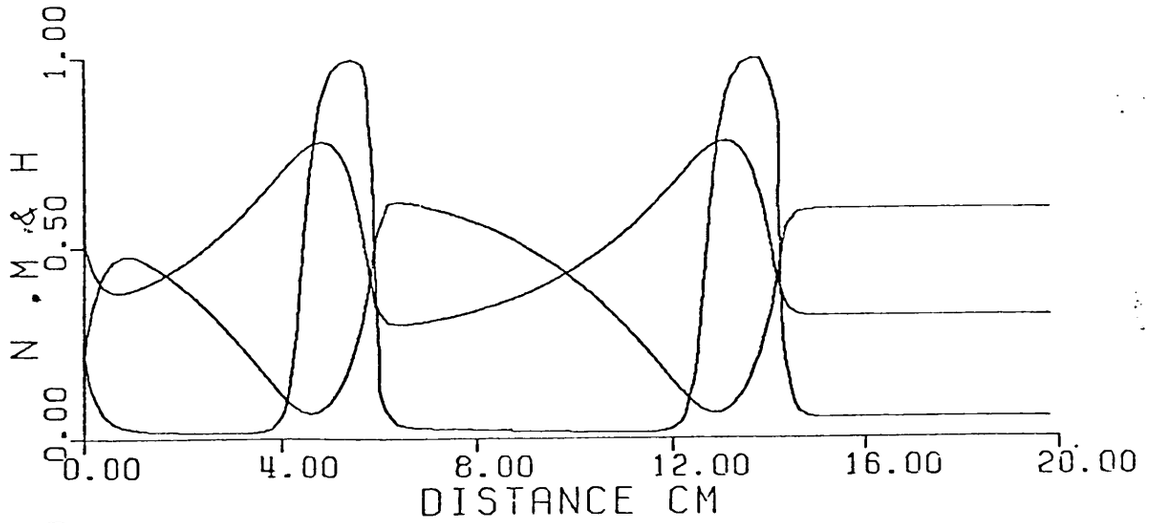

Figure 5.17b

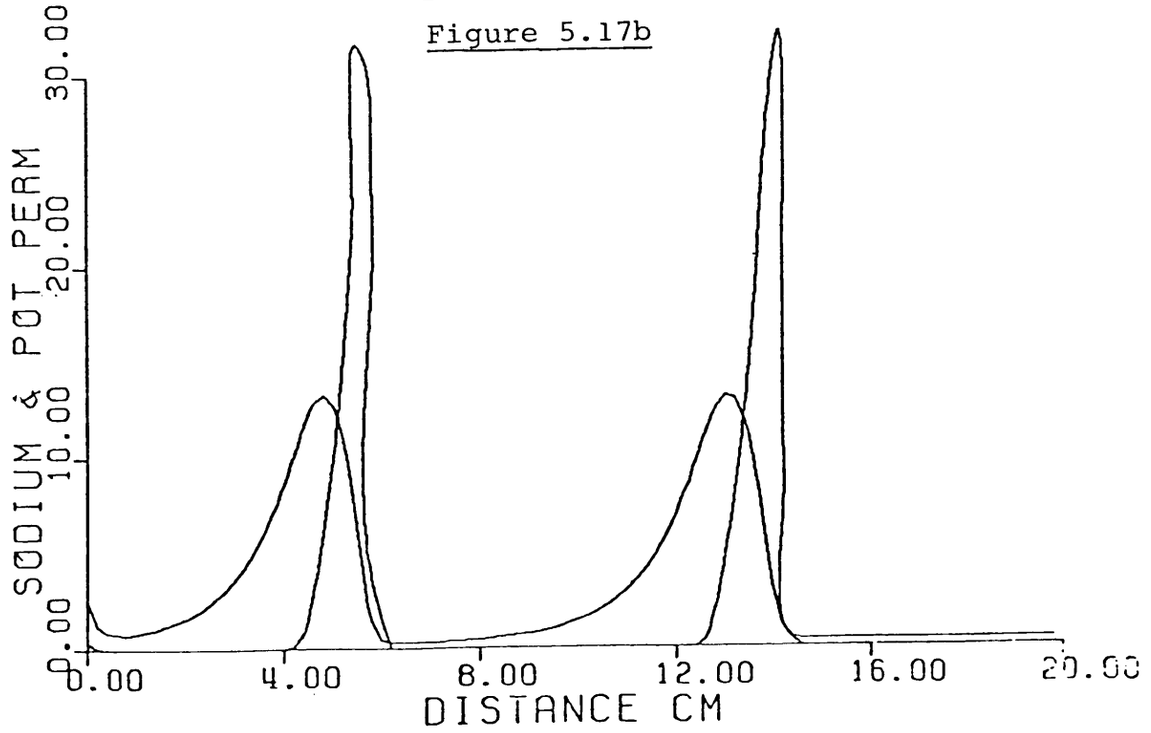

height of the "plateau" potential is slightly higher than the maximum height of a single pulse. The sodium conductance increases to a value much higher than that reached during a proper action potential, the potassium conductance not changing at all.

Figure 5.17a shows a train of pulses, obtained by applying a constant current stimulus (condition 4 on the left-hand boundary, described subsequently). Figures 5.17b and 5.17c depict the corresponding changes in the variables n, m and h and the potassium and sodium conductances, respectively.

Speed: Using the Finite Element scheme described in § 5.5.1 we obtain a value of 18,89 m/sec for the asymptotic speed of propagation for a single pulse at 18,5 °C and for mesh size $h = 0,05$, time-step $k = 0,01$. Hodgkin and Huxley observed a speed of 18,8 m/sec experimentally. Subsequent calculations of Cooley and Dodge [11], using an implicit Finite Difference scheme showed the corresponding value of the speed to be 18,69 m/sec, which is slightly lower than the value obtained presently.

Being interested in the effect of various types of boundary data on the initiation of either a single pulse or train of pulses, we turn our attention to these aspects:

Initial conditions: We assume the nerve to be in a state of rest before applying an external stimulus, therefore (§ 2.3.4)

$$V(x,0) = 0 \quad \text{for all } x > 0.$$

The resting state values of the other three variables are obtained by setting $\frac{\partial n}{\partial t} = 0$, $\frac{\partial m}{\partial t} = 0$ and $\frac{\partial h}{\partial t} = 0$ and substituting

$V = 0$ in the subsidary equations (5.16). These conditions signify a time-independent equilibrium state.

It follows that

$$n(x,0) = \frac{4}{5e-1}, \quad m(x,0) = \frac{5}{8e^{\frac{5}{2}}-3}, \quad h(x,0) = \frac{7e^3+1}{7e^3+107}$$

Boundary conditions:

On the right-hand boundary we use either of

(i) $u(L,t) = 0$ for L large

or (ii) $\frac{\partial u}{\partial x}(L,t) = 0$

On the left-hand boundary one of five different types of boundary conditions are used. Each of these will be discussed separately. For Dirichlet boundary conditions on $V(x,t)$ at the left-hand boundary the variables n, m and h satisfy:

$\frac{\partial n}{\partial t} = 0$, $\frac{\partial m}{\partial t} = 0$ and $\frac{\partial h}{\partial t} = 0$, so that

$$n(0,t) = \frac{\alpha_n(V)}{\alpha_n(V)+\beta_n(V)}, \quad h(0,t) = \frac{\alpha_h(V)}{\alpha_h(V)+\beta_h(V)}, \quad m(0,t) = \frac{\alpha_m(V)}{\alpha_m(V)+\beta_m(V)}$$

The Dirichlet condition on $V(0,t)$ usually implies that $V(0,t)$ is kept at a constant value for a certain duration of time and therefore one expects this to be accompanied by similar constant states of n, m and h, described above.

For a Neumann condition on the left-hand boundary the values of n, m and h were calculated at every time-instant from (5.17) and no extra condition was necessary. The same applies for the right-hand boundary.

Temperature: Hodgkin and Huxley [45] originally did their experiments for temperatures 6,3 °C and 18,5 °C. In this section the latter was chosen for our experiments, the reason being that at the higher temperature the speed of the travelling pulse is higher and a pulse requires less computing time to be initiated.

$$1. \quad V(0,t) = \begin{cases} P & \text{if } 0 \leqslant t \leqslant T \\ 0 & \text{if } t > T \end{cases}$$

A single pulse is produced travelling to the right, provided P and T exceed threshold values, whereafter the nerve returns to a state of rest. The threshold strength and duration curve is time-consuming to calculate. We give, instead, approximations for the minimum values of P and T obtained from our calculations. At 18,5 °C these minimum values are T = 0,065 m sec and P = -13,5 mV. The implication is that any stimulus, however strong, applied for less than 0,065 m sec will fail to produce a pulse. Likewise, a stimulus of modulus strength less than 13,5 mV of however long duration will fail to produce a pulse.

$$2. \quad V(0,t) = P, \quad t \geqslant 0, \quad P \text{ constant.}$$

This boundary condition represents a stimulus applied at the left-hand boundary for an infinite duration of time. A stimulus above threshold produces a single travelling pulse but fails to produce a second pulse. A boundary layer is formed on the left-hand boundary. Contrary to expectations no train of pulses is formed. This coincides with the observations for the simplified models. One can conclude that this Dirichlet type of boundary condition is inappropriate for simulating a constant current stimulation of infinite duration, since in actual experiments

of Hodgkin and Huxley [45], a train of pulses was observed for an infinite constant current applied externally. This requires an explanation: Whereas it was difficult to interpret corresponding results of the simplified models physically, it is possible to do so for the full Hodgkin-Huxley system. The present results can be given a physical interpretation by stating that excitation from a state of rest of the nerve may trigger off a pulse but if one end of the nerve is kept in this excited state the nerve looses the ability to trigger another pulse.

It is essentially the changes in the variables n, m and h that bring the triggering of a pulse about. The reader is referred to § 2.3.1.2 and § 2.3.4 where it is stated that changes in sodium and potassium permeability brings the triggering of pulses about. The sodium conductance variables are m and h and that of potassium is n. If the potential V(0,t) is kept at a constant value, the boundary conditions on the variables n, m and h would imply that they are kept at fixed values and the lack of necessary changes in the values of n, m and h would fail to produce a second pulse.

$$3.\quad V(0,t) = \begin{cases} P & \text{if } n(T_1+T_2) \leqslant t \leqslant n(T_1+T_2)+T_1 \\ 0 & \text{if } n(T_1+T_2)+T_1 < t < (n+1)(T_1+T_2), \end{cases}$$

$$n = 0,1,2, \ldots.$$

This particular boundary condition represents a train of stimuli and is applied with the purpose of producing a train of pulses (repetitive firing). We do obtain the required train but this is subject to certain conditions. A one-to-one correspondence between stimuli and pulses is possible, provided the stimuli do

not follow each other too closely. When a pulse is triggered it is followed by an absolute refractory period ([29] [45]). When a stimulus is given during this period no second pulse will be fired. To verify this the following train of strong but brief stimuli is applied:

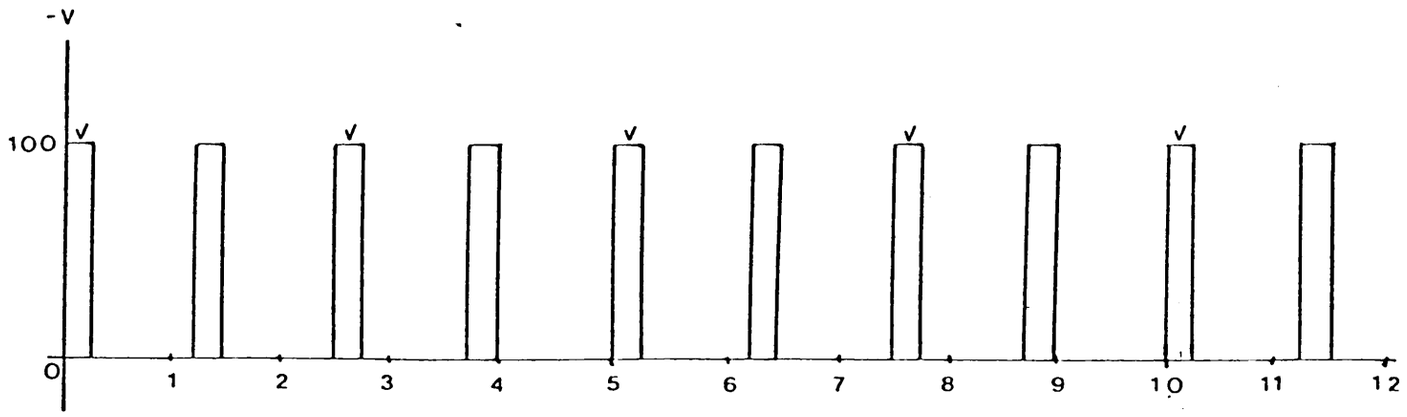

Every second stimulus produces a pulse. This means that the duration of the absolute refractory period is more than 1,25 m sec but less than 2,5 m sec. Moving the second stimulus along in time with steps of 0,01 m sec it was found to trigger a pulse when positioned at 2 m sec. The absolute refractory period for 18,5 °C is therefore in the region of 2 m sec.

For a temperature of 6,3 °C the pulse needs a much stronger stimulus to trigger a pulse. The "width" of the pulse is bigger, too, so that the absolute refractory period is longer too. According to our calculations it is in the region of 9 m sec.

Returning to experiments with a temperature of 18,5 °C and increasing the time lapse between stimuli to more than 2 m sec, we still obtain a one-to-one-correspondence between stimuli and firing.

Decreasing the time lapse between stimuli, that is, allowing the stimuli to follow each other rapidly, results in no train being produced. As example of this consider the following stimulation pattern:

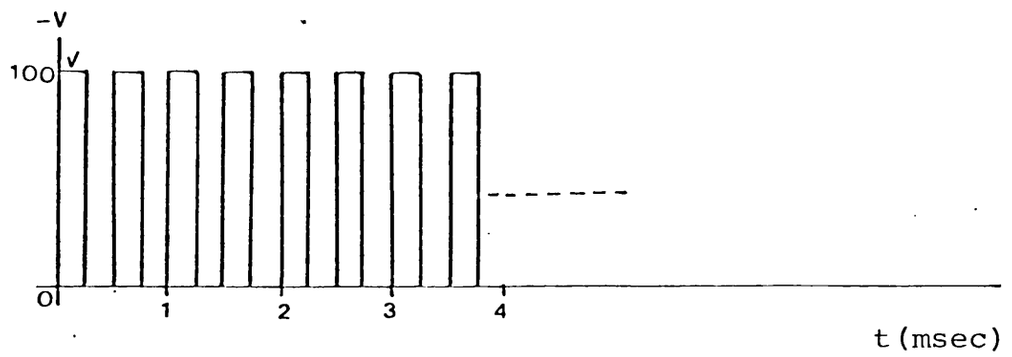

Frequency 2000/msec

A single pulse is triggered whereafter no second pulse is produced.

This behaviour can probably be explained by saying that the variables n, m and h are not allowed enough time to undergo the necessary changes to be able to produce a pulse once more.

We now consider the following Neumann boundary conditions:

$$4. \qquad \frac{\partial V}{\partial x}(0,t) = 0 , \qquad t \geqslant 0.$$

In this case the necessary stimulus was obtained by adding a term acting as stimulus to the right-hand side of the principal equation (5.15). If the stimulating current is given by I_S then the density across the membrane at the stimulated end is

$$\frac{I_S}{2\pi ah} .$$

Letting $I_S = \sum_{i=1}^{N} I_{S_i}(t)\phi_i(x)$, $\quad I_{S_1} \neq 0$

$I_{S_i} = 0, \quad i \neq 1$

the C.N.G. formula (5.18) gains one more term, added to the left-hand side, namely

$$\frac{1}{2\pi ah} \; (I_S, \phi_j)$$

Now let $I_{S_1}(t) = P$ for $t \geqslant 0$. This represents a constant stimulus of infinite duration from an external source. In contrast to Case 1 the first pulse is followed naturally by more pulses to form a train of pulses. The number of pulses in a train depends on the strength of the stimulus and for a certain range of P the number of pulses in a train is infinite. We will now discuss this interesting phenomenon in greater detail.

This particular example, of a stimulus added to the right-hand side of the principal equation (5.15) has also been considered by Cooley & Dodge [11] in a Finite Difference study, the reader is referred to § 3.4.4 where details of their scheme is discussed. Although they do not give actual numerical values for the range of values of P which trigger a train of pulses, they do give a diagram, reproduced here as Figure 5.18, which shows the response for a few parameter values.

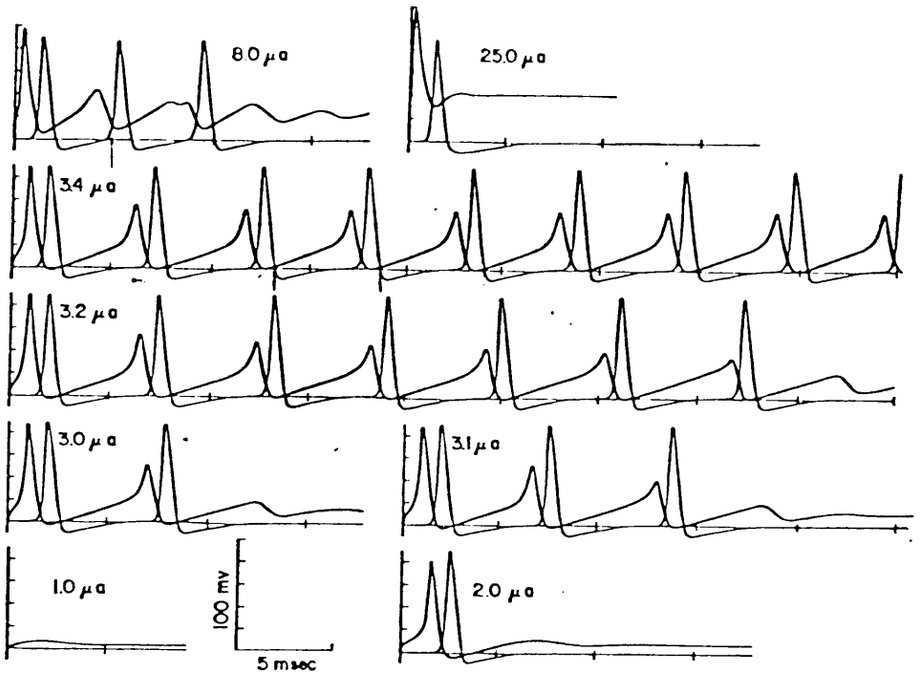

Figure 5.18 : Response of the continuous axon to a steady stimulus of various intensities showing time course of the membrane potential V at x = 0 (heavy lines) and at x = 2 cm (lighter lines) [Reprinted from [11]]

From our numerical experiments we observe the following:

Not all values of P trigger trains of pulses. For a range of P between -2,8 μa and -10,8 μa more than one pulse were triggered. This boundary condition is therefore more appropriate for simulation of an infinite constant current than was Case 2.

Increasing the modulus of the stimulus strength P from 2,8 μa to 10,8 μa we find that close to the lower bound first two (and then three) pulses occur in a train after which a boundary layer forms. The boundary condition on the right hand causes the pulse(s), which were triggered, to leave smoothly across the boundary so that a steady equilibrium state is finally reached across the x-interval. This steady state is non-zero only close to the left-hand boundary, the value on the boundary depending on the stimulus strength.

The number of pulses in a train increases rapidly as the stimulus strength increases to the middle of the range.

It seems likely that the number of pulses in a train resulting from a stimulus in the middle of the range (-5 μa for example) is infinite. The reason for this deduction being that there is no indication of termination at all even if the program is run for a long period of time. An infinite number of evenly spaced pulses is a periodic solution and this could correspond with Rinzel's [71] results on the simplified FitzHugh-Nagumo equation for which he proves the existence of a range of stimulus values for which periodic solutions exist (See § 5.3.2).

For a stimulus strength less than 2,8 μa, bigger than 1,2 μa a single pulse is formed and for a strength less than 1,2 μa no pulse is triggered at all. For a stimulus strength exceeding 10,8 μa only a single pulse is triggered whereafter a boundary layer forms.

We return to experiments for values of stimulus strength in the range exhibiting repetitive firing. As the stimulus strength increases we observe that pulses are produced more rapidly and the distance between travelling pulses decreases. (For P = -10 μa the distance between two adjacent pulses in a train is 7,2 cm and for P = -4 μa the distance is 9,0 cm). These observations do not include the first few pulses in a train of which the behaviour will be discussed in the next paragraph.

To every infinite constant stimulus a corresponding period may be associated. The relation between the strength of the constant stimulus and the corresponding period (time lapse between

two consecutive pulses) can be seen in the graph below. We also show the frequency (and period) against stimulus strength in Figure 5.19.

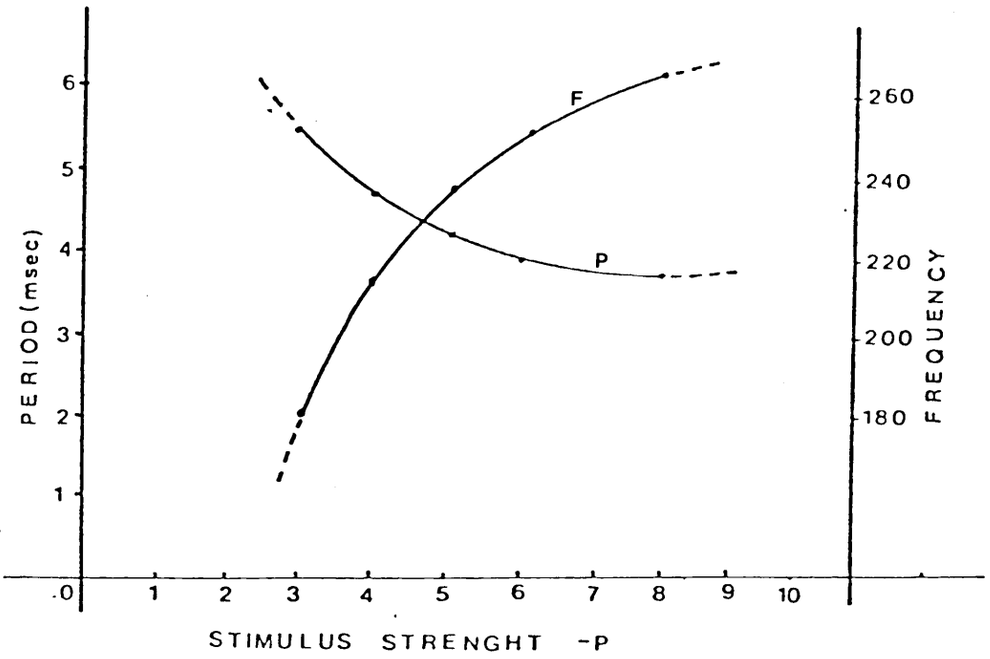

Figure 5.19

The conclusion to be made is that the frequency of the pulses in a train is determined by the strength of the infinite constant stimulus.

The behaviour which we observe with our numerical experiments is supported physiologically by a conjecture of Hodgkin [45]: "Experiments ..... prove that the nervous impulses in one fibre is of constant amplitude and shape and that it's characteristics cannot be altered by changing the strength or the quality of the stimulus. The inference is that the intensity of a sensation or a movement is controlled by varying the frequency of impulses and the number of fibres in action."

5. In this case the stimulus is added to the right-hand side of the principal equation (5.15) as an extra term (as in 4.), that is

$$I_S = \sum_{i=1}^{N} I_{S_i}(t)\ \phi_i(x), \quad I_{S_i} = 0 \quad \text{except when } i = 1.$$

Stimuli is then given in the form of rectangular pulses, that is

$I_{S_i} = P$ (constant) for a certain time duration and for a particular value of P and is then set to zero. This is repeated. All experiments are for 18,5 °C.

We apply trains of stimuli for various values of P, evenly spaced in time and then examine the behaviour of the solutions obtained.

Applying a strong stimulus, such as - 25 μa for a duration of 0,25 m sec at intervals pictured below, every <u>second</u> stimulus fires a pulse.

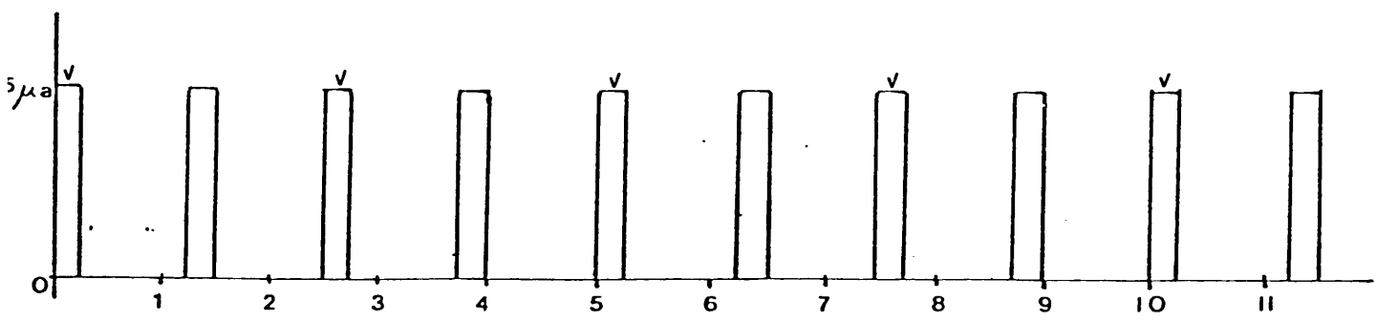

Stimulus frequency 800/sec
Firing frequency 400/sec

Decreasing the strength of the stimulus to -8μa but keeping the

same spacing results in one pulse for every fourth stimulus. A weaker stimulus, therefore, requires longer interstimulus intervals. The effect in the figure above, a pulse for every second stimulus, can be obtained for the weaker stimulus strength of - 8 μa by increasing the time lapse between stimuli as shown below:

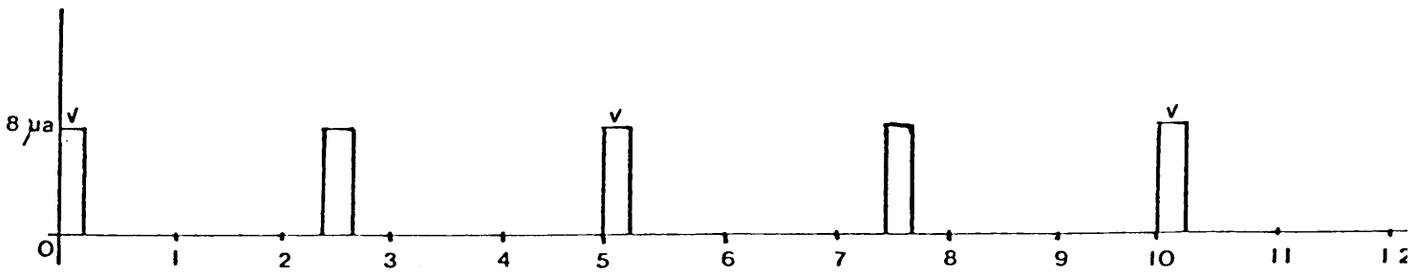

Stimulus frequency 400/sec
Firing frequency 200/sec

Here again every second stimulus produced a pulse. One can conclude that strong stimuli can follow each other more rapidly than weak stimuli to produce the same ratio of number of pulses per number of stimuli.

A likely explanation for this phenomenon comes from the concept of a relative refractory period. According to Hodgkin [44] and FitzHugh [29] the absolute refractory period (during which no pulse can be fired) is followed by a relative refractory period during which a second stimulus can produce a pulse, but the threshold value for this second stimulus is higher than the threshold of the resting fibre. During the relative refractory period, which is of indefinite duration, the threshold falls and gradually approaches it's original resting value. This explains why the stronger stimulus (- 25 μa) can produce a second pulse after a shorter time lapse than in the case of the weaker

stimulus (- 8 μa).

Returning now to case 4 where an infinite constant current was applied we recall that a natural period was associated with every stimulus strength. The pulses were produced at regular time intervals. One is tempted to say that only "certain parts" of the stimulus is necessary to trigger pulses. One would expect that the constant current can be replaced by a sequence of short stimuli to obtain the same results, provided that the period between stimuli is the same as the natural period determined by the stimulus strength.

Our calculations prove this conjecture to be only partly true.

A constant current of infinite duration and of strength I_{S_1} cannot in general be replaced by short stimuli of the same strength and duration and still retain the same frequency of pulses.

For a strength of - 8 μa an infinite current produced pulses every 3,75 m sec. For rectangular pulses of - 8 μa of duration 0,25 m sec a one-to-one correspondence between stimuli and pulses occurred only for stimuli 5 m sec apart.

Keeping the strength of the stimulus fixed (-8 μa) and increasing the duration of the stimulus allows a decrease in the length of interstimulus intervals for which it is possible to obtain a one-to-one correspondence between stimuli and pulses.

The natural period of pulses generated by an infinite constant stimulus of -8 μa is 3,75 m sec. This can be imitated by a sequence of rectangular stimuli as follows:

For the first pulse to be triggered a duration of 0,15 m sec was sufficient.

For the second and subsequent pulses, however, this was insufficient. A stimulus of the same strength (-8 μa) had to be applied for 0,30 msec which is twice the duration required for the first pulse. This can be explained again by the conjecture that the second pulse is triggered in the relative refractory period following the first pulse.

The subject of this paragraph has mainly been the effect of various boundary conditions on the initiation of pulses. In the following paragraph we will concern ourselves with the behaviour of individual, especially the first few, pulses in a train.

5.5.2.3. Changing of speed in trains

In a recent paper of Miller and Rinzel [57] the following conjecture is made concerning the speed of the various pulses in a train: "Propagation speed of an impulse is influenced by previous activity. A pulse following it's predecessor too closely may travel more slowly than a solitary pulse. In contrast, for some range of interspike intervals, a pulse may travel faster than normal because of a possible super excitable phase of it's predecessor's wake".

We have observed this phenomenon too and report our findings in what follows. Miller and Rinzel computed a diagram for the relation between speed and frequency (the dispersion relation) for steadily propagating periodic wave trains for three tempe-

ratures: 6,3 °C, 18,5 °C and 26 °C. A maximum frequency is obtained and the solitary pulse is obtained in the limit as the frequency tends to zero.

We proceed to give results of a few of our numerical experiments, conducted at 18,5 °C. We first consider Case 4 of the preceding paragraph, we recall that this particular boundary condition represented a constant current of infinite duration.

For the range of values of current strength which produced repetitive firing, we investigated the speed of the individual pulses.

The first pulse in a train travelled at the expected speed for a single pulse, determined by temperature alone (see § 5.5.2.3).

The second pulse, however, travelled significantly slower than the first, the third pulse a little slower than the second. The speeds of subsequent pulses were the same (difference less than 10^{-2}). The pulses in a train produced by an infinite constant current therefore presumably travels slower than a single pulse in general.

We now turn to Case 5 of the preceding paragraph, which, as we recall, represents a sequence of rectangular pulses given at fixed intervals.

We apply the following sequence of strong stimuli which produces one pulse per stimulus:

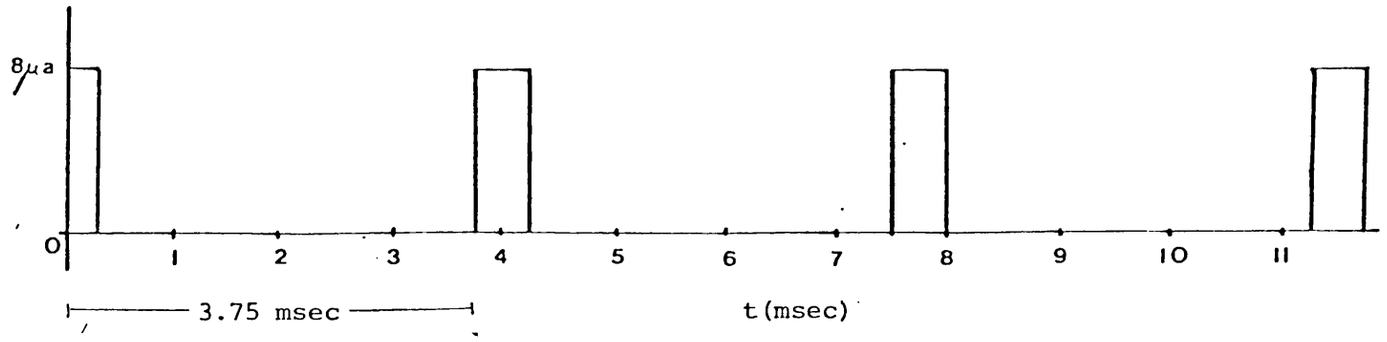

The pulse produced by the first stimulus travels at the single pulse speed (18,89 m/sec), the second travels slower, at 18,3 m sec, the third at 18,1 m/sec. The fourth and subsequent pulses travel at the same speed, namely 18,0 m/sec (speed measured at 5 cm).

A second sequence of stimuli is applied as follows (time lapse

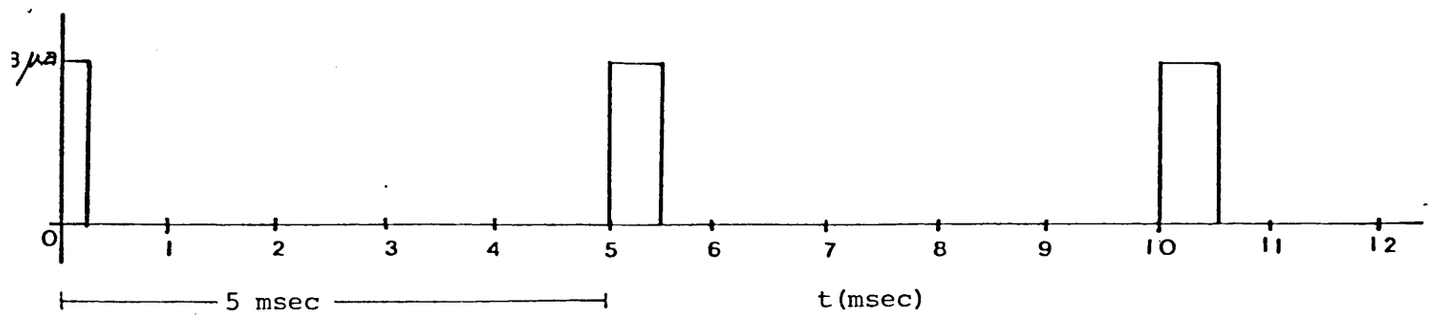

The pulse produced by the first stimulus travels again at the single pulse speed. The second pulse travels faster than the first, at a speed of 19,51 m/sec. The speed of the third pulse is a slight increase on the previous one, but the fourth and subsequent pulses travels at approximately the same speed.

From the two numerical experiments above the question might be asked whether a train of pulses travelling at the same speed

as the first one can be obtained. Our calculations indicate that for stimuli at intervals of 4,78 m sec all pulses in a train travel at the same speed

5.5.2.3. The effect of temperature

We conclude our study by making a few observations concerning the general effect of temperature on a single travelling pulse.

When a single pulse is generated from the left-hand boundary we observe the following: A change of temperature has two major effects on the travelling pulse: The shape of the pulse changes and the speed changes. The latter can be calculated directly and the former will be measured in terms of the amplitude of the pulse. Conversely: The height and the speed of a single travelling pulse is changed only by a change in temperature. (For repetitive firing this does not hold as had been shown in § 5.5.2.2). Boundary or initial conditions does not affect the speed or height of a pulse, provided a pulse is fired. This phenomenon had been referred to previously as the all-or-none response of nerve activity (§ 2.3.3).

The effect of temperature on the speed and amplitude of a single travelling pulse is shown in Figure 5.20.

Turning to the simpler models for impulse propagation (§ 5.2 - 5.4) we see that there is no single parameter playing the role of temperature. Changes in shape and speed of a single pulse is brought about by changes in a and b in Nagumo's model and a, b and d in the FitzHugh-Nagumo model. We expect, therefore, a correlation between these parameters and the Hodgkin-Huxley temperature T.

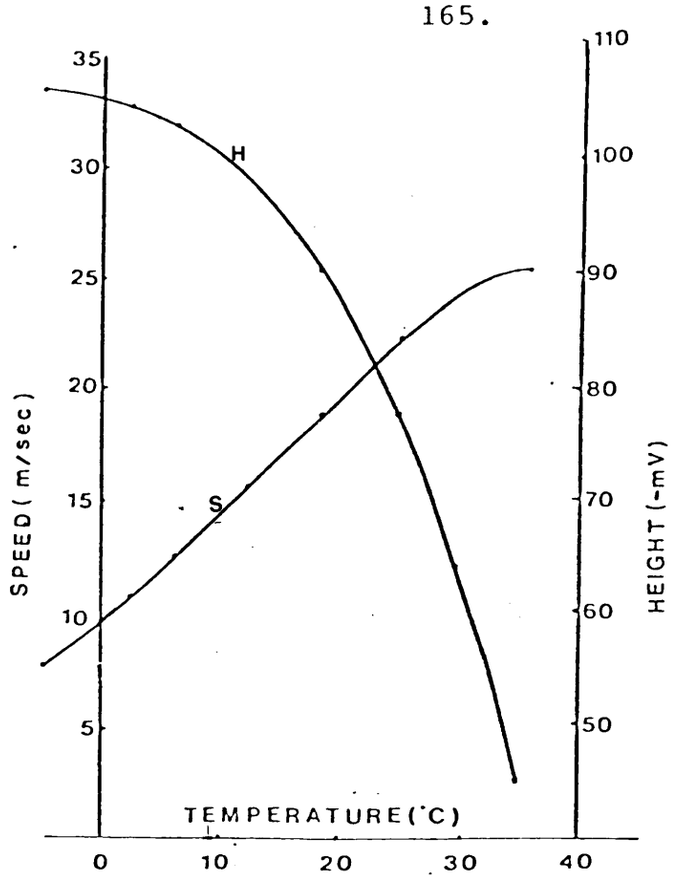

Figure 5.20

In Nagumo's model for a fixed b and decreasing a the height and "width" of a pulse increase as had been observed in § 5.2.2. This corresponds to the results of a decreasing temperature for the Hodgkin-Huxley system. The speed, however, increases for decreasing a (in Nagumo's model) in contrast to the decreasing speed for decreasing temperature in the Hodgkin-Huxley model. The same behaviour is observed for decreasing b. It is therefore not obvious what the exact relation is between parameters a and b and the temperature.

As the temperature increases above 20 °C the height of the single travelling pulse decreases rapidly and for temperatures above 36 °C no travelling pulse can be obtained. This maximum temperature is a little lower than had been observed experimentally by Hodgkin and Huxley — they observed a maximum temperature of 38 °C.

Increased temperature has the effect of speeding up the recovery processes, thus decreasing the refractory period and allowing stimuli to follow each other more rapidly and still produce one pulse per stimulus.

Another effect of increasing temperature is to decrease the threshold to stimulation. For the boundary condition

$$V(0,t) = P \ , \quad t \leqslant T$$
$$= 0 \ , \quad t > T$$

a stimulus of - 100 mV for a duration of 0,065 m sec was sufficient to produce a travelling pulse at a temperature of 18,5 °C whereas at a temperature of 6,3 °C a stimulus of -100 mV for a duration of 0,26 m sec was required.

CHAPTER 6

CONCLUSION

Although the main purpose of the present study was a mathematical one, that is to conduct a numerical investigation into mathematical models of two reaction-diffusion physiological processes, it was also necessary to briefly study the physiological processes themselves and to consider the construction of the mathematical models describing the physical reality. The processes were therefore introduced through a description of their basic features which brought to the fore the existence of interesting physiological phenomena. This knowledge proved to be invaluable, if not essential, for the subsequent mathematical investigation into the models representing these processes. An exposition of the assumptions, on which the mathematical models are based, lead to the framing of the governing equations. The governing equations of these models were then shown to be particular examples of a general system of reaction-diffusion equations.

The present study emphasizes that the importance of numerical work in the study of reaction-diffusion systems cannot be underestimated because of the increasing difficulties encountered when conventional methods of analysis are applied to more realistic models which may be represented by complicated systems of differential equations. It is pointed out, for example, that for Fisher's equation, which is representative of the simpler scalar case, analytical results exist for many different prescribed conditions as opposed to the very little that is available for the more complicated non-scalar Hodgkin-Huxley system.

The vast number of analytical results existing in the literature on the different models are systemized here and provides an overview of available information. The most important feature emerging is the aspect of travelling wave solutions. Special attention is therefore given to results on the existence and stability of travelling wave solutions. The analytical results do not always provide a clear understanding of what the exact relationship is between the existence of travelling wave solutions for various speeds and the asymptotic speed of propagation associated with a particular model.

Numerical investigation, as presented here, gives a clearer picture as to the relationship between these concepts. The travelling wave equation associated with a particular model is an ordinary differential equation and may possess an infinite number of solutions, although only one of these is obtainable from a time-progressing solution of the original partial differential equation, namely the one travelling with asymptotic speed c^*. The numerical solution of Fisher's equation, as presented in this study, shows that concepts such as the stability of an equilibrium state, the asymptotic speed of propagation and convergence to a travelling wave solution are very closely related. For example, for the case when $f(u) = u(1-u)$; any disturbance from the unstable zero steady state will evolve in time to the stable unity steady state, the shape of the disturbance converging in the process to a wave front (or two wave fronts in some cases) travelling with asymptotic speed.

For Fisher's equation in the case where $f(u) = u(1-u)(u-a)$ theoretical results indicate the existence of a threshold property.

This deduction is confirmed by calculated threshold curves, presented here for both the pure initial value problem and initial boundary value problem.

The existence of solutions other than travelling wave solutions, investigated by using a method of Fife [21], rendered only one interesting case, as far as "stationary patterns" are concerned, namely for $f(u) = u(1-u)(u-a)$, $a = \frac{1}{2}$, where the existence of two local adjacent maxima on the potential curve ensures the existence of a stable time-independent steady state.

The matter of extensions to Fisher's model, touched upon when considering the addition of the so-called drift term, leaves an open door for further investigation. The sudden appearance of oscillations is an interesting phenomenon and has been observed in other investigations of similar equations. A non-zero convection term in the general system of reaction-diffusion equations (3.1) requires a more sophisticated numerical technique than that adopted here.

It is apparent from the literature survey that the usual method for investigating reaction-diffusion systems is to transform the given partial differential equations into ordinary differential equations, called the travelling wave equations. On the one hand this approach has it's merits because results for more than one speed, corresponding to stable as well as unstable solutions, may be obtained. The unstable solutions are impossible to obtain from solving the partial differential equations in a time-progressing manner. On the other hand, the partial differential equations represent a physiological process which develops with time and therefore are preferable to be solved in a time-progressing man-

ner. By doing so the actual physiological process is simulated in a more natural and realistic manner.

In this study, for the first time, Finite Element methods have been applied to the numerical study of these models. The Finite Element method with linear test and trial functions gives satisfactory results, not only for Fisher's equation, but also for the models of impulse propagation of the nervous system. For the Hodgkin-Huxley system good agreement is found with results of the Finite Difference method employed by Cooley and Dodge [11]. The employment of quadratic basis functions was found to be impractical from the computational point of view and it is doubtful whether it's use would significantly have added to the actual accuracy obtained.

From the numerical solution of Nagumo's model it is possible to calculate a speed diagram which has not been published before and which resembles the upper part of a diagram proposed by McKean [53]. This speed diagram represents an improvement on the one obtained by Rinzel and Keller [74] for a simplified Nagumo model. One advantage of their diagram, though, lies in the lower parts of these curves which they calculated from solving the corresponding travelling wave equations.

The investigation, carried out here, on the effect of boundary conditions for the Nagumo and FitzHugh-Nagumo models leads to the following conclusions: The Dirichlet boundary condition is not appropriate to model a stimulus of infinite duration. Experimental evidence indicate that a maintained stimulus should produce repetitive firing, which the Dirichlet condition failed to produce. The non-homogeneous Neumann condition (FitzHugh-

Nagumo model) succeeded in producing repetitive firing and may therefore be considered more appropriate to model such a stimulus.

In the case of the Hodgkin-Huxley system the same effect was observed, namely that the Dirichlet boundary condition failed to produce repetitive firing. The homogeneous Neumann boundary condition with the stimulus added as an extra term to the principal governing equation produced the desired firing effect.

Although various numerical studies have been conducted on the Hodgkin-Huxley system, a great deal of work on this interesting model still remains to be done. Numerical results obtained here should contribute to the existing knowledge. In particular, the relationship between stimulus strength and one-to-one correspondence between stimuli and firing established by the present calculations show that the duration of the absolute and relative refractory periods play major roles. Furthermore it is shown that the frequency of a train of pulses is dependent on the stimulus strength, the precise relationship being given by a computed curve which is in quantitative agreement with limited results given by Cooley and Dodge [11] and Stein [81].

An interesting observation recorded in the present study is that a constant stimulus of infinite duration is equivalent to a sequence of short but unequal stimuli. In the calculations the second stimulus had to be applied for twice the duration of the first. Stimuli following one another too rapidly fail to produce a train of pulses. The remarkable phenomenon, investigated by Miller and Rinzel [57], namely that individual pulses in a train may travel with different speeds was confirmed by the present ob-

servations. It is also shown, with examples, that a pulse following it's predecessor too closely will travel with a slower speed. In other cases the second pulse may travel faster and for a special given case all pulses in a train travel with the same speed as the single pulse.

Speed and height diagrams, similar to that obtained for Nagumo's equation, were constructed for the Hodgkin-Huxley system. A comparison between these showed remarkable differences. Summarizing one can say that although it appears that the parameters a and b of Nagumo's model play the same role as the temperature parameter in the Hodgkin-Huxley system, namely that changes in height and speed of single pulses are brought about by changes in these parameters, the exact relationship is not clear. It is clear, however, that Nagumo's model should simply be regarded as a simplification of the Hodgkin-Huxley model which exhibits qualitatively some of the features of the original process.

In conclusion it may be stated that reaction-diffusion equations, because of their wide range of application, will continue to be a subject of great interest for a long period to come. In the studies stimulated by this interest numerical investigations, such as presented here, will increasingly be required as aids in the further analysis of reaction-diffusion systems.

APPENDIX A: GENETICAL BACKGROUND OF RANDOM MATING

Individual of genotype:	aa			aA			AA		
mating with	X			X			X		
individual of genotype:	aa	aA	AA	aa	aA	AA	aa	aA	AA
Offspring (×4):	4aa	2aa/2aA	4aA	2aa/2aA	1aa/2aA/1AA	2aA/2AA	4aA	2aA/2AA	4AA
Density of offspring:	ρ_1^2	$\rho_1\rho_2$	$\rho_1\rho_3$	$\rho_1\rho_2$	ρ_2^2	$\rho_2\rho_3$	$\rho_1\rho_3$	$\rho_2\rho_3$	ρ_3^2

Ratio of densities of the three classes:

Density of aa: $$[\rho_1^2 + \rho_1\rho_2 + \frac{\rho_2^2}{4}] = [\rho_1 + \frac{\rho_2}{2}]^2$$

Density of aA: $$2[\rho_1\rho_2 + \frac{\rho_1\rho_2}{2} + \frac{\rho_2\rho_3}{2} + \frac{\rho_2^2}{4}] = 2[\rho_1 + \frac{\rho_2}{2}][\rho_3 + \frac{\rho_2}{2}]$$

Density of AA: $$[\rho_3^2 + \rho_3\rho_2 + \frac{\rho_2^2}{4}] = [\rho_3 + \frac{\rho_2}{2}]^2$$

APPENDIX B

THE HODGKIN-HUXLEY SYSTEM

$$\frac{a}{2R}\frac{\partial^2 V}{\partial x^2} = C_m \frac{\partial V}{\partial t} + \bar{g}_K n^4 (V - V_K) + \bar{g}_{Na} m^3 h (V - V_{Na}) + \bar{g}_\ell (V - V_\ell) \ldots \quad (1)$$

$$\frac{\partial n}{\partial t} = \alpha_n (1-n) - \beta_n n \quad \ldots\ldots \quad (2)$$

$$\frac{\partial m}{\partial t} = \alpha_m (1-m) - \beta_m m \quad \ldots\ldots \quad (3)$$

$$\frac{\partial h}{\partial t} = \alpha_h (1-h) - \beta_h h \quad \ldots\ldots \quad (4)$$

$$\alpha_n(V) = 0{,}01(V+10)/(\exp(\frac{V+10}{10}) - 1), \quad \beta_n(V) = 0{,}125 \exp(\frac{V}{80})$$

$$\alpha_m(V) = 0{,}1(V+25)/(\exp(\frac{V+25}{10}) - 1), \quad \beta_m(V) = 4 \exp(\frac{V}{18})$$

$$\alpha_h(V) = 0{,}07 \exp(\frac{V}{20}) \quad , \quad \beta_h(V) = \frac{1}{(\exp(\frac{V+30}{10}) + 1)}$$

t = time (m sec)

x = distance along axon from stimulated end (cm)

$V(x,t)$ = membrane potential (mV)

$m(x,t)$, $n(x,t)$, $h(x,t)$ = conductance variables, dimensionless

a = radius of axon (0,0238 cm)

R = specific resistance of axoplasm (35,4 ohm cm)

C_m = specific membrane capacitance (1 $\mu f/cm^2$)

$\bar{g}_{Na}$ = maximum sodium conductance (120 mmho/cm^2)

V_{Na} = sodium equilibrium potential (115 mV)

$\bar{g}_K$ = maximum potassium conductance (36 mmho/cm^2)

V_K = potassium equilibrium potential (- 12 mV)

$\bar{g}_\ell$ = non-specific leakage conductance (0,3 mmho/cm^2)

V_ℓ = equilibrium potential of leakage current (10,5989 mV)

APPENDIX C: DERIVATION OF THE FITZHUGH-NAGUMO SYSTEM

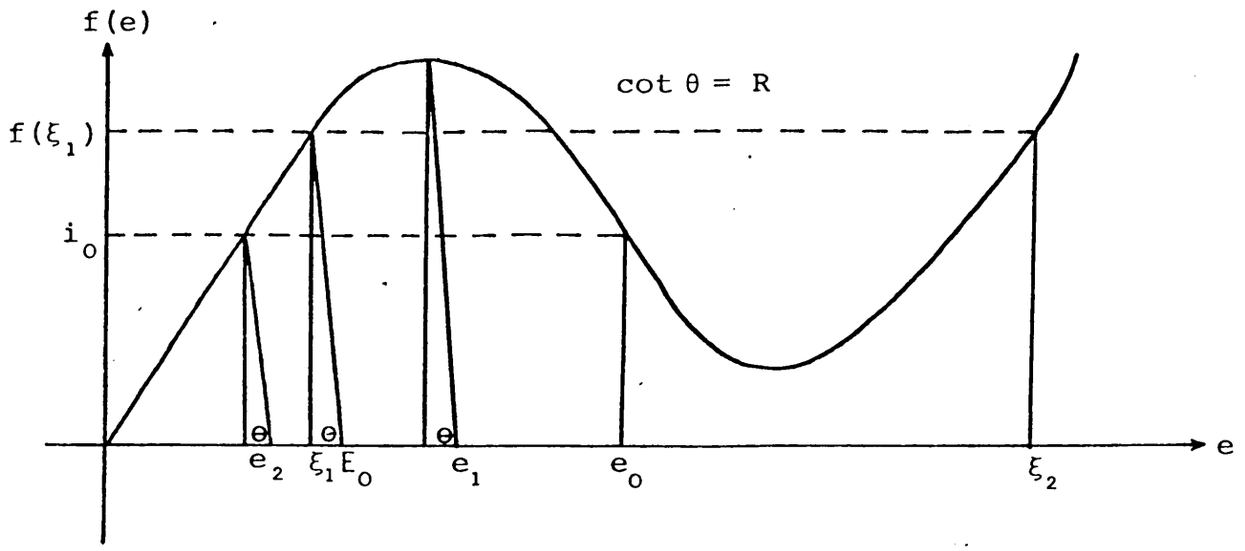

We recall equations (2.31, 2.32):

$$j = c\frac{dv}{dt} - i - f(e) \qquad L\frac{di}{dt} + Ri = -v = e - E_0 \quad \Rightarrow$$

$$j = -c\frac{de}{dt} - i - f(e) \qquad \ldots\ldots (1)$$

$$L\frac{di}{dt} + Ri = e - E_0 \qquad \ldots\ldots (2)$$

$$f(e) = i_0 - \frac{1}{\rho}\{(e - e_0) - \frac{(e - e_0)^3}{3K^2}\}, \qquad \rho > 0,\ K > 0$$

For $e_2 < E_0 < e_1$, ξ_1 and ξ_2 can be found as shown in the figure above.

Equation (1) can be written as $j = -c\frac{de}{dt} - i - [f(e) - f(\xi_1)] - f(\xi_1)$

Then $f(e) - f(\xi_1) = \frac{1}{\rho}\{(\xi_1 - e_0) - \frac{(\xi_1 - e_0)^3}{3K^2} - (e - e_0) + \frac{(e - e_0)^3}{3K^2}\}$

Now let $e^* = \frac{e - \xi_1}{\xi_2 - \xi_1}$ then $e = (\xi_2 - \xi_1)e^* + \xi_1$.

Therefore $f(e) - f(\xi_1) = \frac{1}{\rho}\{(\xi_1 - e_0) - \frac{(\xi_1 - e_0)^3}{3K^2} - (((\xi_2 - \xi_1)e^* + \xi_1 - e_0) - \frac{((\xi_2 - \xi_1)e^* + \xi_1 - e_0)^3}{3K^2})\}$

$$= f^*(e^*)$$

Thus $f^*(0) = 0$, $f^*(1) = 0$, $f^*(\alpha) = 0$ for some $\alpha \in (0,1)$

$$(f(\xi_1) = f(\xi_2))$$

$$\Rightarrow \quad f^*(e^*) = \frac{1}{\rho}\, e^*(e^* - 1)(e^* - \alpha), \quad \alpha \in (0,1)$$

Now let $i^* = i + f(\xi_1)$

then $$j = -c(\xi_2 - \xi_1)\frac{de^*}{dt} - i^* - \frac{1}{\rho}(e^*)(e^*-1)(e^*-a) \qquad \ldots\ldots (3)$$

and $$L\frac{di^*}{dt} + R(i^* - f(\xi_1)) = (\xi_2 - \xi_1)e^* + \xi_1 - E_o \qquad \ldots\ldots (4)$$

But $R\,f(\xi_1) = E_o - \xi_1$ ($\cot\theta = R$ in figure above)

then (4) reduces to

$$L\frac{di^*}{dt} + Ri^* = (\xi_2 - \xi_1)e^* \qquad \ldots\ldots (5)$$

Let $t^* = \dfrac{t}{c\rho(\xi_2 - \xi_1)}$, $J^* = \rho j$, $K_1 = \dfrac{c\rho(\xi_2 - \xi_1)R}{L}$

$$i^{**} = \rho i^*, \qquad K_2 = \frac{c^2\rho(\xi_2 - \xi_1)^2}{L}$$

then (3) and (5) reduces to

$$J^* = -\frac{de^*}{dt^*} - i^{**} + e^*(1 - e^*)(e^* - a) \qquad \ldots\ldots (6)$$

$$\frac{di^{**}}{dt^*} = -K_1\, i^{**} + K_2 e^* \quad K_1 > 0, K_2 > 0, \quad \alpha \in (0,1) \quad \ldots (7)$$

In the case of a propagated action potential we have

$$j = \frac{1}{r}\frac{\partial^2 v}{\partial s^2} \qquad \ldots\ldots (8)$$

or $$J^* = \frac{\rho}{r}\left(-\frac{\partial^2 e}{\partial s^2}\right) = -\frac{\rho}{r}(\xi_2 - \xi_1)\frac{\partial^2 e^*}{\partial s^2}\,.$$

By setting $x = \dfrac{s}{\sqrt{\frac{\rho}{r}(\xi_2 - \xi_1)}}$ we obtain $J^* = -\dfrac{\partial^2 e^*}{\partial x^2}$

so that (6) reduces to

$$\frac{\partial e^*}{\partial t^*} = \frac{\partial^2 e^*}{\partial x^2} - i^{**} + e^*(1 - e^*)(e^* - a) \qquad \ldots\ldots (9)$$

By renaming the variables in (7) and (9) we obtain the system which is usually referred to as the FitzHugh-Nagumo system

$$\frac{\partial u}{\partial t} = \frac{\partial^2 u}{\partial x^2} + u(1-u)(u-a) - w$$

$$\frac{\partial w}{\partial t} = b(u - dw) \quad , \qquad b > 0,\ d > 0,\ a \in (0,1)$$

APPENDIX D: HAMMING'S PREDICTOR-CORRECTOR METHOD, RUNGE-KUTTA FOURTH ORDER METHOD AND GAUSSIAN ELIMINATION

Initial value problem:

$$y' = f(x,y), \quad y(a) = \eta$$

Runge-Kutta fourth order method:

$$y_{n+1} - y_n = \frac{h}{6}(k_1 + 2k_2 + 2k_3 + k_4)$$

$$k_1 = f(x_n, y_n)$$

$$k_2 = f(x_n + \tfrac{1}{2}h, y_n + \tfrac{1}{2}h\,k_1)$$

$$k_3 = f(x_n + \tfrac{1}{2}h, y_n + \tfrac{1}{2}h\,k_2)$$

$$k_4 = f(x_n + h, \; y_n + h\,k_3)$$

Hamming's Predictor-corrector method:

P: $$y_{n+4}^{[0]} - \hat{y}_n^{[1]} = \frac{4h}{3}(2\hat{f}_{n+3}^{[1]} - \hat{f}_{n+2}^{[1]} + 2\hat{f}_{n+1}^{[1]}),$$

M: $$\hat{y}_{n+4}^{[0]} = y_{n+4}^{[0]} + \frac{112}{121}(y_{n+3}^{[1]} - y_{n+3}^{[0]}),$$

E: $$\hat{f}_{n+4}^{[0]} = f(x_{n+4}, \hat{y}_{n+4}^{[0]}),$$

C: $$y_{n+4}^{[1]} - \frac{9}{8}\hat{y}_{n+4}^{[1]} + \frac{1}{8}\hat{y}_{n+1}^{[1]} = \frac{3h}{8}(\hat{f}_{n+4}^{[0]} + 2\hat{f}_{n+3}^{[1]} - \hat{f}_{n+2}^{[1]}),$$

M: $$\hat{y}_{n+4}^{[1]} = y_{n+4}^{[1]} - \frac{9}{121}(y_{n+4}^{[1]} - y_{n+4}^{[0]})$$

E: $$\hat{f}_{n+4}^{[1]} = f(x_{n+4}, \hat{y}_{n+4}^{[1]})$$

Gaussian Elimination

We describe the standard method for solving a tridiagonal system of linear equations of the form

$$Ax = f \ ,$$

where x is the unknown n-dimensional vector, f is an n-dimensional vector of constants, and

$$A = \begin{bmatrix} a_1 & c_1 & & & \\ b_2 & a_2 & c_2 & & \\ & & & & \\ & & & & \\ & & b_{n-1} & a_{n-1} & c_{n-1} \\ & & & b_n & a_n \end{bmatrix}$$

The method involves writing A as the product of two matrices L and U so that

$$Ax = f \Rightarrow LUx = f \ .$$

Letting $g \equiv Ux$, we first solve for g:

$$Lg = f \ ,$$

and then obtain x as the solution of

$$Ux = g \ .$$

The advantage of this method is that the equations for both g and x can be solved by back-substitution.

Step 1. Factor A.

$$A = LU = \begin{bmatrix} \alpha_1 & & & \\ b_2 & \alpha_2 & & \\ & b_3 & \alpha_3 & \\ & & & \\ & & b_n & \alpha_n \end{bmatrix} \cdot \begin{bmatrix} 1 & \gamma_1 & & \\ & 1 & \gamma_2 & \\ & & & \gamma_{n-1} \\ & & & 1 \end{bmatrix}$$

where $\alpha_1 = a_1$,

$\gamma_1 = c_1/\alpha_1$,

$\alpha_i = a_i - b_i\gamma_{i-1}$, $i = 2, \ldots, n$,

$\gamma_i = c_i/\alpha_i$, $i = 2, \ldots, n-1$.

Step 2. Solve for g .

$$Lg = f \Rightarrow g_1 = \frac{f_1}{\alpha_i}$$

$$g_i = (f_i - b_i g_{i-1})/\alpha_i \ , \quad i = 2, \ldots n .$$

Step 3. Solve for x .

$$Ux = g \Rightarrow x_n = g_n$$

$$x_i = g_i - (x_{i+1})\gamma_i \ , \quad i = n-1, \ldots, 2, 1 .$$

If several systems of equations must be solved using the same matrix A (i.e., with different f vectors), then only steps 2 and 3 need be repeated.

REFERENCES

1. D G Aronson and H F Weinberger: Nonlinear diffusion in population genetics, combustion and nerve pulse propagation. Lecture Notes in Mathematics, vol. 446, Berlin Springer-Verlag, 1975.

2. D G Aronson and H F Weinberger: Multidimensional nonlinear diffusions arising in population genetics. Advances in Math. 30 (1978) 33-76.

3. K F Bonhoeffer: Activation of passive iron as a model for the excitation of nerve. Journal of General Physiology 32 (1948) 69-91.

4. G A Carpenter: Periodic solutions of nerve impulse equations. Journal of Mathematical Analysis and Applications 58 (1977) 152-173.

5. R Casten, H Cohen and P Lagerstrom: Perturbation analysis of an approximation to Hodgkin-Huxley theory. Quart Appl. Math. 32 (1975) 365-402.

6. M E Cochran: A generalisation of McKean's nerve axon model. B.A. Thesis, University of Tennessee, 1978.

7. K S Cole: Electrodiffusion models for the membrane of squid giant axon. Physiological Reviews 45 (2) (1965) 340-378.

8. K S Cole, H A Antosiewicz, P Rabinowitz: Automatic computation of nerve excitation. J. SIAM 3 (3) (1955) 153-172.

9. C Conley: On the existence of bounded progressive wave solutions of the Nagumo equation. (In manuscript, 1975).

10. E Conway, D Hoff, J Smoller: Large time behaviour of solutions of systems of nonlinear Reaction-Diffusion Equations. SIAM J. Appl. Math. 35 (1)(1978)1-16.

11. J W Cooley and F A Dodge (Jr): Digital computer solutions for excitation and propagation of the nerve impulse. Biophysical Journal 6 (1966) 583-599.

12. J Cooley, F Dodge, H Cohen: Digital computer solutions for excitable membrane models. Cell. & Comp. Physiol. 66 (1965) 99-110.

13. B Copeland: A guide to programs which solve variations of the FitzHugh-Nagumo equations and the equations for spreading depression. Technical report no. 79-13 (March 1979). University of British Columbia, Vancouver, Canada.

14. J E Dendy (Jr), B Swartz and B Wendroff: Computing travelling wave solutions of a nonlinear heat equation. Topics in Numerical Analysis 77 (1977) 447-463.

15. J C Eilbeck, S D Luzader, A C Scott: Pulse evolution on coupled nerve fibres. (Preprint 1979, submitted to the Bulletin of Mathematical Biology).

16. J W Evans: Nerve axon equations I-IV. Indiana Univ. Math. J. 21 (1972) 877-885, 22 (1972) 75-90, 22 (1972) 577-594, 24 (1975) 1169-1190.

17. G Fairweather: Finite element Galerkin methods for differential equations. Marcel Dekker, Basel 1978.

18. P C Fife: Stationary patterns for Reaction-Diffusion equations. Nonlinear Diffusion 81 - 121 (eds. W E Fitzgibbon and H F Walker) Research Notes in Mathematics 14. Pitman 1977.

19. P C Fife: Asymptotic states for equations of reaction and diffusion. Bull. Amer. Math. Soc. 84 (5) (1978) 693-726.

20. P C Fife: Results and open questions in the asymptotic theory of Reaction-Diffusion equations. Nonlinear Evolution equations 125-139. Ed. M G Crandall. Academic Press 1978.

21. P C Fife: Long time behaviour of solutions of bistable nonlinear diffusion equations. Arch. R. Mech. 70 (1) (1979) 31-46.

22. P C Fife: The bistable nonlinear diffusion equation: Basic theory and some applications. Applied nonlinear analysis. 143-159. Ed. V Lakshmikanthan. Academic Press 1979.

23. P C Fife and J B McLeod: The approach of solutions of nonlinear diffusion equations to travelling front solutions. Arch. Rat. Mech. & Anal. 65 (1977) 335-361.

24. P C Fife and J B McLeod: A phase plane discussion of convergence to travelling fronts for nonlinear dif-

fusion. MRC Technical Summary Report # 1986 University of Wisconsin (1979).

25. P C Fife and L A Peletier: Nonlinear diffusion in population genetics. Arch. R. Mech. 64 (2)(1977) 93-109.

26. R A Fisher: Gene frequencies in a cline determined by selection and diffusion. Biometrics 6 (1950) 353-361.

27. R A Fisher: The wave advance of advantageous genes. Annals of Eugenics. 7 (1937) 355-369.

28. R FitzHugh: Impulses and physiological states in theoretical models of the nerve membrane. Biophysical Journal. 1 (1961) 445-466.

29. R FitzHugh: Mathematical models of excitation and propagation in nerve. Biophysical Engineering 1-85. H P Schwan (Ed), McGraw-Hill, N.Y., 1969.

30. R FitzHugh: Motion picture of nerve impulse propagation using computer animation. Journal of Applied Physiology. 25 (1968) 628-630.

31. R FitzHugh and H A Antosiewicz: Automatic computation of nerve excitation - detailed corrections and additions. J. SIAM 7 (4)(1959) 447-458.

32. R A Gardner: Asymptotic behaviour of semilinear Reaction-Diffusion systems with Dirichlet boundary conditions. MRC Technical Summary Report # 1896, University of Wisconsin. November 1978.

J. Math. Oxford 27 (2) (1976) 123-134.

43. S P Hastings: Addendum to the existence of periodic solutions to Nagumo's equation. (In manuscript, 1976)

44. A L Hodgkin: The conduction of the nervous impulse. Liverpool University Press 1964.

45. A L Hodgkin and A F Huxley: A quantitative description of membrane current and it's application to conduction and excitation in nerve. J. Physiol. 117 (1952) 500-544.

46. A L Hodgkin and A F Huxley: Movement of radioactive potassium and membrane current in giant axon. J. Physiol. 121 (1953) 403-414.

47. T J R Hughes (Ed): Finite element methods for convection dominated flows. American Soc. Mech. Engineers. A.M.D. Vol 34 (1979).

48. A F Huxley: Ion movements during nerve activity. Annals New York Academy of Science. 81 (1959) 221-246.

49. E Isaacson and H B Keller: Analysis of numerical methods. Wiley 1966. London.

50. A Kolmogoroff, I Petrovsky, N Piscounoff: A study of the equation of diffusion with increase in the quantity of matter and it's application to a biological problem. Bjul. Moskouskogo Gos Univ 1 (7)(1937) 1-72.

51. J D Lambert: Computational methods in ordinary differential equations. Wiley 1973.

52. M Lees: On extrapolated Crank-Nicolson difference scheme for quasi-linear parabolic equations. Nonlinear Partial Differential Equations, W. F. Ames, Ed., Academic Press 1967.

53. H P McKean (Jr): Nagumo's equation. Advances in Mathematics 4 (3)(1970) 209-223.

54. H P McKean: Applications of Brownian motion to the equation of Kolmogorov-Petrovskii-Piskounov. Communications on pure and applied mathematics, vol. XXVIII (1975) 323-331.

55. K Maginu: Stability of periodic travelling wave solutions of a nerve conduction equation. J. Math. Biol. 6 (1978) 49-57.

56. A Meiring, A R Mitchell, B D Sleeman: Numerical studies of Reaction-Diffusion. Report NA/39, February 1980, University of Dundee.

57. R N Miller and J Rinzel: The dependence of impulse propagation speed on firing frequency, dispersion, for the Hodgkin-Huxley model, preprint (submitted to Biophysical Journal).

58. A R Mitchell: Computational methods in partial differential equations. John Wiley and Sons. 1969.

59. A R Mitchell, D F Griffiths and A Meiring: Finite element Galerkin methods for Convection-Diffusion

and Reaction-Diffusion. To appear in Proceedings of Second Conference on Asymptotic Methods held in Holland 1980, published by Academic Press.

60. A R Mitchell and R Wait: The finite element method in partial differential equations. John Wiley and Sons 1977.

61. R M Muira: Accurate computation of travelling wave solutions: The FitzHugh-Nagumo equations stable solitary wave. (Preprint 1979).

62. J D Murray: On travelling wave solutions in a model for the Belousov-Zhabotinskii reaction. J. Theor. Biol. 56 (1976) 329-353.

63. J D Murray: A pattern formation mechanism and it's applications to mammalian coat markings Lecture Notes in Bio-Mathematics. Springer-Verlag (1980)(to appear).

64. J Nagumo, S Arimoto and S Yoshizawa: An active pulse transmission line simulating nerve axon. Proceedings of the IRE 50 (1962), 2061-2070.

65. J Nagumo, S Yoshizawa and S Arimoto: Bistable transmission lines. IEEE Transactions on Circuit Theory, Vol CT-17, no 3 (1965) 400-412.

66. D Noble: Applications of Hodgkin-Huxley equations to excitable tissues. Physiological Reviews 46 (1966) 1-50.

67. D Noble and R B Stein: The threshold conditions for initiation of action potentials by excitable cells. J. Physiol. 187 (1966) 129-162.

68. R E Plant: The geometry of the Hodgkin-Huxley model. Computer Programs in Medicine 6 (1976) 85-91.

69. J Rauch and J Smoller: Qualitative theory of the FitzHugh-Nagumo equations. Adv. in Math. 21 (1978) 12-44.

70. J Rinzel: Neutrally stable travelling wave solutions of nerve conduction equations. J. Math. Biol. 2 (1975) 205-217.

71. J. Rinzel: Repetitive nerve impulse propagation: Numerical results and methods. Nonlinear Diffusion 186-212 (Eds. W.E. Fitzgibbon and H.F. Walker). Research Notes in Mathematics 14. Pitman 1977.

72. J Rinzel: Repetitive activity and Hopf bifurcation under point stimulation for a simple FitzHugh-Nagumo nerve conduction model. J. Math. Biol. 5 (1973) 363-382.

73. J Rinzel: Spatial stability of travelling wave solutions of a nerve conduction equation, Biophysical Journal 15 (1975) 975-988.

74. J Rinzel and J B Keller: Travelling wave solutions of a nerve conduction equation. Biophysical Journal 13 (1973) 1313-1337.

75. F Rothe: Convergence to travelling fronts in semilinear parabolic equations. Proc. Roy. Soc. Edin. (A) 80 (1978) 213-234.

76. N H Sabah and R A Sprangler: Repetitive response of the Hodgkin-Huxley model of the squid giant axon. J. Theor. Biol. 29 (1970) 155-171.

77. M E Schonbek: Boundary value problems for the FitzHugh-Nagumo equations. Journal of Differential Equations 30 (1)(1978) 119-147.

78. M E Schonbek: Some results on the FitzHugh-Nagumo equations. Nonlinear Diffusion 213-218 (Eds. W.E. Fitzgibbon and H.F. Walker) Research notes in Mathematics 14 Pitman 1977.

79. B D Sleeman: FitzHugh's nerve axon equations. J. Math. Biol. 2 (1975) 341-349.

80. B D Sleeman: Instability of certain travelling wave solutions to the FitzHugh-Nagumo nerve axon equations. Journal of Math. Anal. & Appl. 14 (1)(1980) 106-119.

81. R B Stein: The frequency of nerve action potentials generated by applied currents. Proceedings of Royal Society of London. B167 (1967) 64-86.

82. A N Stokes: Nonlinear diffusion wave shapes generated by possibly finite disturbances. J. Math. Anal. & Appl. 61 (1977) 370-381.

83. W C Troy: Bifurcation phenomena in FitzHugh's nerve conduction equations. J. Math. Anal. & Appl. 54 (1976) 678-690.

84. W C Troy: Oscillation phenomena on the Hodgkin-Huxley equations. Roy. Soc. Edinburgh Proc. A 74 (1976) 299-310.

85. University of Pretoria Medical Lecturing notes: (MBCHB II) (1972).

86. B van der Pol: On relaxation oscillations. Phil. Mag. 2 (1926) 978-992.

87. B van der Pol and J van der Mark: The heartbeat considered as a relaxation-oscillator and an electrical model of the heart Phil. Mag. 6 (1928) 763-775.